Effect of LD Slag and Copper Slag as Sand Replacement on Self-Sensing Properties of Cementitious Composites

A thesis report submitted

In Partial Fulfilment of the Requirement for the Award of the Degree of

Masters of Engineering

In

Structural Engineering

Submitted by

Achleshwar Singh Raizada

802224031

Under the Guidance of

Dr. Shruti Sharma
Professor
Department of Civil Engineering
TIET, Patiala

Dr. Arpit Goyal
Assistant Professor
Department of Civil Engineering
TIET, Patiala

DEPARTMENT OF CIVIL ENGINEERING

THAPAR INSTITUTE OF ENGINEERING AND TECHNOLOGY

(DEEMED TO BE UNIVERSITY)

PATIALA-147004 (PUNJAB)

December 2024

DECLARATION

I hereby declare that this is a bonafide work which is presented in this minor design project report/seminar report entitled "**Effect of LD Slag and Copper Slag as Sand Replacement on Self-Sensing Properties of Cementitious Composites**" as per requirement for the award of master of engineering in Structure Engineering, submitted in the department of Civil Engineering, Thapar Institute of Engineering and Technology (TIET), Patiala. This work is carried out under the guidance and supervision of DR. Shruti Sharma and Dr. Arpit Goyal. It is declared that this work is original and has not been submitted anywhere else for the award of any other degree or certificate.

Date: 20/09/2024

(Achleshwar Singh Raizada)

(802224031)

CERTIFICATE

This is to verify that the above statement made by candidate is correct to the best of our knowledge.

(DR. SHRUTI SHARMA)

Professor

Department of Civil Engineering

TIET, Patiala

(DR. ARPIT GOYAL)

Assistant Professor

Department of Civil Engineering

TIET, Patiala

i

ACKNOWLEDGEMENT

This research thesis would not have been possible without the assistance and guidance of several individuals who offered insightful input, whether directly or indirectly. I would like to extend my sincere gratitude to Dr. Shruti Sharma, professor in the department at Thapar Institute of Engineering and Technology, Patiala, and Dr. Arpit Goyal, an assistant professor in the same department, for their vital support, guidance and putting innovative ideas into practice. For the motivation and inspiration that triggered me throughout my work. I also want to express my gratitude to the entire Institute staff for giving me all the support and resources I needed to finish the research. Moreover, I would like to acknowledge the financial support provided by Thapar Institute of Engineering & Technology from M.E contingency. Lastly, I would want to thank my family for unwavering support and encouragement, especially during my academic career.

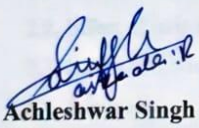

Achleshwar Singh Raizada

(802224031)

Table of Contents

LIST OF TABLES

LIST OF FIGURES

ABSTRACT

The abstract of the thesis "Effect of LD Slag and Copper Slag as Sand Replacement on Self-Sensing Properties of Cementitious Composites" investigates the possibility of using copper slag and LD slag as conductive fillers in cement mortar. The study aims to improve the electrical and mechanical properties of cementitious composites by adding these industrial by- products. Copper slag, a by-product of the copper smelting process, is known for its excellent mechanical and conductivity qualities, making it an ideal filler. LD slag, a by-product of the steel making process, has significant concentrations of calcium oxide and other inorganic components, which contribute to its cementitious qualities. The study investigates the effects of various materials on workability, compressive strength, and flexural strength, electrical and piezoelectric properties of cement mortar. Furthermore, the research involves microstructural characterization using SEM to better understand the interaction between the fillers and the cement matrix. The findings indicate that the addition of copper slag and LD slag may significantly improve the electrical and mechanical performance of cement mortar, giving a sustainable and cost-effective choice for the construction sector. The study highlights the potential of these by-products in substituting natural resources such as river sand, therefore resolving environmental concerns and improving the use of waste materials in construction. This concludes with recommendations for future research to improve the usage of these components in cementitious composites.

CHAPTER 1

INTRODUCTION

1.1 General

Over time, more emphasis has been placed on the need to monitor and evaluate concrete performance utilizing a variety of materials and condition assessment technologies during maintenance or service life. A method called Structural Health Monitoring (SHM) has the capability to identify performance imperfection in a structure before they cause a significant loss of capacity. The term "SHM" refers to a technology that continually assesses a structure's condition to identify developing defects and avoid collapse or failure. An early damage-monitoring instrument that can be applied to the load-bearing structural system is one the prominent solutions (Kuang et al., 2009). The greatest benefit is the ability to assess a vulnerability as soon as it is identified and, if required, undo the harm. Accurately evaluating a structure's functionality, monitoring its efficacy over time, and giving current information on its state are the goals of "SHM". The rate of corrosion, humidity, alkali reactions, loads, strains and stresses are few of the factors that can be tracked with SHM. Structural health monitoring uses a sensory system to continuously and precisely measure how well a structure is working, because they are piezo resistive, recently developed cement-based sensors can be utilised to directly sense stress or strain by evaluating their electrical resistance. These sensors sometimes referred to as smart (self-sensing) structural composites that can be fully or partially integrated into a structure, providing structural as well as applied stress and damage response capabilities. In recent decades, there has been increased interest in cementitious materials that contain conductive particles and have the ability to self-sense for SHM. Structural health monitoring (SHM), which uses specialized instruments including piezoelectric transducers, magneto elastic stress sensors, and fiber-optic sensors, is thought to be one of the useful methods for preventing unanticipated structural failures and monitoring damage occurrences in crucial zones. The low sensitivity, short service life, low durability, and high cost of these sensor-based instruments all contribute to the deterioration of the mechanical characteristics of the structural elements in which they are placed. The development of new sensor types that not only improve the mechanical characteristics of their host element but also have low cost, long service life, high durability, and compatibility would be very helpful in overcoming these drawbacks.

The structural material functions, electrical conductivity, and piezo resistivity qualities of electrically conductive cementitious composite (ECCC) are widely used in snow melting, electromagnetic shielding, cathodic protection systems, and SHM. Given its capacity to fill molecular holes, lessen concrete shrinkage, and greatly increase electrical conductivity, nano-graphite is a perfect ECCC functional filler. On the other hand, large concentrations of nano-graphite can cause particle aggregation and are rather expensive.

The cement-based composite is considered an insulating material with high resistivity, ranging from 106 Ω·cm to 109 Ω·cm. On the other hand, the composites that are reinforced with conductive fillers exhibit high conductivity and piezo-resistivity. In their review, Wang et al. examined twelve conductive fillers that improved the electrical characteristics and self-sensing capabilities of the electrically conductive cementitious composite (ECCC). Because of its notable conductivity, lightweight nature, and stability during operation, carbon-based materials are the most widely used in engineering practice. Carbon fibres have better conductive qualities than steel fibres, although they cost more, according to Banthia et al. The best compressive strength with comparatively high conductivity is confirmed to be achieved with an optimal 0.5wt% for carbon fibres.

Furthermore, carbon based nanomaterials gained international interest due to their excellent conductivity and versatile applications, made possible by innovative nanotechnology. The mixture of nano-graphite can decrease the autogenous shrinkage and reduce the porosity of the concrete. But when components are utilized in significant dosages, the crystal microstructures of the nanoscale carbon fillers become unstable. This is because the mechanical attributes pertaining to the microstructure, hydration speed and rheological features are neglected by smooth micro surfaces and particle aggregation. Therefore, in addition to figuring out its threshold, it is crucial to mix in additional fillers to offset the lubricating effect.

Copper slag by-product of the copper manufacturing and refining procedure, is an excellent supplementary filler due to its exceptional mechanical and conductivity properties. Depending upon the slow and fast cooling, copper slag particles formed are amorphous or crystalline. China is likely to produce almost 40% of the total world copper smelter production, followed by Japan (8%), Chile (6%) and Russian Federation (5%) according to

International Copper Study Group, 2019). Currently, copper slag is widely used in the construction of road infrastructure, train ballast, and full-scale cement factories. Substituting some of the aggregated with copper slag will result in substantial energy savings required for cement manufacturing. Moreover, it will effectively repurpose a residual material, offering possible ecological and financial advantages for all participating companies. Khalifa et. al conducted a study in which they found that replacing sand with 40-wt% of copper slag can result in formation of HPC that possesses exceptional toughness and resilience. Additionally, the use of copper slag as a fine aggregate has been shown to significantly increases the abrasion resistance of cement mortar. Additionally, coarse texture can counteract the mechanical loss resulting from graphite. The utilisation of the carbon materials in conjunction with the copper slag resulted in improved electrical conductivity, cost effectiveness, and mechanical qualities. Nevertheless, the mixture of nano-graphite and copper slag by conventional blending methods fails to achieve the desired properties due to inadequate dispersion of particles within the matrix. In addition, the difference in surface properties of nano-graphite and copper slag impeded the process of combining them. Hence, it is imperative to employ suitable modification techniques to achieve the desired dispersion while simultaneously acquiring favourable mechanical and conductive characteristics.

For development of communities, steel industry is the most important industry. It contributes the significant development to India's economic. Steel has played a substantial role in the economic progress of India. Based on the 2022 data from the world steel association, the global production of the crude steel amounted to 1878 million tons. Approximately 73.2% of the worldwide production of crude steel is derived from oxygen furnaces. Statistics in India indicate that 45% of the overall crude steel production is derived from the basic oxygen furnace method, while the remaining 55% is manufactured using electric furnace. Ferrous slag is a residual substance that is generated when molten steel is separated from impurities of the steel making procedure. Slag is a viscous liquid formed by melting and is composed of a mixture of silicates and oxides. It solidifies upon cooling. Slag is typically regarded as refuse, is disposed of in landfills, so occupying the significant amount of land and contaminating environment, and surroundings because of the release of alkaline substances. Slags are classified in four types that is Blast Furnace Slag (BFS), Basic Oxygen Furnace Slag (BOF slag) or Linz Donawitz slag (LD slag), Electric Arc Furnace slag (EAF slag), and Ladle Furnace slag (LF slag). The first stage in steel production is blast furnace steelmaking, where raw iron one is transformed into pig iron. Pig iron contains different levels of carbon,

silicon, manganese, sulphur, and phosphorus. By introducing limestone into the process, the impurities are eliminated and a resulting slag as high levels of calcium, silica, aluminium, and magnesium oxides. This slag has a similar appearance to cement but with differing proportions, making it valuable component in cement production. The molten iron undergoes additional processing and utilized in the LD steelmaking process. Unlike LD slag, EAF slag is produced using high power electrics arcs. In LD method large portion of molten iron and a smaller amount of steel scrap. In contrast, the EAF process primarily relies on the steel scrap as its main input material.

Linz-Donawitz slag used for various purposes, such as soil stabilization, fertilization, road aggregate, and cement binding. Presence of CaO and MgO causes volumetric expansion which prohibited the use of LD slag as aggregate in concrete and concrete mixes. Free lime content of LD slag can range from 1% to 10%. After undergoing weathering over a period of almost 12 months, slag can be seen as an effective remedy for different expansion problems, as its CaO content decreases below 2%. After the LD steelmaking process LD slag is removed and disposed, where it still contains a significant amount of free lime. LD slag has the ability to absorb moisture (H2O) and carbon dioxide from the air. Calcium oxide (CaO) undergoes a chemical reaction with water (H2O) to produce calcium hydroxide (Ca(OH)2). The Ca(OH)2 compound undergoes a reaction with CO2, resulting in the formation of calcium carbonate (CaCO3). The reaction produces additional amount of CaCO3, formed by the combination of Calcium oxide and Carbon dioxide. (Ca(OH)2) typically results in enlargement and degeneration. Therefore, as the reactions occur repeatedly, the free lime content gradually decreases over time, resulting in a decrease in the expansion for slag. As a result, the duration of aging can vary proportionally. Wang et al. established the usefulness criteria by making predictions about the volumetric expansion of steel slag. A formula was derived to determine the maximum permissible amount of free lime in slag in order for it to be suitable for use as a granular material in the base or subbase course. The acceptable range for the free lime content in the pavement construction, which has a 10 cm thick layer at the top, is between 3.7% and 3.9% Kambole et al. provided specific restriction for the expansion of LD slag when used as a construction materials found in asphalt mixtures in a number of countries, including South Africa (7%), Brazil (3%), China (2%), Japan (1.5%), and Canada (1%). Wang and colleagues found that a free lime content of 2.09% was considered appropriate, and that using steel slag was a good way to ensure the durability of hardened concrete.

1.2. Need for self-sensing cementitious concrete

Self-sensing cementitious concrete enables the continuous and immediate monitoring of the structural integrity of buildings, bridges, and other infrastructures. This allows for the early detection of cracks, deformations, or other forms of deterioration, which can prolong the lifespan of the structure.

Self-sensing cementitious concrete can enhance safety by providing real-time information on the behaviour of a structure, thereby enabling more informed decision-making during maintenance and repair activities. Self-sensing cementitious concrete can help reduce maintenance expenses by detecting deterioration at early stage and enabling targeted and efficient repairs.

Self-sensing cementitious concrete provides data on the internal moisture level of the concrete, facilitating corrosion avoidance. Self-sensing cementitious concrete can provide valuable insights into the behaviour of a structure during the design process. This information can help enhance the performance of the structure and reduce costs by enabling more informed decisions regarding material selection, shape, and loading conditions. (Ren, et. al, 2022)

1.3. Process of making self-sensing cementitious concrete

- Begin by combining the concrete in accordance with the guidelines provided by the manufacturer. Concrete mixes typically consist of cement, water, aggregates (such as sand and gravel), and admixtures. In this stage, the sensor materials are included into the mixture.
- Using a high-shear mixer or a paddle mixer, the sensor materials are equally distributed throughout the concrete mix. This ensures that the sensors are evenly dispersed and do not cluster together.
- Once the concrete is well mixed, it is then poured into molds and left to harden for a period of several days. Throughout this duration, it is imperative to ensure that the sensor materials remain devoid of moisture and any form of impurities.
- Once the concrete has solidified, it is necessary to calibrate the sensors to ensure accurate measurement of the desired values. The sensor's output is determined by measuring it after known loads or stresses are applied to the concrete.

- The sensors are connected to a data acquisition system using either wires or fibre optic cables. This enables the transmission and analysis of sensor data by a computer or other monitoring equipment.
- The usefulness and precision of the self-sensing concrete are assessed by subjecting it to different loading conditions. The process may entail subjecting the concrete to different loads or stresses and closely monitoring the sensor's output.
- The sensors may degrade or become damaged over time due to environmental factors or normal usage. Regular sensor maintenance and replacement are necessary to ensure their continued appropriate and reliable performance.

1.4. Challenges of self-sensing cementitious concrete

Difficulties associated with self-sensing cementitious concrete. Self-sensing concrete sensors are still somewhat costly in comparison to standard concrete sensors. Implementing self-sensing concrete on a wide scale becomes challenging.

One of the most challenging elements of self-sensing concrete is integrating sensors into the matrix without affecting its mechanical properties. The sensors must possess a small size, low weight, and be able to withstand the extreme conditions found in concrete. Concrete self-sensing sensors need to exhibit long-term reliability and precision. The sensors must possess the capability to provide dependable measurements under diverse environmental conditions, encompassing temperature, humidity, and load.

Concrete self-sensing sensors need to be compatible with other structural elements, such as reinforcing bars and admixtures. This requires meticulous selection of sensor materials and precise installation processes. (Ren, et. al, 2022)

1.5. Types of Conductive Fillers

Copper slag: Copper slag is a by-product of copper industry, which is extracted through smelting. During smelting, impurities from slag, which floats on the molten metal. When damped in water, the slag produces angular granules. These granules are either disposed of as waste or utilized in other certain ways. For instance, copper slag in grit blasting and landfilling. Additionally researchers have discovered its use as a concrete aggregate, finding that it can be more sustainable than other Ordinary Portland cement. The use of copper slag as a fine aggregate has been shown to significantly enhance the abrasion resistance of cement

mortar. The angular granules of copper slag contribute to its effectiveness in blasting operations. This shape enhances its conductivity and makes it suitable for various uses. (Gupta, et al., 2019)

Figure 1.1. Copper Slag

Linz-Donawitz slag (LD slag): LD slag is a by-product produced throughout steelmaking procedure within a Basic Oxygen Furnace (BOF) or LD converter. Essentially, the molten by-product that separates from purified metal during refining. LD slag is characterised by its high calcium oxide (Cao) content, typically ranging from 42% to 50%. Additionally, it contains other inorganic elements like SiO2, Al2O3, FeO, Fe2O3, and MnO. While LD slag finds some applications in construction due to its hardness and cementitious properties, its high phosphorus content limits its broader use in industries like ironmaking and cement production. It can be used as a conductive filler in certain applications due to its potential to form conductive pathways within a composite material. This is because LD slag contains metallic phases, such as iron oxides and unoxidized metal particles, which can facilitate electrical conductivity when dispersed within a conductive matrix. (Singh, et. al, 2023)

Figure 1.2. LD slag

Carbon nanotubes (CNTs): Carbon nanotubes (CNTs), with their remarkable mechanical properties and unique electrical characteristics, hold immense potential for the development of next-generation construction materials. Incorporation of CNTs into cementitious composites has been shown to enhance tensile strength, flexural performance, and improve crack resistance through improved interfacial bonding and stress transfer mechanism. Additionally, the inherent electrical conductivity of CNTs opens avenues for the exploration of multifunctional building materials with embedded sensor capabilities for real-time health monitoring of structures. However, challenges persist regarding cost-effective, large-scale production methods for CNTs and ensuring their uniform dispersion within the cementitious matrix. (Rathinavel, et. al, 2021)

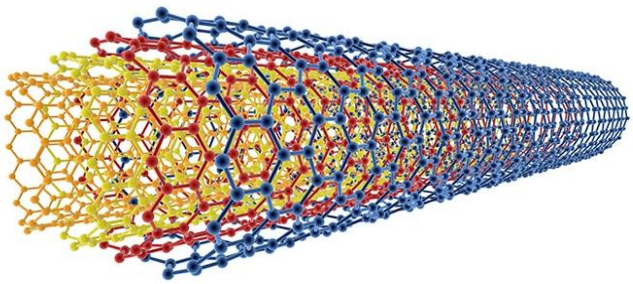

Figure 1.3. Multilayer Carbon nanotubes

Steel slag: Steel slag is a by-product manufactured during the steelmaking process. It's the waste material formed when the impurities are removed from molten iron. Composed of magnesium oxide, calcium oxide, and silica, steel slag is usually granulated for easier handling. Its high density and hardness make it resistant to wear and tear, ideal for applications like concrete aggregate, and asphalt. By employing steel slag, the consumption of natural resources such as sand and gravel is minimized, leading to their conservation. Additionally, it aids in waste management by providing a meaningful purpose for an industrial by-product. Frequently, steel slag proves to be more cost-effective than conventional construction materials, rendering it a compelling choice for extensive projects. Enhanced characteristics of concrete: By substituting a portion of the cement content, steel slag can increase the strength, durability, and resistance to freezing and thawing of concrete. (Kang, et. al, 2024)

Figure 1.4. Steel slag

Carbon Fibre (CF): The incorporation of carbon fibre (CF) into construction materials has emerged as a promising strategy for the development of next-generation composites. CF reinforcement offers a unique opportunity to synergistically enhance the mechanical performance of cementitious matrices while simultaneously introducing electrical conductivity. This paves the way for the exploration of multifunctional building elements with embedded functionalities such as de-icing capabilities, electromagnetic shielding, or even self-heating properties. The ability to tailor the electrical conductivity of CF-reinforced composites opens doors for innovative applications in building design. For instance, conductive composites could be strategically incorporated into structures to provide efficient

de-icing capabilities in cold climates, thereby enhancing safety and reducing maintenance costs. Furthermore, the inherent electrical conductivity of CF presents intriguing possibilities for the development of "smart" construction materials with integrated sensor capabilities for real-time structural health monitoring. Such advancements could revolutionize preventative maintenance practices and improve the overall safety and longevity of structures. However, significant research efforts are still required to optimize the CF-matrix interface to achieve the desired balance between enhanced electrical conductivity and robust mechanical performance. Achieving this balance is crucial for ensuring the structural integrity of the composite material while enabling the desired electrical functionalities. Additionally, addressing the scalability and cost-effectiveness of large-scale CF-reinforced composite production remains a crucial challenge for their widespread adoption in the construction industry. Overall, CF presents a fascinating avenue for advancing the functionality and performance of construction materials, but further research is necessary to overcome these critical considerations for successful implementation.

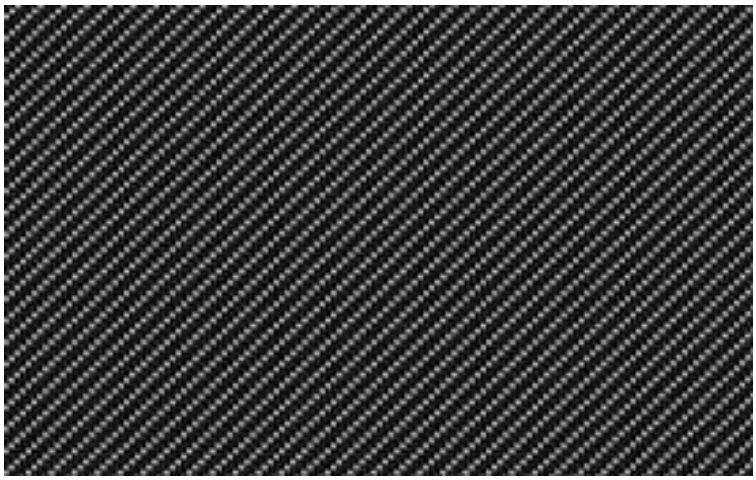

Figure 1.5. Carbon fibre

1.6. Measurement of sensing signal of cement mortar composite

Piezo resistivity, electrical resistivity, dielectric constant, conductivity, and capacitance are a few methods that can be used to evaluate how responsive concrete is (Han, et al., 2015). Reliability in measuring sensitivity can be achieved by employing electrical resistance, also known as resistivity. Variations in temperature, damage, or stress can all impact a cement-based composite's electrical resistivity. The conductivity of the fibers inside the material can also have an impact. Electrodes composed of the right materials are used to evaluate

electrical conductivity in various configurations (Han, et al., 2015). Three things need to be thought through before selecting an electrode: design, placement location, and substance. The material should possess two essential characteristics: a minimal electrical resistance and a consistent conductive property. The electrodes can be attached to the surface of the composite, implanted into the composite to a significant depth, or arranged in a clipping arrangement. Out of these options, embedding and attaching are the two most frequently used approaches. Experiments can be conducted utilizing either a two-probe technique or a four-probe setup, where both electrodes serve as the current and voltage terminals (Han, et al., 2015).Unlike the two-probe method, the four-probe technique utilizes inner probes to measure voltage and exterior probes to detect current. Two-probe technique is more accurate and easy to carry as compared to four-probe technique (Figure 1.6). The four-probe method is commonly used to accurately measure low resistance values because of its extraordinary precision in producing accurate results (Han, et al., 2015).

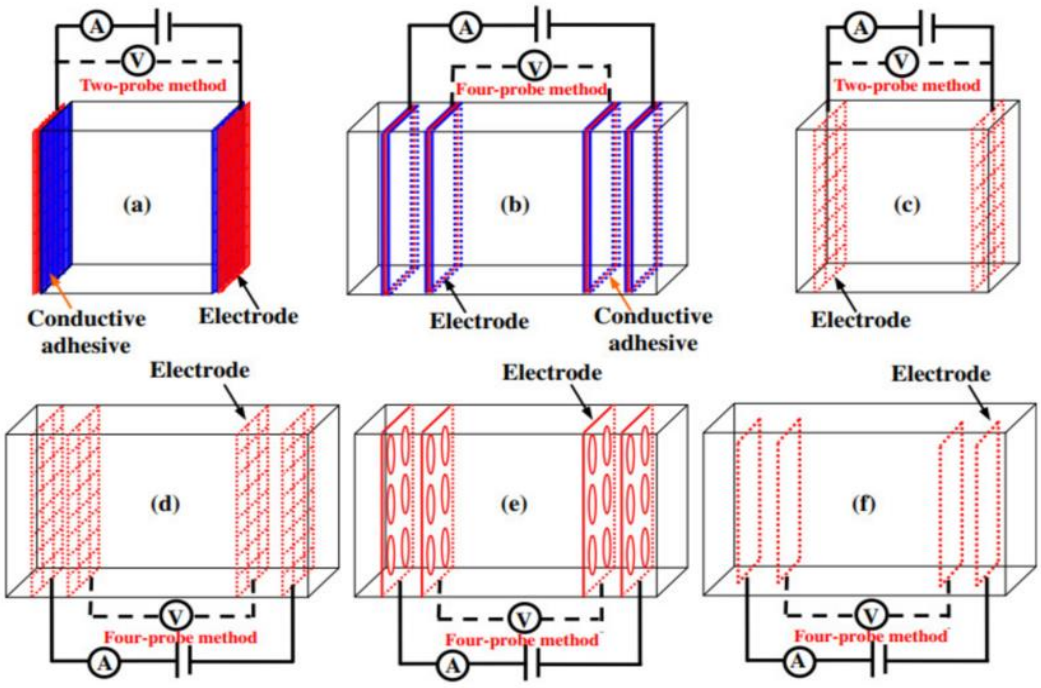

Figure 1.6 Setting the electrode configuration and style in self-sensing (a, b): surface mounted electrode; (c-f): embedded mesh, perforated plate, or loop electrode. (Han,et al.,2015)

1.7. Electrical Resistivity

While resistance is influenced by a material's electrical properties, it is also dependent on its size and shape, such as length. To compare the conductivity of different materials objectively, regardless of their geometry, electrical resistivity (measured in Ohm-m) is a crucial parameter. It essentially captures the intrinsic resistance of a material. Since resistivity is the ratio of resistance to length (as shown in Equation 1.1), it serves as a standardized metric for evaluating a material's ability to conduct electricity. This allows for a more accurate comparison of conductivity between different materials, including cementitious composites.

$$\rho = \frac{RA}{L} \qquad 1.1$$

Where, A (m^2) represents the cross-sectional area, whereas the variable l (m) represents the distance between two voltage electrodes. Electrical conductivity, denoted by σ (S/m), is a quantitative measure of a material's ability to conduct electric current. It is the inverse of electrical resistivity. Equation 1.2 may be used to articulate the conductivity in correlation to resistivity.

$$\sigma = \frac{RL}{A} = \frac{1}{\rho} \qquad 1.2$$

1.8. Piezo Resistivity

Piezo resistivity is the phenomenon where a material's electrical resistivity changes when mechanical strain is applied. This is distinct from the piezoelectric effect, where an applied force generates a voltage. In piezo resistivity, the external force alters the material's band structure and carrier mobility, ultimately affecting its conductivity. The piezo resistance coefficient is a material property that dictates the extent and direction of the resistivity change under stress. It can be positive (piezo resistance) or negative (piezo conductivity), depending on the material and the type of stress applied. The Fractional change in Resistivity (FCR) is a measure of stress/strain value in a piezo-resistive sensor.

The FCR is defined as the ratio of the initial electrical resistivity to the change in electrical resistivity. The FCR is used as an indicator of stress & strain sensing since it reacts proportionally and reversibly to the observed strain by a sensor (wang & zhang, 2022).

$$\mathbf{FCR}\ (\%) = \frac{\boldsymbol{\rho 1 - \rho 0}}{\boldsymbol{\rho 0}}\boldsymbol{X100}\ = \frac{\boldsymbol{\Delta \rho}}{\boldsymbol{\rho 0}}\boldsymbol{X100}$$

1.9. Aim and Objectives of the work

The aim of the study is to create self-sensing cementitious (SSC) composites by including by-products of industrial based materials, such as copper slag, LD slag as sand replacement for smart structural health monitoring. The objectives of the planned research may be summarized as follows:

- To study the influence of addition of copper slag and LD slag on the mechanical properties of cementitious composite.
- To create copper slag and LD slag based self-sensing cementitious sensor that can monitor stress generating in concrete
- To analysis the electrical characteristics of copper slag and LD slag which includes electrical resistivity and piezo-resistivity.
- To evaluate performances of developed bulk form reinforced mortar beam as a sand replacement with copper slag and LD slag.

1.10. Organisation of thesis

Chapter 1 – Introduces Structural Health Monitoring (SHM) and SSC composites and explores several kinds of materials with their respective characteristics.

Chapter 2 – Focuses on the different researcher's studies on various conductive fillers, including copper slag, LD slag, carbon fibre, silicon powder and carbon nanotubes. The chapter explores the impact of these conductive fillers in self-sensing characteristics, such as electrical resistivity and piezo-resistivity, as well as other mechanical properties.

Chapter 3 – Provides an explanation of an experimental design, encompassing the utilized materials and aspect taken into account. This chapter also presents a depiction of mortar mixture design.

Chapter 4 – Provides the findings and evaluation of the mechanical properties, namely compressive and flexural strength. This chapter provides a more in-depth analysis of the discoveries of electrical properties, namely electrical resistivity and piezo resistivity.

Chapter 5 – Provides a summary and conclusion of the study's results, and discusses the potential future directions of the research.

CHAPTER 2

LITERATURE REVIEW

2.1. General

This chapter focuses on the extensive research conducted by numerous authors over the years about the characteristics of Copper Slag, LD slag, Steel fibres, Carbon nanotubes (CNTs) and Carbon fibre (CF) when added to cementitious composites. Two main categories were established based on the analysis of qualities: mechanical properties and self-sensing characteristics. Self-sensing involves analysing the main sensing mechanism using piezo resistivity and electrical resistivity. Mechanical attributes include compressive and flexural strength.

2.2. Effect of industrial by-products on mechanical Properties on cementitious composites

Singh, et al., (2023): The rise in industrialization and urbanization has resulted in the over exploitation of natural resources such as river sand and coarse aggregates, necessitating the search for sustainable alternatives in the manufacturing of concrete. Linz-Donawitz (LD) slag, which is a by-product of steel making, has become a promising alternative because of its plentiful availability and positive impact on the environment. Research has demonstrated that substituting fine particles with LD slag can improve the compressive strength of concrete. For example, replacing up to 50% of fine aggregates with LD slag in Normal Strength Concrete (NSC) and 25% in High Strength Concrete (HSC) has resulted in improved mechanical qualities when compared to traditional mixtures. The rough surface texture of LD slag enhances the stronger bonding with cement paste. The increased water absorption and non-uniform particle shape of LD slag can decrease the workability of concrete. Moreover, it enhances the endurance of the material by creating a more condensed and tightly packed mixture, particularly when used at the recommended levels of substitution as shown in figure 2.1. Consequently, there is a decrease in sorptivity coefficients and an improvement in abrasion resistance. Using LD slag in concrete not only decreases the requirement for natural aggregates but also tackles the environmental concerns linked to slag disposal. It facilitates sustainable development by reducing waste and promoting the circular economy. Utilizing LD slag in concrete mixtures provides a practical

approach for sustainable building, improving both the mechanical and durability characteristics while reducing environmental effects.

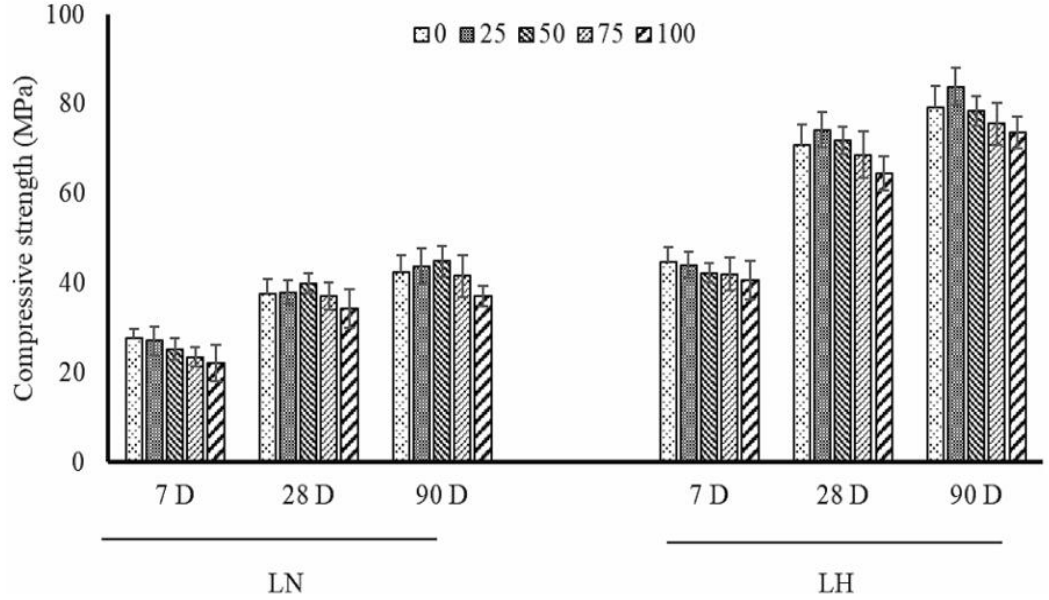

Figure 2.1. Compressive strength for NSC and HSC mixes
Singh, et al., (2023)

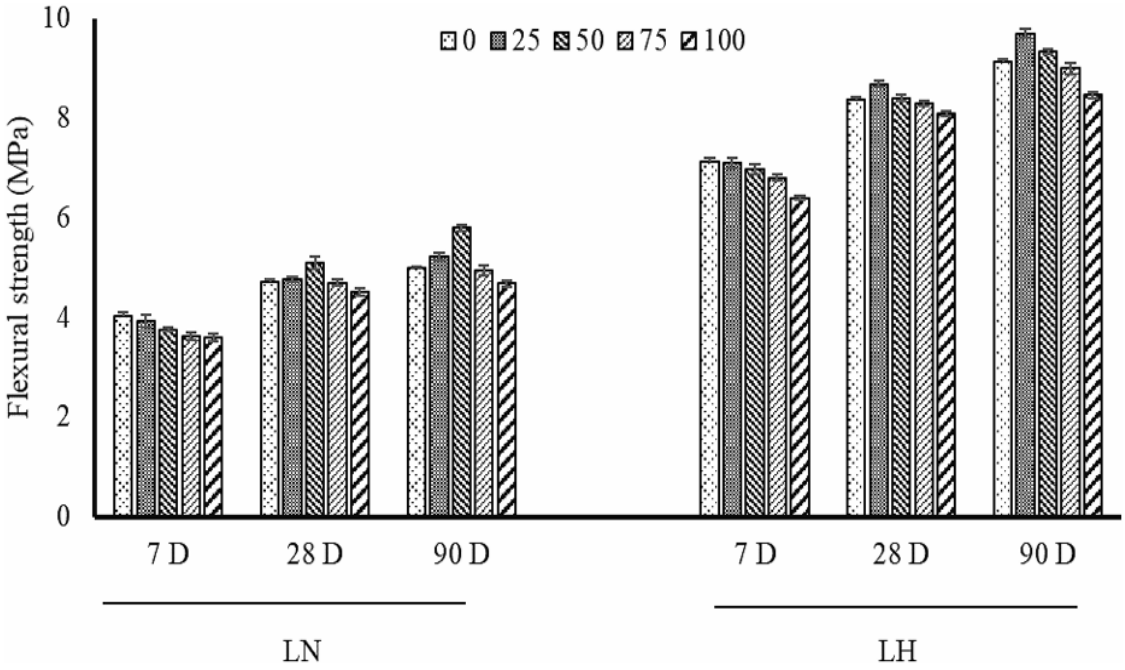

Figure 2.2. Flexural strength for NSC and HSC mixes
Singh, et al., (2023)

The study examined the utilization of LD slag in NSC and HSC as substitutes for fine aggregates. The findings indicated that including LD slag up to 50% in normal strength concrete (NSC) and up to 25% in high strength concrete (HSC) caused changes in the microstructure of the concrete, resulting in increased compressive strength and enhanced flexural strength as shown in figure 2.2. The incorporation of LD slag also led to enhanced interconnections with adjacent particles, resulting in elevated MOE values. Increased slag content also intensified drying shrinkage, concrete expansion, micro-cracks, and pores, facilitating greater water evaporation. The condensed mixture produced by LD slag led to reduced sorptivity coefficients.

Gupta, et al., (2019): Copper slag, a by-product of the copper manufacturing industry, has been successfully utilized as a substitute for a portion of the fine aggregates in self-compacting concrete (SCC). Research has shown the inclusion of copper slag improves the compressive strength, and splitting tensile strength of self-compacting concrete. Studies suggest that the workability of SCC enhances as the proportion of copper slag increases, glass-like texture and minimal water absorption. The compressive strength and splitting tensile strength exhibit an increase up to a specific percentage of copper slag substitution shown in figure 2.3 and figure 2.4. The development of calcium silicate hydrate gel in self-consolidating concrete mixes including copper slag has been confirmed by the use of methods like SEM, EDS, and XRD, leading to improved micro-structural properties.

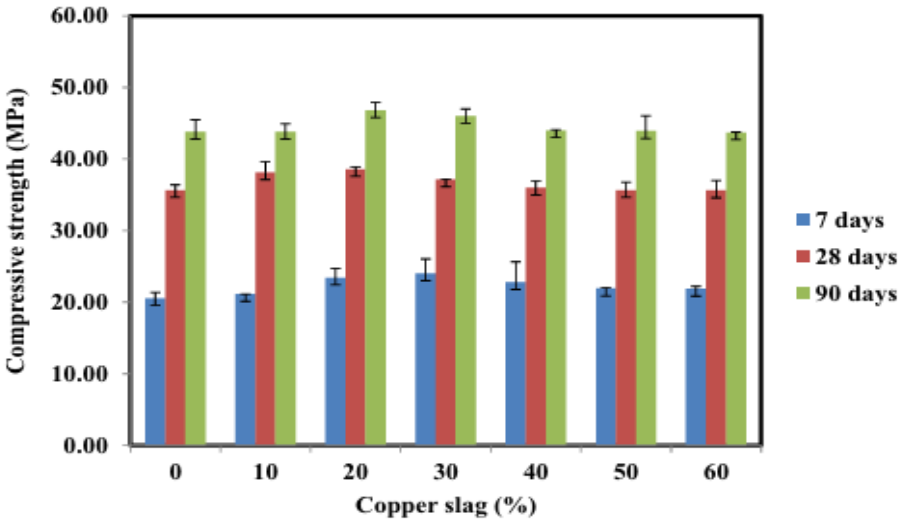

Figure 2.3. Compressive strength of SSC mix.
(Gupta, Siddique at el., 2019)

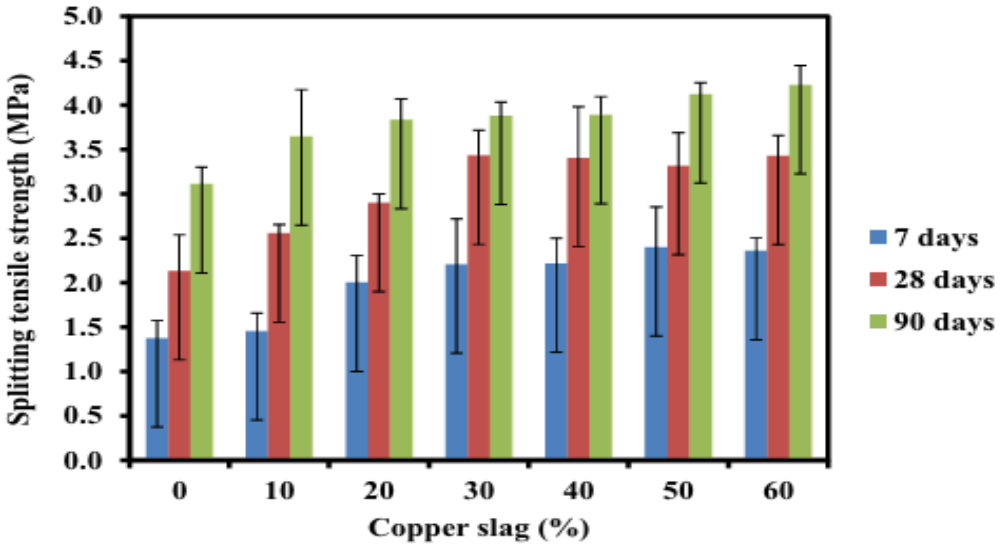

Figure 2.4. Splitting-tensile strength of SSC mix
(Gupta, Siddique et al., 2019)

Gupta, et al., (2020): The usefulness of copper slag in self-compacting concrete (SCC) with regard to its fresh and hardened properties was investigated in this study. In this investigation, copper slag was substituted for natural sand in different ratios, ranging from 0% to 60%, with a 10% increment. In addition, fly ash was added to replace 20% of the cement content. Every other characteristic, including the ratio of water to cement and the quantity of super plasticizer, remained unchanged. Consequently, compressive strength testing was done to evaluate the mechanical characteristics of SSC that can be seen in figure 2.5.

The research investigated if adding up to 30% copper slag to mixes of self-compacting concrete (SCC) might significantly increase their compressive strength throughout all time periods. After 28 days, the control concrete's compressive strength rose from 35.63 MPa to 37.13 MPa when a 30% copper slag self-compacting concrete (SCC) mix was applied. In the same way, after 90 days and 365 days, respectively, the strength of the 30% copper slag SCC mix improved from 43.78 MPa to 46.00 MPa and from 45.56 MPa to 47.43 MPa. The concrete matrix's bonding was improved by the slag particles' sharp edges. Between the seventh and the twenty-eighth day, the compressive strength increased at the fastest pace. The SCC mix with 60% copper slag was determined to have lowest compressive strength. At any of the curing ages, its strength did not drop below that of control concrete.

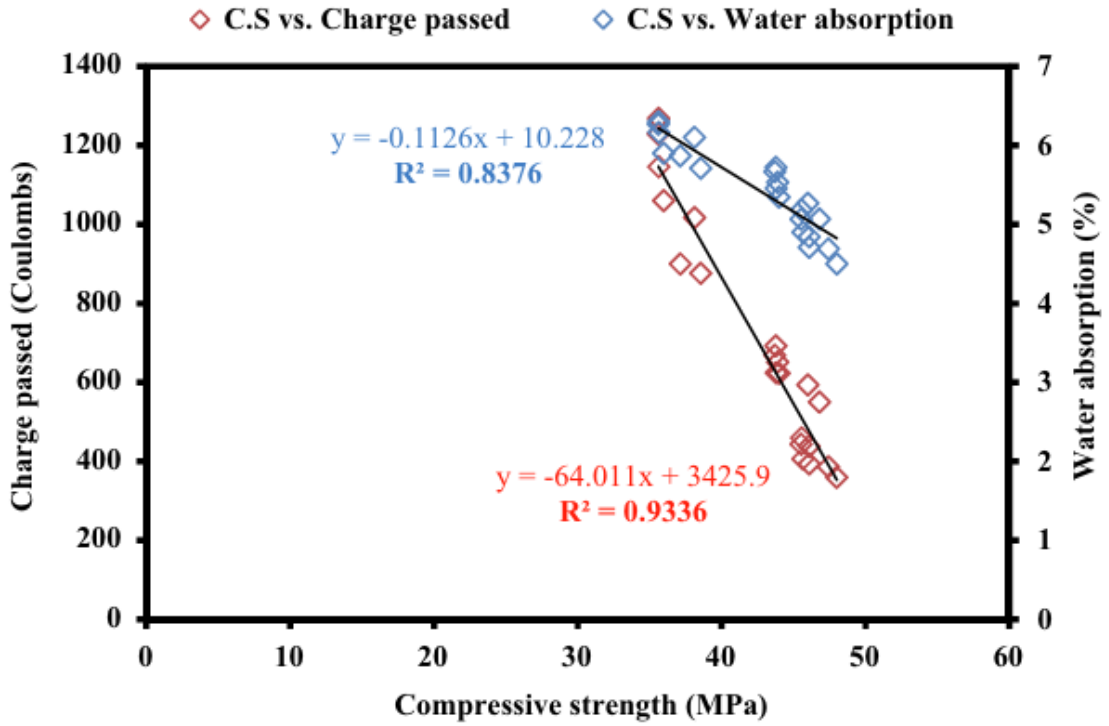

Figure 2.5. Correlation of compressive strength of SCC with charge passes and water absorption Gupta, (Siddique et al., 2020)

Singh, et al., (2022): Experimentally investigated the level of LD Slag that should be used to replace coarse aggregates. At the ratios of 25, 50, 75, and 100 percent, coarse aggregates were substituted with Linz-Donawitz Slag. This study tested a variety of mechanical and durability qualities, including but not limited to the following: hardened concrete density, ultrasonic pulse velocity, compressive strength, split tensile strength, flexural strength, modulus of elasticity, drying shrinkage, water absorption, sorptivity, and abrasion resistance. Compressive strength tests and Ultrasonic Pulse Velocity (UPV) were carried out on cubes of dimensions 150 mm at 7, 28, 90 days of water curing that can seen in figure 2.9. Flexural strength was carried out on 500 x 100 x 100 mm prisms at 7, 28, 90 days. Modulus of elasticity and Split tensile strength tests were carried out on cylinders of 150 mm diameter and 300 mm length and is cured for 7, 28, 90 days.

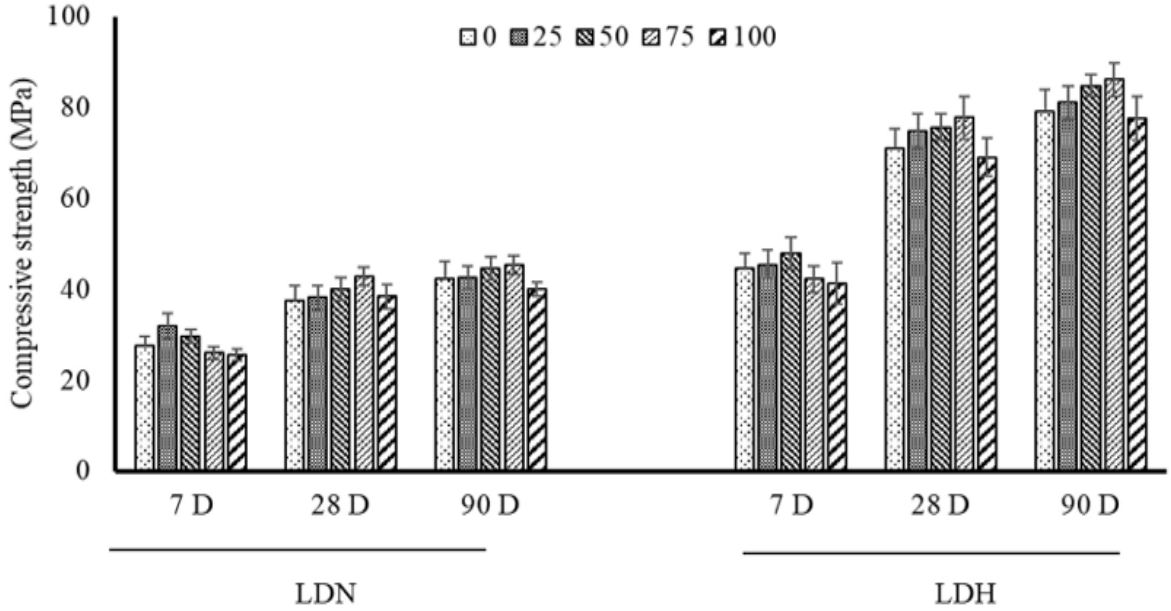

Figure 2.6. Compressive strength at different testing stages (Singh, et al., 2022)

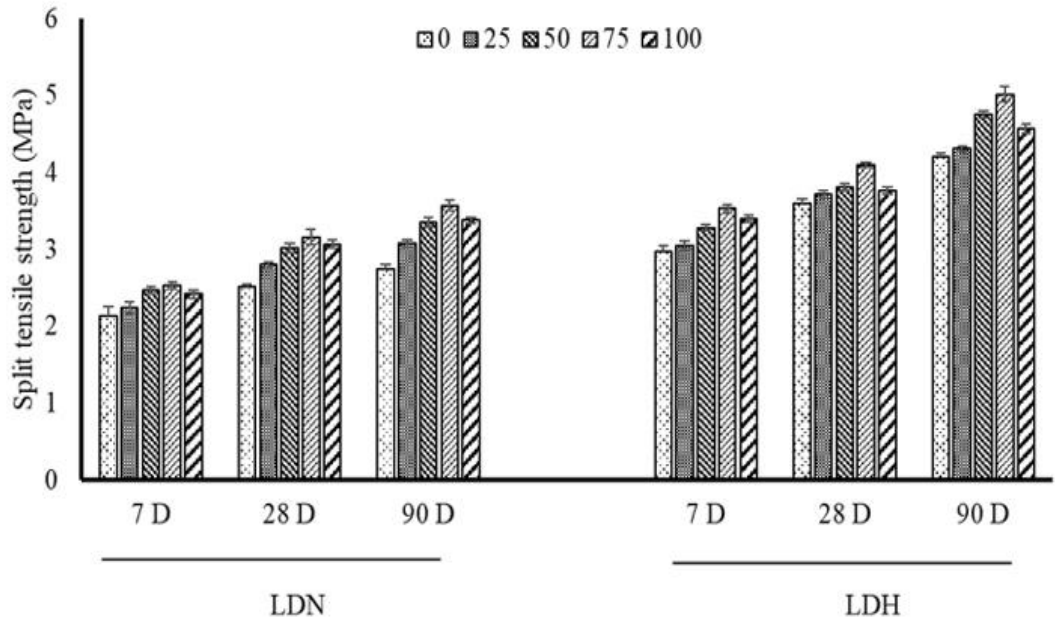

Figure 2.7. Split tensile strength at different stages (Singh, et al., 2022)

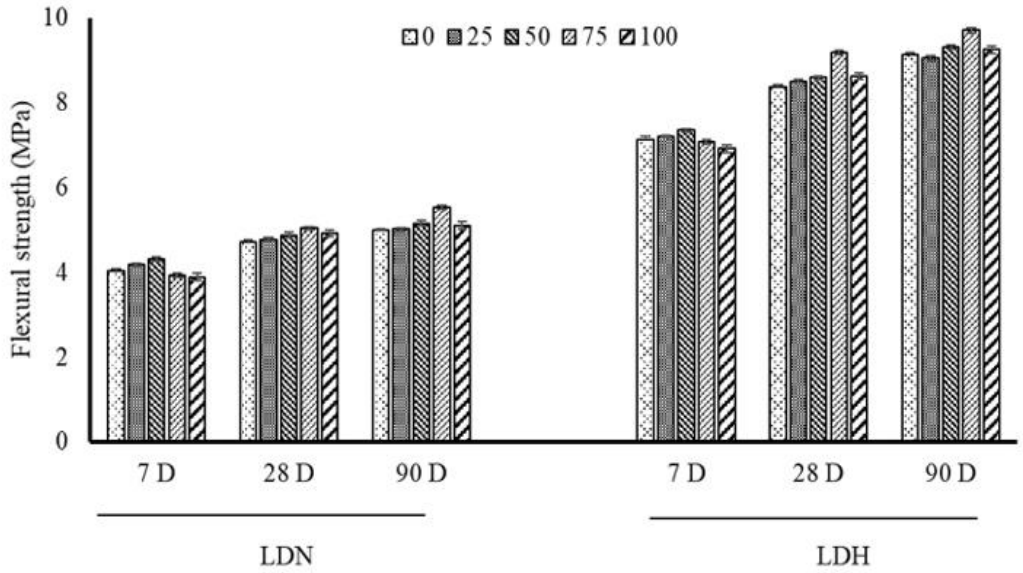

Figure 2.8. Flexural strength at different stages (Singh, et al., 2022)

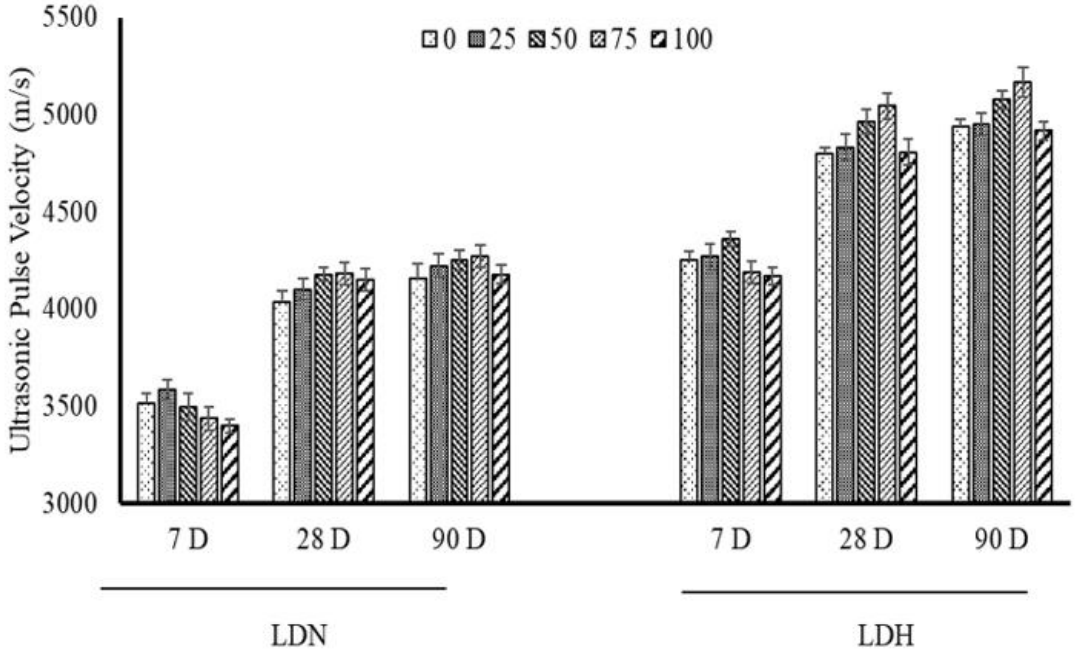

Figure 2.9. Ultrasonic Pulse Velocity at different testing ages (Singh, et al., 2022)

The study on normal concrete and high strength concrete containing LD slag found that LD Slag has superior mechanical characteristics as compared to natural coarse aggregates. However, it also experiences volumetric expansion because of the presence of CaO. Higher the content of LD slag, decreases workability because of its coarse surface and increases the

concentration of concrete due to its greater specific gravity. The substitution of 75% of the LD slag with coarse aggregates determined to be the most effective for both types of concretes figure 2.6 and figure 2.7. After 90 days, the concrete samples containing 75% LD Slag exhibited a 2-5% increase in pulse velocity, resulting in decreased porosity and improved surface characteristics. The compressive strength showed a rise ranging from 7 to 9%, while the split tensile strength and flexural strength also improved. The improved interfacial transition zone (ITZ) between the aggregates made from LD slag and the cement paste played a significant role in these enhancements.

Ren, et al., (2022): The materials examined in the study were extent to which fine aggregate was replaced with copper slag, and nano-graphite. The water to cement ratio was maintained at 0.43. The proportion ratio of the copper slag replacement were 0%, 20%, 40%, and 60% and proportion ratio of nano-graphite (NG) were 3%, 6%, and 9% respectively. The following treatment approaches were employed in this research:

- The chemical activation method
- Ultrasonic vibration
- Combined activation

Concrete samples underwent unconfined compressive strength and flexural strength tests to determine the effect of conductive fillers on the mechanical properties of the material. In order to perform the compressive test, 129 cubic design samples with 50 mm of edge length were created and allowed to cure for 7, 14, and 28 days, respectively. Moreover, specimens 40 × 40 × 160 mm in size were made especially for the experiment on flexural properties.

This study examines the mechanical characteristics of concrete with nano-graphite and copper slag modified using ECCC. The findings indicate that the addition of nano-graphite greatly enhances the electrical conductivity of concrete. However, the impact on mechanical qualities decreases once the concentration above 3%. A recommended NG percentage of 3% is advised to fulfill the mechanical and electrical requirements of ECCC. The inclusion of copper slag greatly enhances the mechanical strength and conductivity of ECCC, exhibiting a direct correlation with its concentration. At 28 days, the resistivity of copper slag drops considerably from 503000 Ω·cm to 19840 Ω·cm, a decrease of 95%, after copper slag content increases from 0% to 20% without the addition of NG figure 2.10. Chemical activation improves the mechanical characteristics of materials by using sodium hydroxide

to enhance the volcanic reaction action of the fly ash-cement system. Utilization of ultrasonic vibration enables the even dispersion of particles, hence enabling the integration of nano-graphite and copper slag to occupy voids in conductive concrete network and enhance its mechanical characteristics. The combined activation method is the most effective approach for enhancing both conductivity and mechanical properties can be seen in figure 2.11. The specimen consisting of 60% copper slag and 3% NG combination activated ECCC exhibited the maximum UCS and flexural strength.

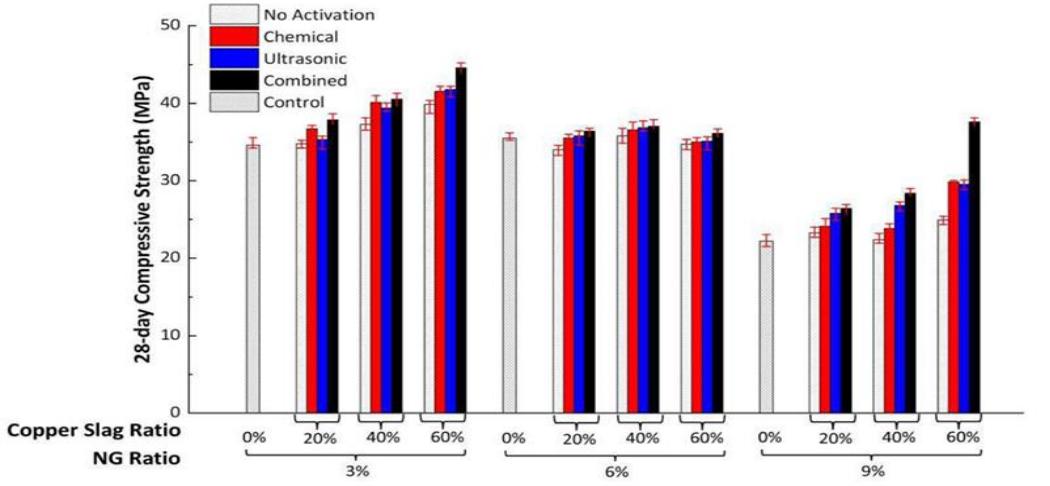

Figure 2.10. Effect of activation approaches on UCS, specimens containing copper slag and nano-graphite. (Ren, et al., 2022)

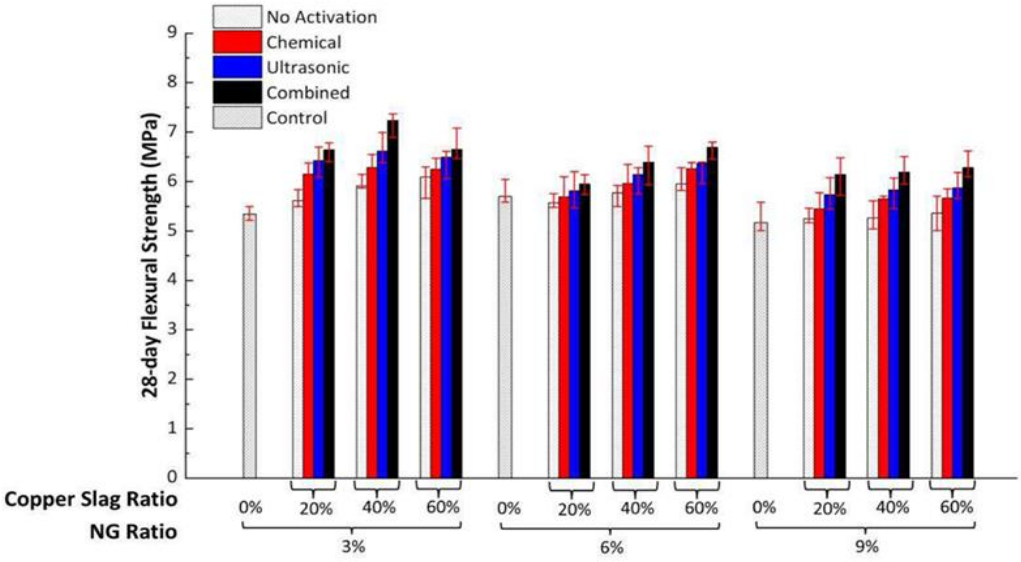

Figure 2.11. Effect of activation approaches on UCS, specimen containing copper slag and nano-graphite. (Ren, et al., 2022)

Xu, et al., (2024): Development of Ultra high performance concrete (UHPC) has been significant advancement in construction materials, known for its exceptional mechanical properties. However, research into more sustainable alternatives has been prompted by its high cost and environmental impact, because of its greater durability and smaller carbon footprint, geopolymer concrete (GPC), which is created by polymerizing industrial by-products like fly ash and ground granulated blast furnace slag (GGBS), has become a promising green substitute figure 2.12. The goal of recent research has been to improve Ultra-High Performance Geopolymer Concrete's (UHPGC) performance through the use of different industrial wastes. Steel slag a by-product of steel industry that contains CaO, SiO_2, and $Al3O_3$.

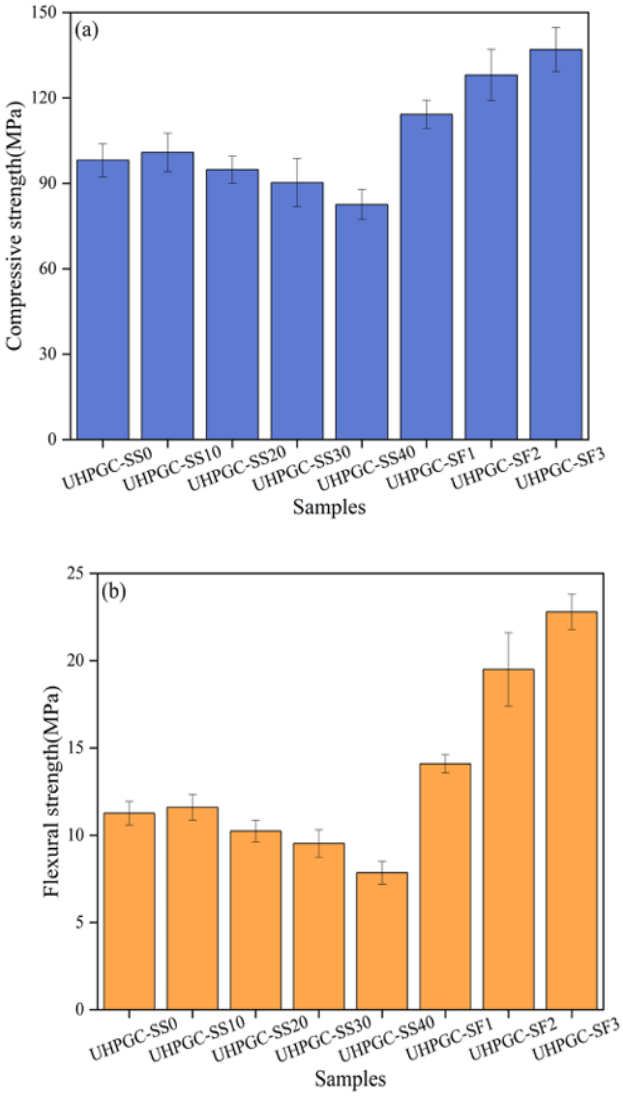

Figure 2.12. Effect on mechanical performance with different steel slag and steel fibre dosage: (a) compressive strength, (b) flexural strength. (Xu, et al., 2024)

Because of this, it has been suggested as a possible precursor material. Steel slag has been shown in studies by Piro et al. (2022) and Zhu et al. (2023) to enhance the mechanical characteristics and durability of UHPGC, but its low reactivity makes early strength development difficult. Furthermore, it has been demonstrated that adding steel fibres greatly improves UHPGC2's mechanical strength and toughness. Aisheh et al. (2021) found that adding 3% steel fibre could result in a 53% increase in compressive strength and a 22% increase in splitting tensile strength, albeit at the expense of less flowability.

Overall, the incorporation of steel slag and steel fibres into UHPGC not only encourages the use of industrial waste but also advances the creation of high-performing, environmentally friendly building materials. Optimal dosage of about 10-20% steel slag and 2% steel fibres improve flexural and compressive strength while maintain flowability. The environmental benefits of using industrial waste materials in UHPGC are substantial, promoting sustainability in construction. Future research should explore higher steel slag dosages and different curing methods to further optimize UHPGC's performance and environmental impact.

2.3. Effect of industrial by-products on self-sensing behaviour

Rehman, et al., (2018): The percentage change in resistance was determined using electrical resistivity tests. The self-monitoring ability of the control specimen and cement mortar incorporating nano Fe2O3 is under investigation. It was found that the nano Fe2O3 cement mortar exhibited greater sensitivity in monitoring tension compared to the control specimen, which was shown to be ineffective in monitoring its own stress. Instead of focusing solely on resistivity, they discovered that the key to self-sensing lies in a fractional alteration in resistance. The FCR (Fineness and Consistency Ratio) for the control cement mix exhibited a very low value. The addition of 15% carbon black and 3% nano FE203 resulted in an increase in the FCR, or strain sensing characteristics.

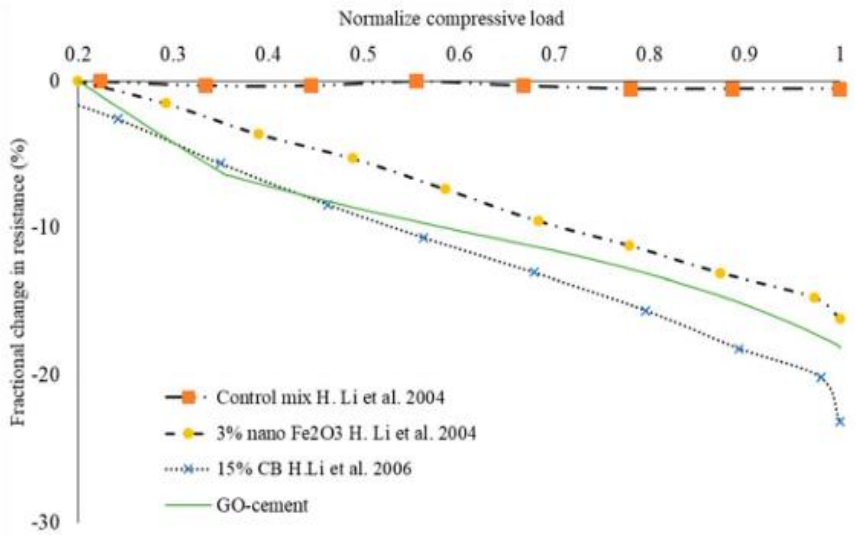

Figure 2.13. Fractional change in resistance against normalized compression load for various samples (Rehman, et al., 2018)

This study shows the potential of using copper slag into self-compacting concrete (SCC) mixes, which is a safe material, to enhance the workability and strength characteristics. The compressive strength of self-compacting concrete (SCC) mixes improved by up to 30% when 30% of the copper slag was used as a replacement. Similarly, the split tensile strength increased by up to 60% with the same substitution. The increase in strength is due to the presence of sharp corners on the grains of copper slag, which facilitate the bonding of the concrete mixture. A marginal reduction in strength was noted in self-compacting concrete (SCC) mixes containing above 30% copper slag, whereas SCC mixes with 40% copper slag exhibited the presence of ettringite crystals as shown in figure 2.13.

Sarwary, et al., (2019): The present research on self-sensing investigations use small specimens without the use of steel reinforcement, which might lead to damage to the structures being monitored. Chen incorporated carbon fibres into the concrete to create combinations that can detect faults by measuring changes in electrical characteristics, which are linked to the strain conditions during loading. Multiple studies have investigated the most effective techniques for mixing electrically conductive substances into cement-based matrices. These investigations have aimed to identify the ideal amounts required to establish a seamless conductive network. A research has been carried out on the self-sensing characteristics of infrastructures under various loading conditions, utilizing reduced-scale samples such as cylindrical, cubic, and prismatic shapes. This study aims to fill this void by

assessing the performance of large-scale reinforced mortar beams that have been enhanced with either carbon fibres or multi-walled carbon nanotubes when subjected to flexural pressure.

Preliminary tests were conducted to precisely sense the damage during four-point loading using electrical measurements. Carbon-based materials (CF) were chosen for their self-sensing properties, and a thin PVC cling film protected the connections between the specimens and the loading heads of a universal testing apparatus. Electrical measurements were obtained from electrodes that were implanted within beam specimens. Brass plate electrodes were selected for their ease of embedding and their ability to provide satisfactory sensing outcomes. The mortar mixes were cast in the same direction as the embedment direction of the electrodes, and the electrodes had sufficient stiffness for easy embedment. The electrical properties of the specimens were assessed by employing an alternating current (AC) technique with a two-probe configuration and a direct current (DC) technique with a four-probe configuration. The AC technique proved to be more effective in capturing electrical measurements in comparison to the DC strategy using the four-probe method. The electrodes were placed directly beneath the tension side of the specimen, in alignment with the loading heads of the universal testing apparatus, to get the most accurate measurements of electrical properties. The study determined that in order to enhance the ability to detect damage based on changes in electrical characteristics, it is necessary for concrete systems to have a high level of electrical conductivity. Additionally, the applied load should reach a specific threshold to induce actual damage in the conductive network as shown in figure 2.14. Electrical data were obtained from electrodes positioned closely beneath the loading heads of the universal testing apparatus throughout the investigation.

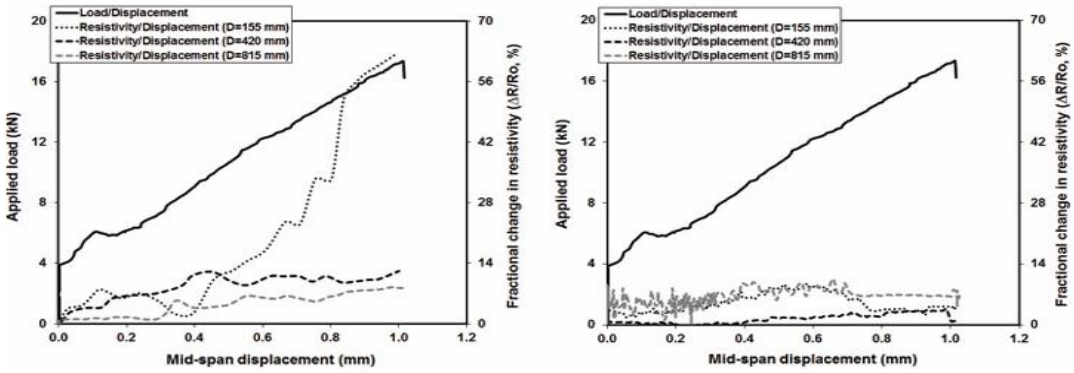

Figure 2.14. (a) Self-sensing behaviour with AC-2 probe setup (b) DC-4 probe setup (Sarwary, Yildirim at el., 2019)

The study assesses the mechanical and structural properties, as well as the self-sensing ability, of large-scale reinforced beam samples. These samples contain either chopped carbon fibres (CF) or multi-walled carbon nanotubes (CNT). The evaluation is done by subjecting the samples to four-point bending stress. The beams containing carbon fibre (CF) experienced failure when subjected to bending, exhibiting a ductile response. On the other hand, the specimens containing carbon nanotubes (CNT) displayed increased brittleness and rigidity, along with a reduced capacity for dissipating energy. Both beams exhibited successful self-sensing capabilities when the level of damage inflicted was minimal. Nevertheless, after a specific threshold was reached, the relationship between the ability to sense and the occurrence of harm became less consistent for specimens containing CF. When it comes to processing large amounts of mortar mixtures, it is recommended to utilize CFs because they are more cost-effective, easier to mix in dense cementitious systems, and have better overall performance.

Ding, Liu et al., (2019): This study investigates the mechanical and self-monitoring capabilities of concrete beams reinforced with steel fibre (SF), carbon black (CB), and carbon fibre (CF) when exposed to bending forces. This study examines the impact of using multiphase conductive materials on two aspects: the compressive strength of the concrete and the link between load, deflection, and fractional change in impedance (FCI) of the concrete beam. The study additionally examines the correlations between FCI and crack opening displacement (COD) as well as sensitivity (gauge factor). A forced mixer is used for mixing. The compressive strength of 100mm cube specimens is measured after 28 days. The specimens used for bending testing are rectangular beams measuring 100mm x 100mm x 400mm. The beams are then removed from the molds 24 hours after being cast and subsequently subjected to ambient conditions (25°C) with a relative humidity of 100% for a duration of 28 days to facilitate curing. The impedance is determined through the utilization of the four-electrode-AC technique, wherein four different types of conductive glue, labelled as A, B, C, and D, are employed as electrical contacts. Contact A and D, which are spaced 190mm apart, are intended for conducting alternating current with a frequency of 50Hz. On the other hand, contacts B and C, which are spaced 100mm apart, are used for measuring voltage. The purpose of Voltmeter equipment V1 is to measure the voltage between the inner contacts B and C figure 2.15 and figure 2.16. V2 is utilized to measure the voltage across the fixed resistor (RF). The current is determined by measuring the voltage drop across the

fixed resistor, which allows us to compute the electrical impedance between the inner contacts of the specimen using Ohm's law.

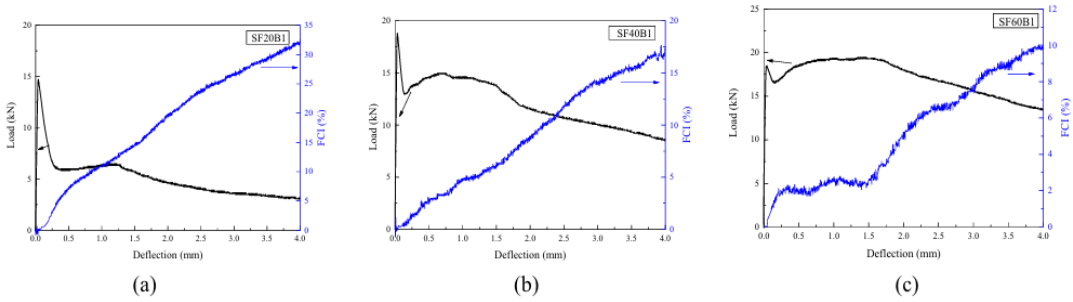

Figure 2.15. Load-deflection-FCI Relationships (a) SF20B1, (b) SF40B1, (c) SF60B1 (Ding, et al., 2019)

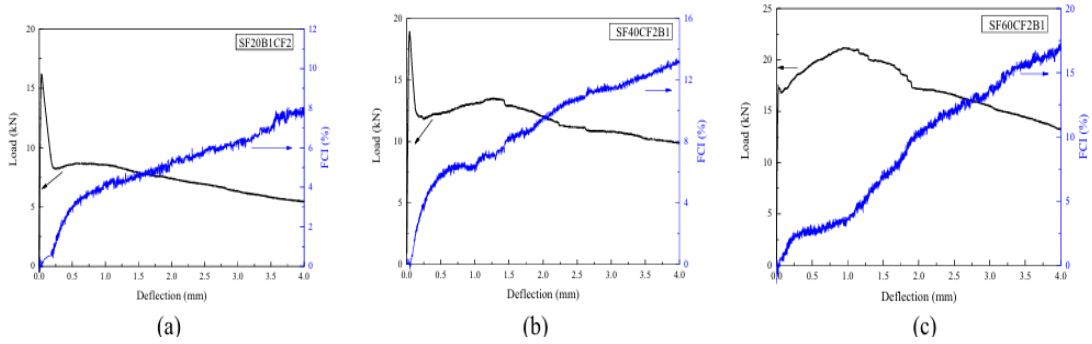

Figure 2.16. Load-Deflection-FCI Relationship (a) SF20B1CF2, (b) SF40B1CF2, (c) SF60B1CF2 (Ding, et al., 2019)

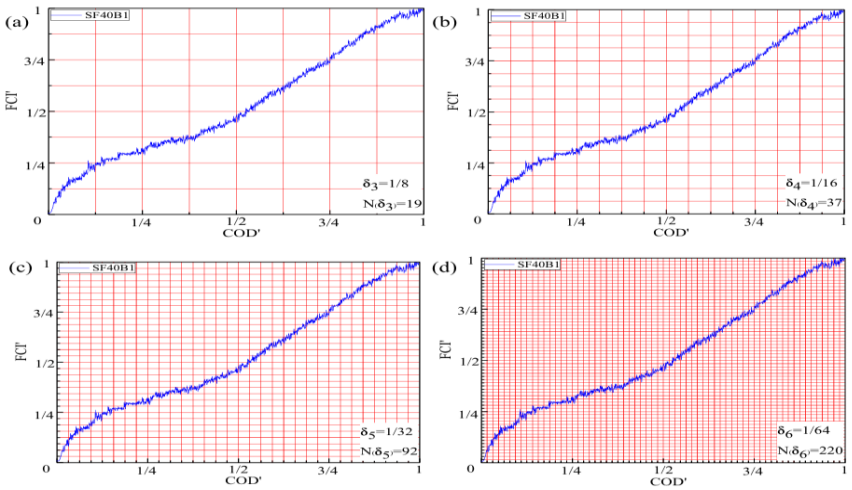

Figure 2.17. Normalized FCI-COD (FCI'-COD') curve covered with different grid sizes (Ding, et al., 2019)

Steel fibres are essential for the enhanced durability and ability of conductive concrete to withstand repeated cracks. The load bearing capacity decreases significantly at initial cracking, resulting in an increase in the FCI of all beams can be seen in figure 2.17. An upward tendency is detected in specimens with one or more cracks, following a bi-linear pattern. The fractal dimension can be used to examine the noise signals, and beams without carbon compounds exhibit higher noise signals. Carbon black and steel fibres can enhance the self-sensing capability of concrete.

Tian, et al., (2019): The construction material used in self-sensing concrete is combined with an electrically conductive infill material. It is possible to monitor stress, deformation, and damage with this novel material since it can sense changes in its electrical characteristics when exposed to outside forces. Many advantages come with the sensor, including its high sensitivity, long lifespan, excellent compatibility, mechanical strength, durability, and minimal maintenance costs. Applications like weight in motion, traffic identification, parking management, and monitoring the health of structures could all benefit from its use. The mechanism of self-sensing concrete, its production process, and each component's makeup and purpose are all thoroughly reviewed in this study.

Self-sensing concrete achieves its functionality through the piezo resistive effect of the filler material that is spread within the matrix material. Due to the non-conductive nature of the concrete matrix, the conductive filler has a significant influence on the electrical properties of self-sensing concrete. These electrically sensitive particles disperse randomly in the matrix, creating a conductive network within the concrete matrix that depends on the concentration of the filler. External loading can significantly alter the network created within a specific range of filler content, known as the percolation threshold.

When producing self-sensing concrete, the dispersion material can assist in achieving a homogeneous mixture with the filler, resulting in a more responsive electrical conducting network within the composite. It is evident that NaDDBS is commonly employed in the dispersion of nano-scale fillers, such as CNT, with the assistance of a sonication method and an anti-foam admixture. Unlike other fibrous fillers, carbon black has greater flexibility when disseminated in cement composites. A water reduction agent, sometimes known as a superplasticizer, can effectively disperse these substances using a simpler method.

Self-sensing concrete is created by incorporating micro or nano-scale filler components into the concrete, enabling it to sense changes in stress, strain, and damage. This technique is

essential for civil structures such as dams, bridges, power plants, and high-rise skyscrapers. Compared to standard embedded electrical components, it provides the advantages of low maintenance cost, real-time monitoring, and continuous monitoring. Researchers are investigating filler materials such as carbon fibre, carbon nanotubes, carbon black, steel fibre, nickel powder, graphene oxide, and graphene Nano platelets in order to identify cost-effective options. Ongoing study is primarily concerned with the structural elements of mortar and concrete, as the properties of the coarse aggregate can have an impact on their sensing capabilities. The dispersion material is crucial in enhancing electrical qualities, while it can also result in adverse effects such as air entrainment and breakage of fibres or nanotubes as shown in figure 2.18. Subsequent research will prioritize the assessment of the dependability of this composite material, given the intricate nature of concrete, which undergoes constant alterations in its microstructure, durability, mechanical characteristics, and exposure to environmental variables.

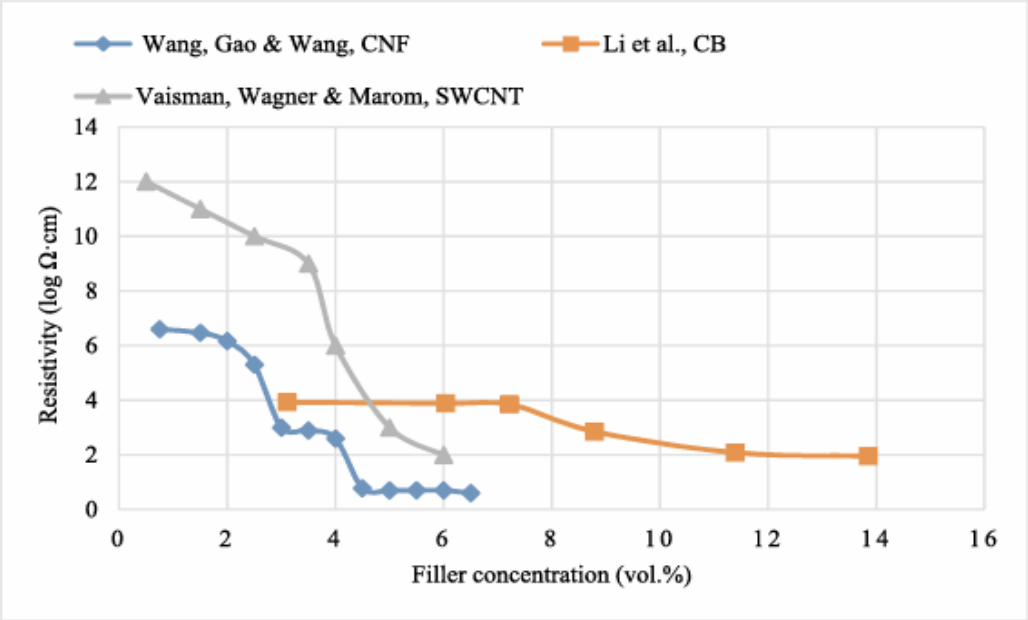

Figure 2.18. Relationship between initial resistivity and filler content (vol%). (Tian, et al., 2019)

Dong, et al., (2021): The electrical resistivity of cementitious composites lacking conductive GNP was comparable to that of normal cement paste. However, only cementitious composites containing GNP were subjected to piezo resistivity testing. The alteration in electrical resistivity and compressive strain. The objective is to analyse the behaviour of a cementitious composite when subjected to compressive stress in order to

ascertain. Piezo resistive response to different loading rates and magnitudes. The fractional changes in resistivity and strain varied in direct proportion to the magnitude of the loading. The values at the stress peaks were fitted using a linear model, and the square deviation of the fitting curves was displayed. The parameters R12 and R22 represent the fractional change in resistivity and compressive strain, respectively. The variations in loading rates and magnitudes of the compressive cycles resulted in square deviations of 0.999 and 0.992, indicating that these the resistivity change figures exhibited a remarkable linear correlation with the compressive stress, regardless of their loading rates and magnitudes. Moreover, it was revealed that compressive strain of the specimen exhibited a similar level of linearity as the compressive stress. Nevertheless, the relationship between fractional fluctuations in resistivity is less linear, exhibiting larger deviation with values of 0.991 and 0.970, respectively. The cumulative microdefects in the cementitious material. The nonlinearity may be explained by the composite effect resulting from each compression. Table 1 presents the square. The variation of the cementitious composites under various stress levels, as determined by linear analysis. Regression analysis is used to demonstrate the impact of stress magnitude. It was determined that the linearity of fractional changes in resistivity and compressive strain deteriorated when subjected to low levels of stress. Higher stress magnitudes result in larger magnitudes. This could potentially be associated with cementitious materials. The unstable porosity architectures and microstructures of composites result in changes to their conductivity. Routes and opposition to the flow of electricity. The electrical resistivity undergoes small changes under low stress conditions, and the fractional changes of resistivity (FCR) are easily influenced by resistivity variations resulting from unstable constructions can be seen figure 2.19. Conversely, high FCR levels are considerably more stable and free from disruptions caused by unstable variations in resistivity under high-stress situations. It can be concluded, that the cementitious composite is better suitable for assessing compressive strength.

Table 2.1. Square deviation of cementitious composite under stress magnitudes (Dong, et al., 2021)

Group	Square deviation	Ranges of stress magnitudes		
		$0 \leq \sigma \leq 5$ MPa	$5 \leq \sigma \leq 10$ MPa	$0 \leq \sigma \leq 10$ MPa
1% GNP and 2% SHP	R_1^{2*}	0.998	0.999	0.999
	R_2^{2*}	0.989	0.998	0.991
2% GNP and 2% SHP	R_1^2	0.993	0.994	0.992
	R_2^2	0.966	0.999	0.970

Note: R_1^2 means the square deviation of the FCR; R_2^2 represents the square deviation of compressive strain

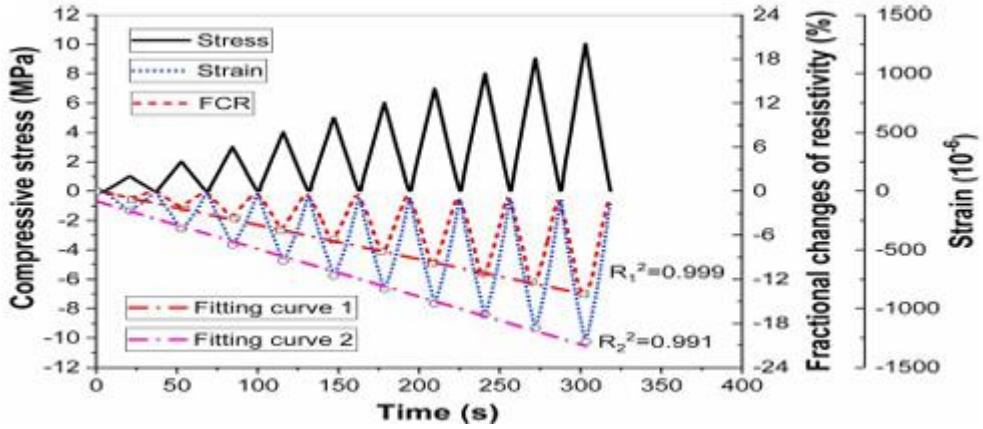

(a) With 1% GNP and 2% SHP

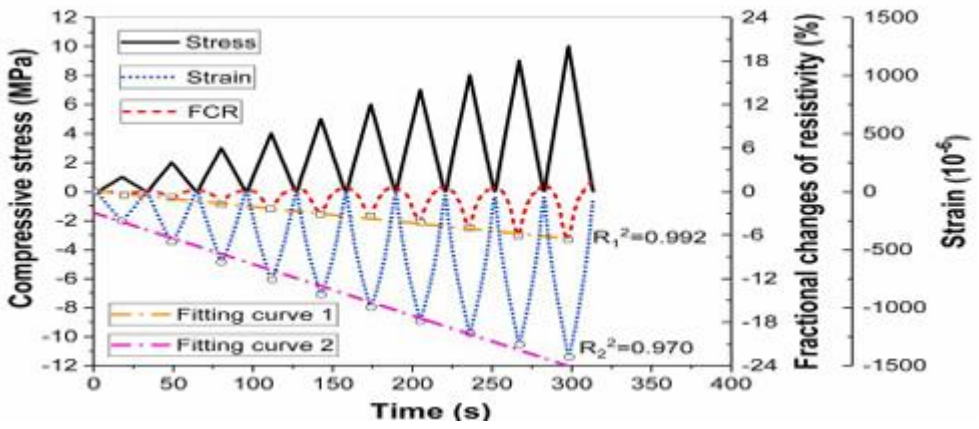

(b) With 2% GNP and 2% SHP

Figure 2.19. FCR as a function of compressive stress and strain of cementitious composite with 2% SHP (Dong, et al., 2021)

Wang, Zhang et al., (2022): Recent advancements have led to the development of self-sensing cementitious composites, which includes the functional filler like carbon fibre (CFs), carbon nanotubes (CNTs), and graphene nano plates (GNPs) to form conductive paths. These composites offers good mechanical properties, high sensitivity, and durability at a lower cost compared to conventional sensors. The synergistic effect of combining different fillers, such as 1D CNTs and 2D GNPs has shown to enhance the mechanical and electrical properties of cementitious composites. Studies have shown that hybrid fillers improve signal quality, reliability, and sensitivity. For instance, Azhari and Banthia (2012) reported enhanced piezo-resistivity in composites with hybrid CNTs/CFs. The hybrid combination of GNPs (graphene nano plates) and CNTs (carbon nanotubes) exhibits exceptional mechanical characteristics, electrical conductivity, and piezo resistivity because of their distinctive architectures. The composites demonstrate substantial enhancements in stress and strain sensitivity, rendering them well suited for structural health monitoring (SHM) applications. Nevertheless, there are still obstacles to overcome in order to achieve consistent distribution of these additives throughout the cement matrix as shown in figure 2.20.

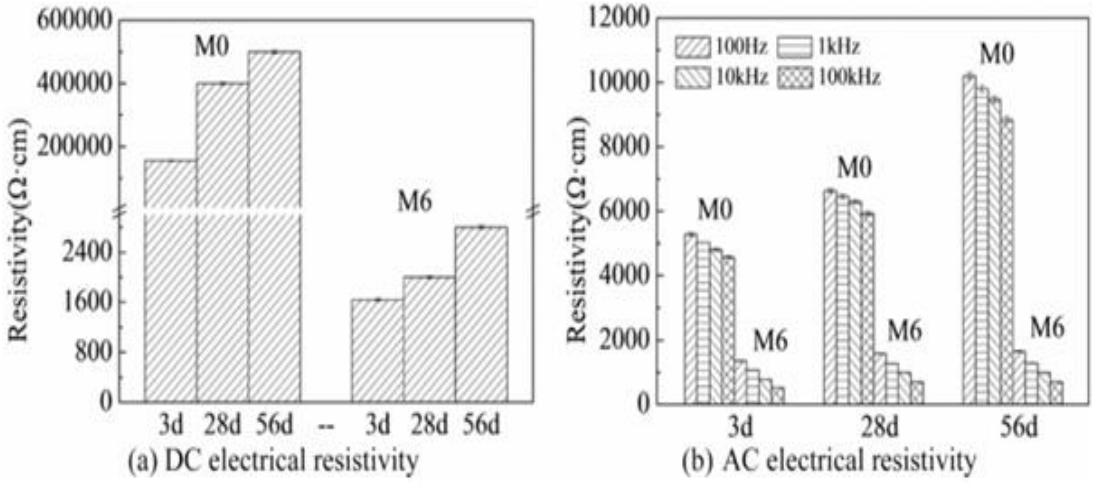

Figure 2.20. Electrical resistivity of cementitious composite containing GNPs/CNTs (Wang, Zhang et al., 2022)

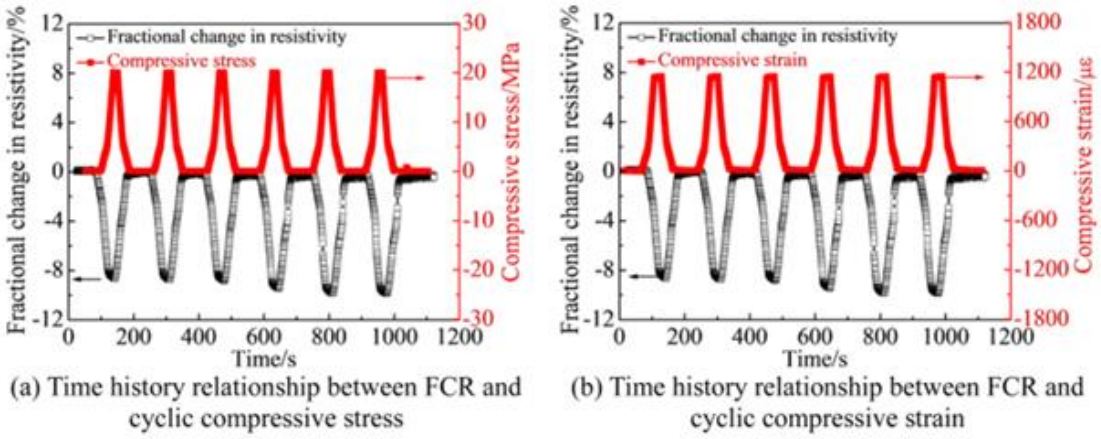

Figure 2.21. Time history relationships between FCR and cyclic compressive stress/strain of M6 (Wang, Zhang et al., 2022)

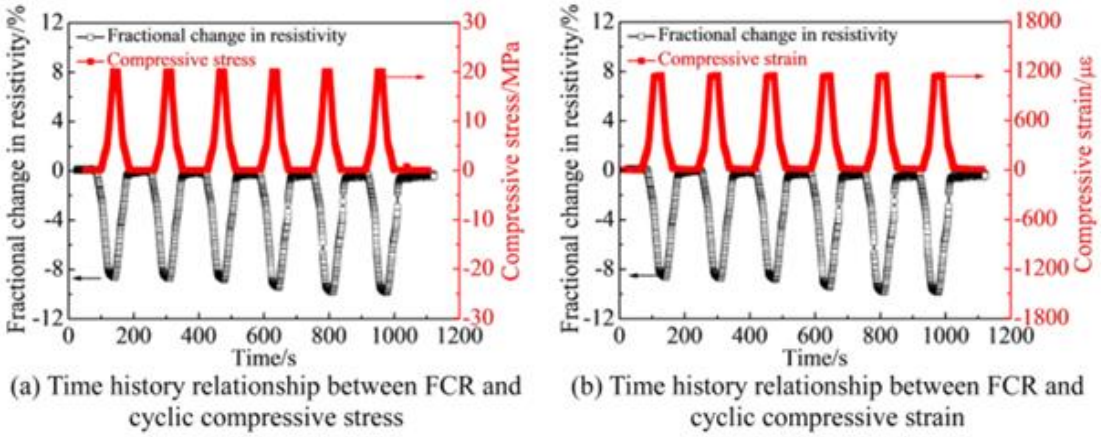

Figure 2.22. Time history relationships between FCR and cyclic compressive stress/strain of M0 (Wang, Zhang et al., 2022)

The use of hybrid GNPs and CNTS in cement-based composites signifies a promising progress in structural health monitoring technology. These composite materials have a dual function: they act as both structural components and sensors figure 2.21 and figure 2.22. This makes them a cost-effective and long-lasting option for monitoring the condition of civil infrastructures.

Saldarriaga, Montoya at el., (2021): Conventional non-destructive testing (NDT) techniques such as visual inspection, ultrasonic, and infrared thermography necessitate human involvement and are expensive. SHM provides ongoing monitoring using permanently placed sensors, resulting in cost reduction and enhanced reliability. These materials, such as cement-based composites containing carbon nanotubes (CNTs), have the ability to support heavy loads and offer ways to detect and respond to damage figure 2.23.

Carbon nanotubes (CNTs) exhibit exceptional mechanical and transport capabilities, making them highly promising. The majority of research concentrate on large-scale construction, which is not economically efficient. Practical solutions for existing infrastructures can be found in alternative such as coatings and embedded sensors figure 2.24. Self-sensing composites can detect damage through changes in electrical resistance, making them suitable for SHM applications.

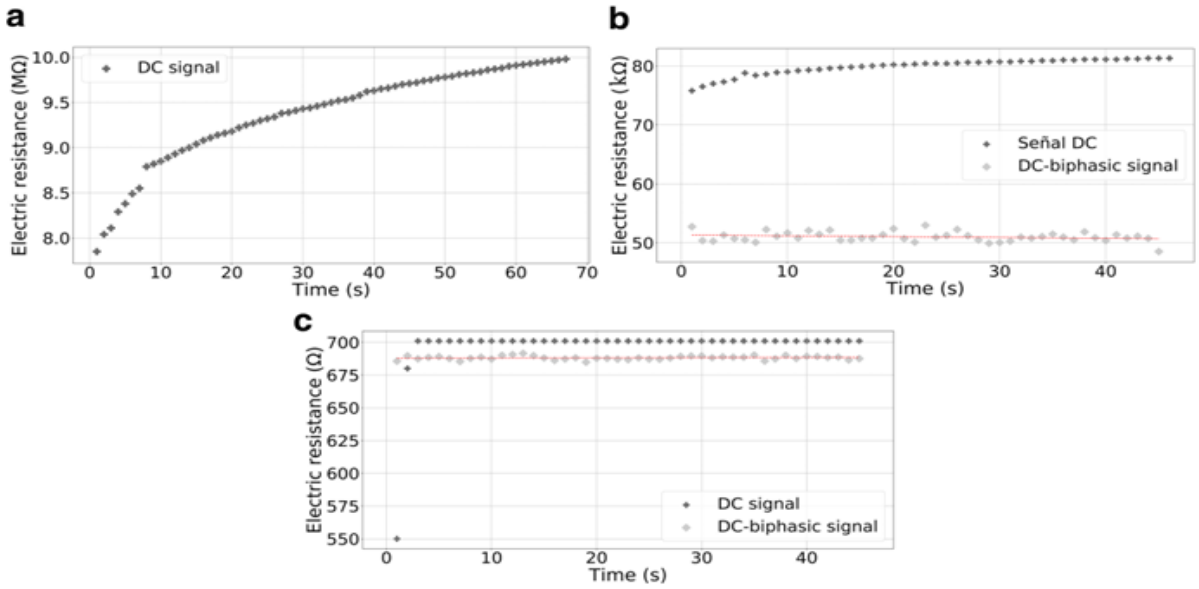

Figure 2.23 Comparison using DC and BDC for samples of (a) 0.2%wt of CNTs, (b) 0.5%wt, (c) 0.8%wt (Saldarriaga, Montoya at el., 2021)

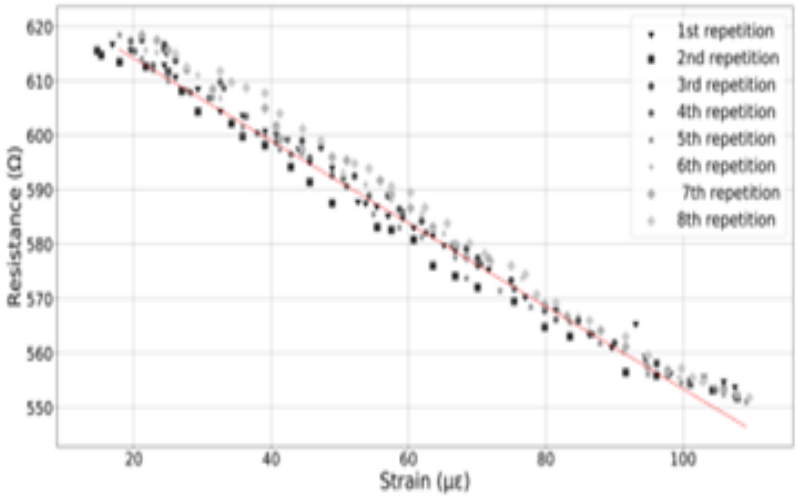

Figure 2.24. Piezo-resistivity phenomenon characterization for sample with 0.8%wt of CNTs (Saldarriaga, Montoya at el., 2021)

2.4. Summary

Based on many review papers on electrical properties on electrical characteristics such as piezo-resistivity, electrical resistivity, and stress sensitivity, it is evident that there is very minimum research done on the electrical properties of Copper slag and LD Slag. This thesis has experimental self-sensing tests on different materials such as Copper slag and LD slag and of different amount of replacements of river sand.

2.5. Research Gaps

- There is limited research done using Copper slag and LD slag to make the concrete self-sensing
- The study of the piezo resistive ability of cement containing Copper slag and LD slag is still uncommon.
- Most of the work is done using the nano materials, which is not economical in the construction.
- Nano materials has been used for the bulk form of SSC, not the by-products of the industry, which may have good electrical characteristics.
- The construction sector is yet to explore potential using SSC in areas such as corrosion monitoring and fracture identification.

CHAPTER 3

EXPERIMENTAL DESIGN AND METHODOLOGY

3.1. General

The aim of the experimental investigation is to examine the characteristics of cement mortar when different proportions of Copper slag and LD slag were added. An analysis were conducted on the self-sensing characteristics, which includes electrical resistivity and piezo-resistivity and further on its mechanical parameters. This chapter covers the essential assessments of cement mortar.

3.2. Materials Used

3.2.1. Ordinary Portland Cement Grade 43 (OPC-43)

Ordinary Portland cement (Ultratech make) of Grade 43 (OPC-43), which met the requirements of BIS code IS 8112-1989 (Reaffirmed 2005), was used in the tests. The cement was made from same batch. The manufacturer provides the details about OPC-43, which are shown in the following Table 3.1 below:

Table 3.1 Physical characteristics of OPC-43 used

Physical characteristics	**Values as per IS 8112-1989**
Initial setting time (minutes)	Not less than 30
Final setting time (minutes)	Not less than 600
Fineness (%)	10 max
Specific Gravity	3.15 max

3.2.2 River Sand

River sand that comply with grading Zone II of IS 383:1970. The river sand was initially sieved using a 4.75 mm sieve, and particles larger than 4.75 mm were eliminated.

3.2.3. Water

Water is a crucial element in experimental research. This serves the purpose of both casting and mixing. It must be free from acidic, chloride, sugar, oil, and organic substances. Tap water was utilized in this experimental study.

3.2.4. Steel reinforcement

High yield strength bars of Fe550 were using comply with the IS 800:2007 standards having diameter of 12mm were used in tension and compression steel whereas 8mm bars were used for stirrups.

3.2.5. Superplasticizer

Superplasticizers are the additives in the concrete to improve its workability while retaining its strength. Superplasticizers, when used in the correct dosage, can increase the flow ability of concrete mixtures, making it easier to place and compact the material. Increasing the recommended dosage of superplasticizer can result in various adverse consequences. The superplasticizers used in the combination was MasterGlenium 51. MasterGlenium 51 is an advanced admixture that incorporates a modified polycarboxylic ether as its primary ingredient. The product has been specifically engineered for utilization in high-performance concrete applications that require optimal durability and performance. MasterGlenium 51 is chloride-deficient and has a low alkali concentration. It is compatible with all types of cements without exception.

3.2.6. Copper Plates

The electrical characteristics has been tested by using four copper plates of the dimensions of (70 x 20mm) for the cube moulds of the size of (50 x 50mm) at the distance of 10mm between them and for the prism of size (160 x 40 x 40mm), two copper plates, separated by 20mm each, are positioned 80mm apart with the other two copper plates. The specifications of the plates used can be seen below in Table 3.3.

Table 3.2. Specifications details of Copper plates

Specimen type	Size of plates (mm)	Number of plates in each specimen	Spacing (mm)
Cube	70 x 20	4	10
Prism	70 x 20	4	20

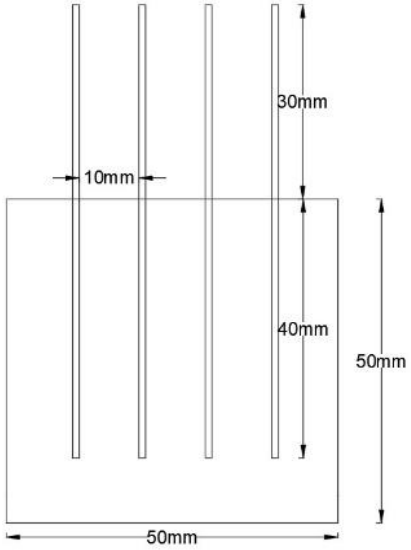

Figure 3.1(a) Cube with copper plates embedment

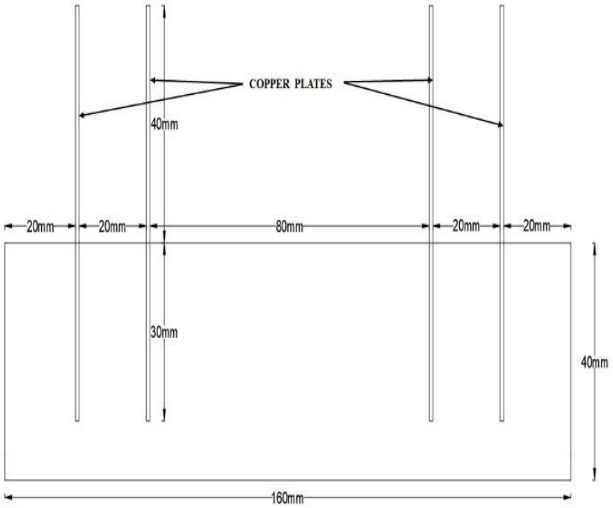

Figure 3.1 (b) Prism with copper plates embedment

Figure 3.2. Copper plate's embedment in cube and prism samples

3.2.7. Copper Slag

Copper slag, a residual material produced during the copper refining process, is obtained by separating impurities that rise to the surface of the molten metal during smelting. When submerged in water, it forms angular granules that can either be discarded as waste or utilized in grit blasting and landfill applications. Copper slag, when used as a fine aggregate, has been discovered to be more environmentally friendly than standard Portland cement. Additionally, it greatly improves the ability of cement mortar to withstand abrasion.

3.2.8. LD Slag

LD slag is a molten by-product that is formed during the refining process of steelmaking in a Basic Oxygen Furnace (BOF) or LD converter. It separates from the purified metal. The high calcium oxide concentration, which ranges from 42% to 50%, together with other inorganic components such as SiO2, Al2O3, FeO, Fe2O3, and MnO, make it well suited for construction purposes due to its hardness and ability to act as a cement. Nevertheless, the presence of a significant amount of phosphorus restricts its applicability in sectors such as ironmaking and cement manufacture. LD slag can serve as a conductive filler in specific applications because of its metallic phases, which enhance electrical conductivity when distributed inside a conductive matrix.

Table 3.3. Physical characteristics of Copper and LD slag

PROPERTY	COPPER SLAG	LD SLAG
Appearance	Black, Glassy Texture	Angular, Irregularly Shaped
Specific Gravity	3.11	2.04
Water absorption (%age)	0.36	4.5
Unit weight (kg/m^3)	2000	2114

3.3. Batching, Mixing and Casting of Specimens

3.3.1. Cement mortar samples with LD and Copper slag

Samples of mortar were created with 1:3 cement-to-sand ratio in accordance with ASTM C-109 guidelines. Replacement ratios of LD slag and copper slag were 20%, 25%, 30% and 25%, 50%, 75% respectively.

Table 3.4. Mix proportions of cementitious cube specimens with Copper and LD slag

No. of mix	C/S Ratio	W/C Ratio	SP (by weight of cement)	Copper slag %
Mix 1	1:3	0.42	0.2	25
Mix 2	1:3	0.42	0.2	50
Mix 3	1:3	0.42	0.2	75

No. of Mix	C/S Ratio	W/C Ratio	SP (by weight of cement)	LD slag %
Mix 1	1:3	0.485	0.8	20
Mix 2	1:3	0.485	0.8	25
Mix 3	1:3	0.485	0.8	30

3.3.2. Casting of Specimens

The moulds were cleaned and greased before the process of casting. Screws were tightened properly with accurate measurements before casting. By carefully determining the optimum proportions of components, we utilized 50x50x50mm moulds to measure the compressive strength and piezo resistivity of the specimens. Utilizing moulds with dimensions of 40x40x160mm as specified in the (IS 4031-Part 6) standard, samples will be prepared for measuring flexural strength and electrical resistivity.

Therefore, casting involves the following process:

- River sand and different proportions of LD and Copper slag was exactly weighed beside cement.
- Properly cleaned tools were used in the mixing process.
- Operate a mortar mixer machine at a low rpm to thoroughly mix dry cement and sand for a duration of 60 seconds.
- To create a homogeneous composition, superplasticizer (MasterGlenium 51) of corrected amount was mixed with the different proportions of Copper and LD slag sand replacements in a mortar mixer.

Figure 3.3. Digi mixer for preparing the mix

- Ultimately, the mortar mixer was programmed to operate for an additional 120 seconds at high rpm. Each batch's components were managed separately.

- Cubes and prisms composed of varying LD and copper slag proportions will undergo electrical resistivity and mechanical properties including compression and flexural test evaluations at curing ages of 7, 28, and 56 days post-casting. Additionally, piezo-resistivity characteristics will be conducted on 28 and 56 days of cured specimens.

Figure 3.4. Casting of Cubes & Prism

3.3.4. Design mix proportions for reinforced concrete beam

The beam specimens were casted using M25 concrete mix by IS code along with the use of properties of materials that were discussed earlier. High yield strength bars of Fe550 were using comply with the IS 800:2007 standards having diameter of 12mm were used in tension and compression steel whereas 8mm bars were used for stirrups.

By casting of beams in bulk form, we hereby have used 20% of the proportion for LD slag and 25% of copper slag as a sand replacement for the beam casting maintaining 0.485 and 0.42 water/cement ratio and 0.2 and 0.8 of the super plasticizer (MasterGlenium 51) of cement. Reducing the use of natural resources like river sand is crucial for preserving the environment and helping to save the future availability of natural resources. We can assess their impact on the concrete's mechanical properties such as compressive strength and flexural strength. Comparing the performance of concrete made with these different

proportions of LD and copper slag with control mix sample can help determine potential economic benefits.

To enable self-sensing within the tension zone of a concrete beam, a conductive path is established by incorporating conductive waste by-products, i.e. LD and copper slag into the mortar mix. Embedded copper plates within the beam will subsequently monitor and record the induced strain and stress variations.

3.3.5. Casting of reinforced mortar beams

In this experimental study, two beams were designed following IS 456:2000. Beams have same cross-sectional dimensions of 150mm x 150mm. The length of the beam was 700mm was casted with twelve copper plates of dimensions 150 x 50mm were placed in the beam casting. These plates were arranged in three groups of four. The first and the third group were positioned symmetrically at 70mm from each beam end, with plates spaced at 40mm intervals. The second group was in centre within the beam, with groups of plate were at 100mm from each other. Casting of beams with LD and copper slag allows determining the self-sensing behaviour of the beam as well as the performance of these materials as a replacement for river sand in mortar mix.

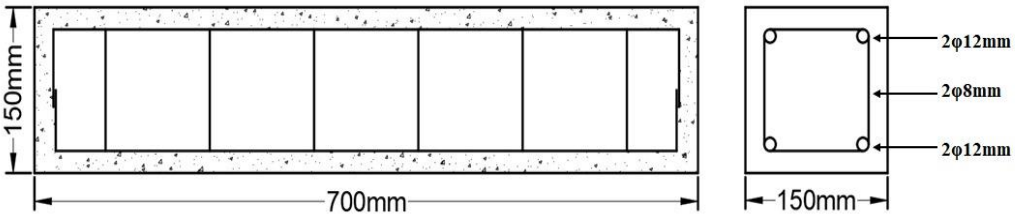

Figure 3.5. Longitudinal Detailing; cross-sectional view of beam specimen

In preparation for casting; the moulds for the beam were properly cleaned, bolted, and greased. A rotary concrete mixer was used for mixing of materials. At first, the process of dry mixing involved combining the sand and cement in the mixer until a uniform mixture was obtained. Subsequently, a fraction of the necessary quantity of water was incorporated to attain a consistent mixture. The concrete mixture was poured into molds in two separate stages. A vibrator was used to achieve compaction during the casting procedure. This

process is performed in order to eliminate any voids of air from the recently poured concrete and guarantee a uniform and even surface.

Following concrete casting, the de-moulding process was completed after one day and the specimens were prepared for curing in water tank. For specimens to reach their maximum strength, they were cured for 28 days.

Figure 3.6. Beam after casting

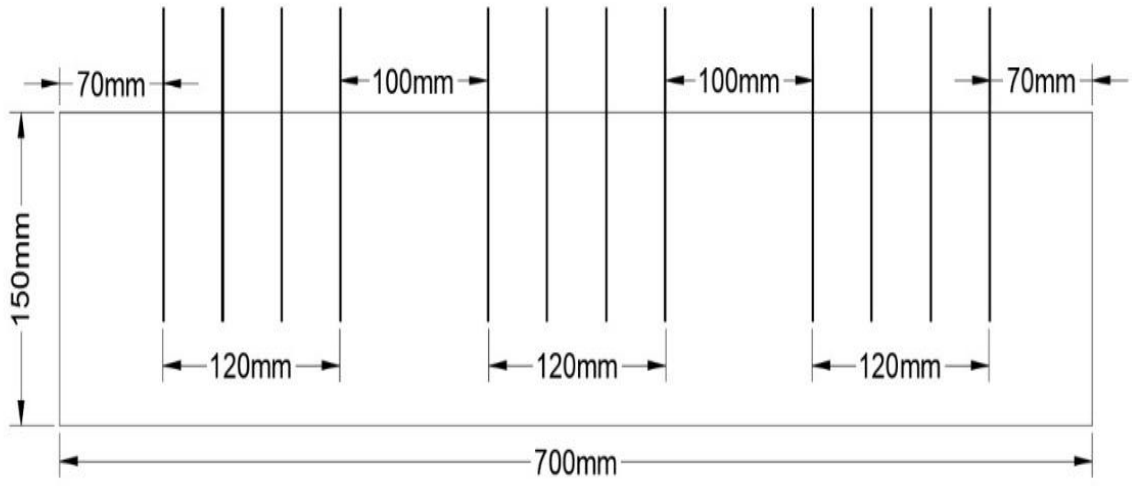

Figure 3.7. Copper plates embedment in beam

3.4. Experimental methods

Figure 3.8. presents the test matrix and technique illustrating different proportions of CS and LD slag along with the many parameters tested throughout the procedure.

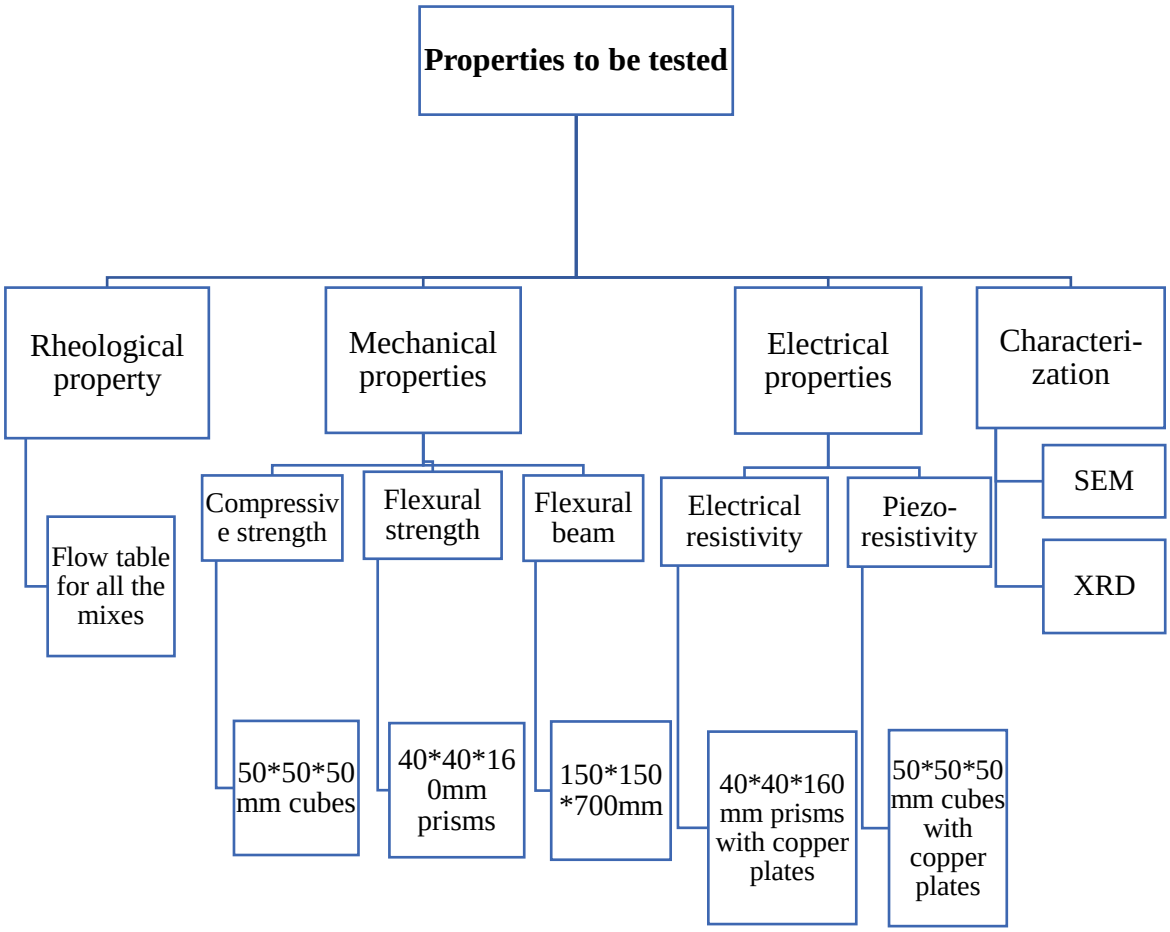

Figure 3.8. Schematic of research methodology

3.4.1. Workability

The workability of the mix was performed by following the prescribed method as per ASTM C1437, which involved carrying out a flow table test. The sample was positioned on a circular, flat-flow table apparatus that was fixed on a tripod platform. The experimental procedure involved inserting a specimen into a flow mold shaped like a truncated cone, with

a base diameter of 70 mm, upper diameter of 60 mm, and a height of 40 mm. The specimen was placed in the mold in three equal layers and each layer was compressed using 25 strokes of a tamping rod. Once the specimen was levelled, the mold was lifted vertically after 1 minute, and then 25 blows were applied to the table. The standard defines a range of flow rates from 105% to 115%.

Figure 3.9. Measurement of workability

Percentage increase in the average diameter of the spreading concrete over the base diameter of the mould is called flow of concrete. Its formula is given as:

$$\textbf{Flow } \% = \frac{\textbf{Spread diameter in mm} - \textbf{70}}{\textbf{70}} \textbf{ X 100}$$

3.4.2. Flexural strength test

Flexural strength of mortar prisms was assessed at various curing ages using a flexure strength test. The specimens were tested using the 3-point bending method. The experiment was conducted on three prisms for a duration of 7, 28, and 56 days, and the mean value should be recorded as the test outcome. The loading rate was configured to be 0.05kN/m, whereas the maximum capacity of the flexibility testing equipment was 100kN.

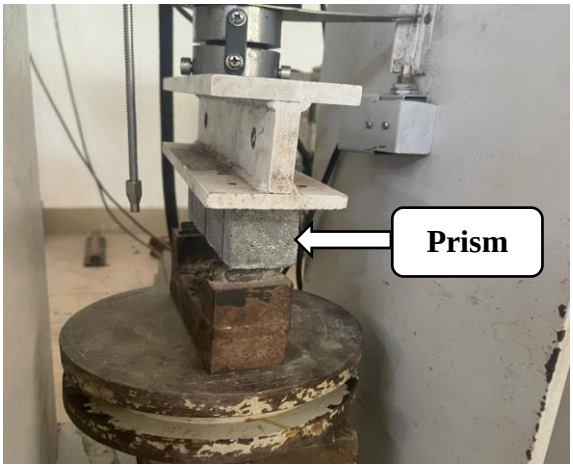

Figure 3.10. Flexural testing of prism

3.4.3. Compression strength test

Compression testing of LD and copper slag at varying curing ages of 7, 28, and 56 days let certain the compressive strength of mortar cubes. Samples were dried at room temperature after taking them out from the water tank for nearly 10-15 minutes. Samples were assessed using a compressive testing machine (CTM) using 0.5kN/s loading rate. Highest capacity of CTM is 5000kN.

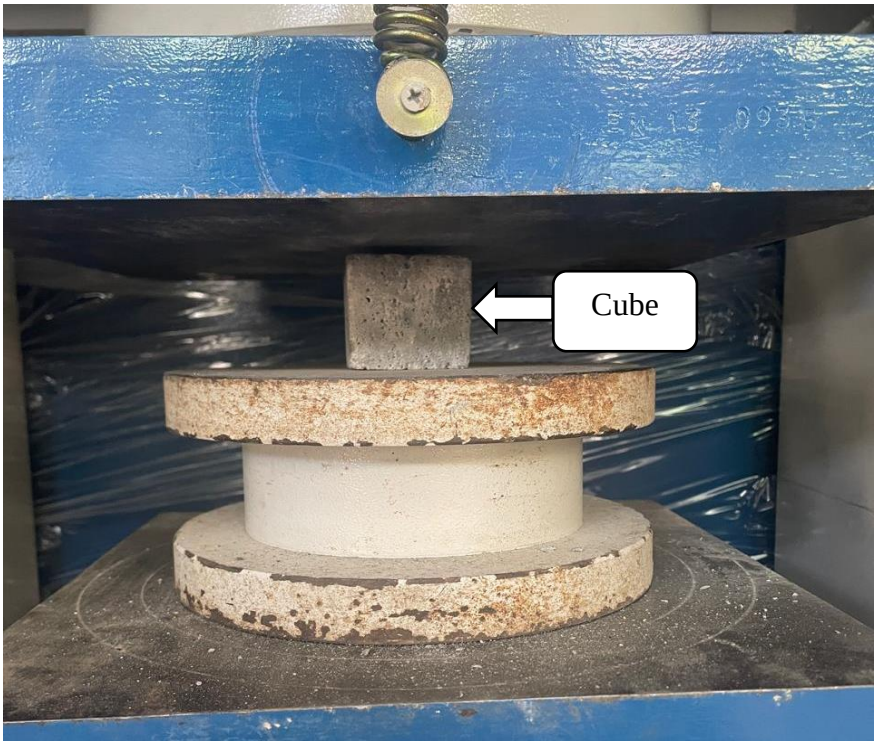

Figure 3.11. Testing of cubes using CTM

3.4.4. Electrical Resistivity test

The electrical resistivity test was conducted using the four-probe method. All the connections are arranged in a series configuration. One end of the wire was attached to the +ve terminal of the power source and the other end was linked to the rheostat. The other terminal of the rheostat was linked to the external plate of the specimen. The -ve terminal of the power supply was linked to the 22d exterior plate of the specimen. This circuit was fully assembled. The DPS-305CF power supply provided a steady direct voltage (U) of 10 V to the two probes, while a digital multi-meter was used to measure the current difference (I).

Using Ohm's law, Equation 3.1, one computed the sample's electrical Resistance (R).

$$\boldsymbol{R = \frac{V}{I}} \qquad \textbf{3.1}$$

The specimens were initially dried completely until their weights remained constant, and thereafter subjected to polarization for a duration of 20 to 30 minutes. The two outside probes were linked to a reference resistor (R1 ohms) in a series circuit driven by a direct current source with a constant voltage of 10V. Two voltage measurements were recorded, one across the resistor (V1) and one between the inner probes (V2) using a high impedance multimeter. Equation 3.2 determined the value of electrical resistance.

$$\boldsymbol{\rho = \frac{RA}{L} = \frac{\left(\frac{V2xR1}{V1}\right)}{L}} \qquad \textbf{3.2}$$

where, ρ = Electrical resistivity, R = Resistance of sample, L = Distance b/w two internal electrodes of the sample and A = Cross sectional area within electrodes.

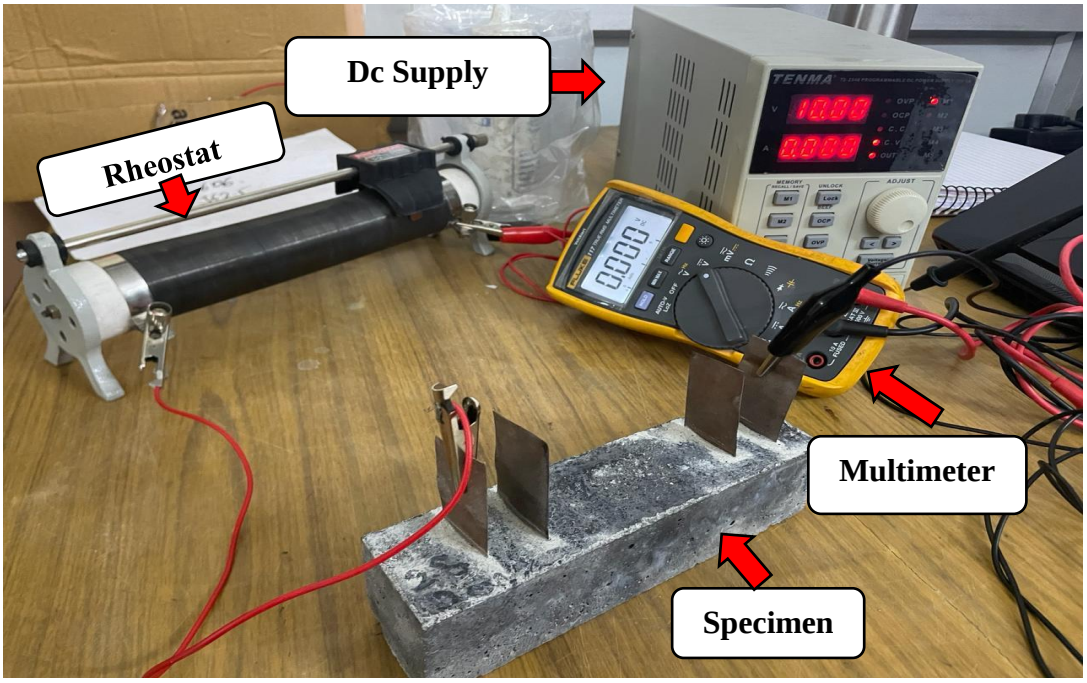

Figure 3.12. Setup for Electrical resistivity test

3.4.5. Piezo Resistivity test

The piezo-resistivity of the composites was analysed by concurrently measuring their deformation and electrical resistance while applying a monotonic compressive load (Figure 3.12). FCR is commonly computed as a percentage. The FCR was calculated using Equation 3.3 (Wang and Zhang 2022)

$$\mathbf{FCR}\ (\%) = \frac{\boldsymbol{\rho 1 - \rho 0}}{\boldsymbol{\rho 0}} \boldsymbol{X 100} = \frac{\boldsymbol{\Delta \rho}}{\boldsymbol{\rho 0}} \boldsymbol{X 100} \qquad \mathbf{3.3}$$

Where, $\boldsymbol{\Delta}\rho$ represents the change in resistivity in ohms per meter**, "**ρ1" represents the resistivity following the application of stress or strain, while "ρ0" represents the initial resistivity, $\boldsymbol{\Delta}$R is the change in electrical resistance in ohms, R represents the initial electrical resistance in ohms.

The experimental procedure for piezo-resistivity measurement was as follows:-

- The computer was first linked to the CTM, and all the initial testing settings, such as loading rate, specimen type, curing age, and specimen dimensions, were allocated.
- The next step entailed configuring the wire connections, which included a resistor, a data recorder, a DC supply unit, and plate connectors.

- A four-point electrode setup was utilized to conduct the piezo-resistivity measurement. A data recorder was employed to quantify the disparity in electric current (I) between the inner and outer copper plates. Additionally, a stable direct voltage (U) of 10 V was administered to the outer two copper plates via a power supply (DPS-305CF).
- Subsequently, the computer executed a command that initiated the process of compressing and loading data.
- The data recorder's recording function was activated before the test began to collect all the necessary data for the electrical resistivity recording.
- In addition to the data logger, a computer was capturing a Force-time graph of the imposed compressive stress until the specimen reached its point of failure.
- The data-recording feature was disabled after the test, and all physical connections were disconnected in preparation for the next sample.
- After calculating resistivity, FCR was finally calculated using Equation 3.3.
- The resistivity was calculated by utilizing a variety of parameters, including the area, length, current, and voltage output of the inner and outer plates (Figure 3.12).

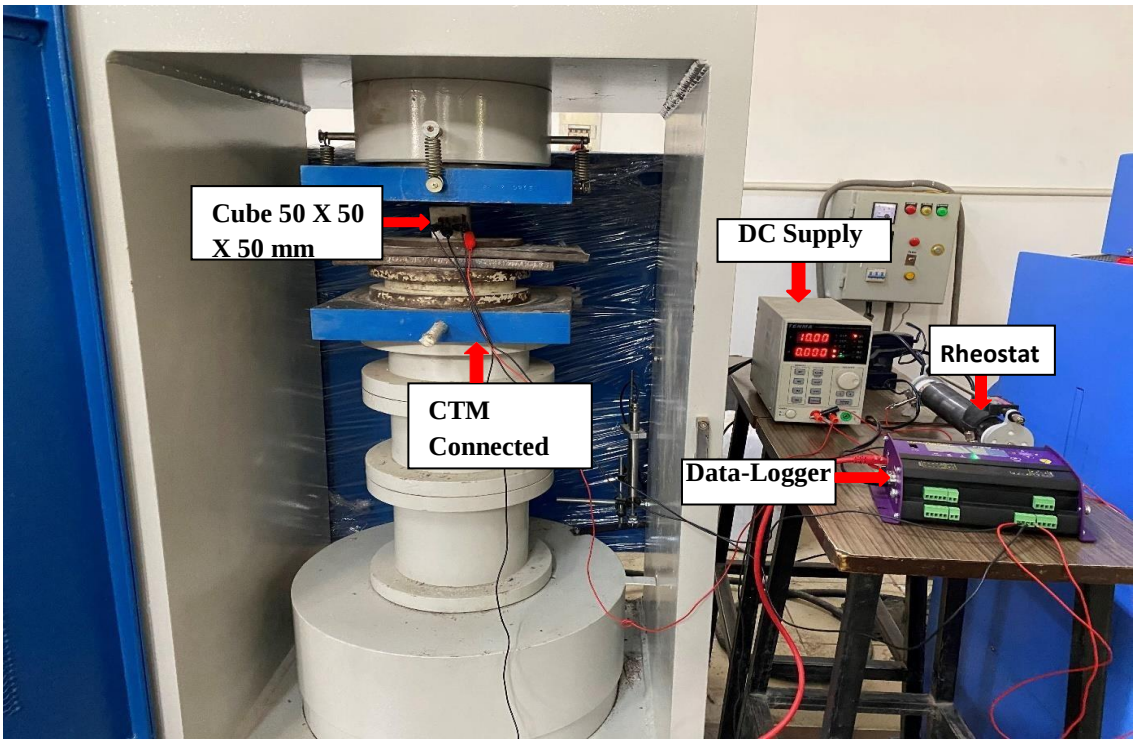

Figure 3.13. Setup for Piezo Resistivity test

3.4.6. Testing of Mortar Beam

We have casted two beams in the bulk form incorporating copper slag and LD slag as a sand replacement to test it as a sensor form under the flexural loading and to observe the electrical characteristics which includes electrical resistivity and piezo-resistivity.

The experimental procedure for beam was as follows:

- The beam was tested using the four point bending technique and the universal testing machine.
- The computer was initially linked to the UTM, and all the basic testing settings (loading rate, specimen type, curing age, and specimen dimensions) were assigned.
- The subsequent phase involved the wire-connection configuration, which consisted of a resistor, a data recorder, a DC supply unit, and plate connectors (Figure 3.13).
- To ascertain the strain value, the strain gauge was fixed in the region experiencing tension. The strain gauge was connected to the data logger using cables, allowing for instantaneous recording of the strain in the data logger.
- The measurement of piezo-resistivity was performed using a setup consisting of four-point electrodes. A data recorder was utilized to quantify the disparity in electric current (I) between the inner and outer copper plates. Additionally, a stable direct voltage (U) of 10 V was administered to the outer two copper plates via a power supply (DPS-305CF).
- The computer then displayed a command, which triggered the compression loading process.
- The data recorder's recording function was activated before the test started to collect all the necessary data for the electrical resistivity recording. The data logger also records the strain value with time. Furthermore, alongside the data logger, a computer was capturing a Force-time graph of the imposed compressive stress until the specimen experienced failure.
- The data recording function was off after the test, and all wired connections were disconnected in preparation for the next specimen.
- After calculating resistivity, FCR was finally calculated using Equation 3.4 (wang & zhang, 2022)

$$\mathbf{FCR}\ (\%) = \frac{\boldsymbol{\rho 1 - \rho 0}}{\boldsymbol{\rho 0}} \boldsymbol{X100}\ = \frac{\boldsymbol{\Delta \rho}}{\boldsymbol{\rho 0}} \boldsymbol{X100} \qquad \textbf{3.4}$$

- The resistivity was determined by considering many characteristics, such as the area, length, current, and voltage output of both the inner and outside plates (Figure 3.12).

Figure 3.14. Setup for Beam testing

3.6. Summary

This chapter detailed the experimental experiments that were conducted. Materials and sample preparation details were disclosed. The electrical characteristics and mechanical properties of the mix proportions of LD and Copper slag were assessed in the testing program, which was divided into two sections. Compressive and flexural strength are two mechanical qualities that are measured. Simultaneously, electrical properties involve evaluations of piezo-resistivity and electrical resistivity.

CHAPTER 4

RESULTS AND DISCUSSION

4.1. General

This Chapter represents the results of the experimental investigations. The previous chapter discussed the various experimental procedures performed to identify the changes in the electrical characteristics and mechanical properties resulting from the addition of Copper and LD slag in the casted mortar samples. This chapter examines the ability of Copper slag and LD slag as self-sensing materials for reinforced concrete constructions. This chapter offers a complete exposition of the obtained results and thoroughly examines the impact of Copper and LD slag.

4.2. Workability

Fig. 4.1. Illustrates how adding various amounts of copper slag to the mixture affects how workable concrete is. Workability greatly improves when the percentage of copper slag increases from 25% to 75%, with flow values increasing from 100 mm to 150 mm. This pattern suggests that it is easier to handle and lay concrete when more copper slag is added. The precision of the data could be somewhat impacted by any errors in mixing, measuring, or other experimental conditions, which could cause this improvement in workability to not be precisely linear.

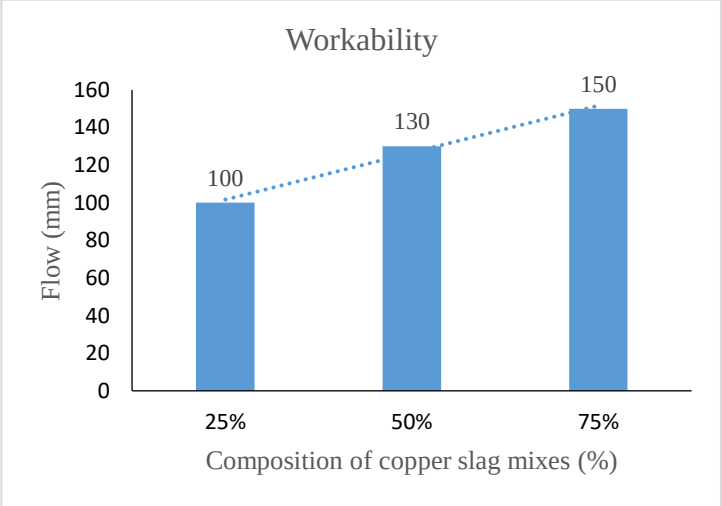

Figure 4.1. Workability characteristics of copper slag

Fig 4.2 indicates that the concrete mix gets more difficult to deal with as the proportion of LD slag increases. When LD slag makes up 20% of the mix, the concrete flows with ease, measuring 93 mm. However, the flow decreases to 72 mm and 60 mm as the LD slag is increased to 25% and 30%, making the concrete more difficult to work with and stiffer. This implies that adding more LD slag reduces the concrete's workability; therefore, to keep the concrete workable, it may be necessary to make adjustments such adding more water or other additives.

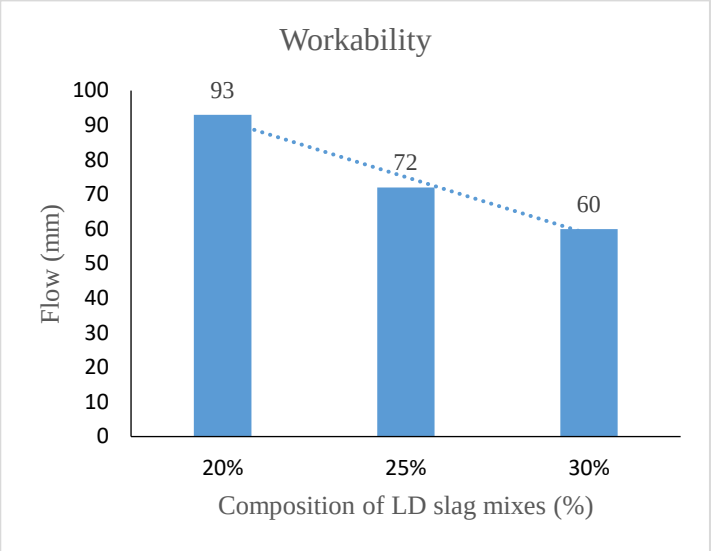

Figure 4.2. Workability characteristics of LD slag

4.3. Flexural strength

The flexural strength of self-compacting concrete (SSC) mixes over 7, 28, and 56 days is shown in fig 4.3 (a), at various LD slag replacement percentages (0%, 20%, 25%, and 30%). At 56 days, the control mix, which does not include LD slag replacement, shows the highest flexural strength of any of the time period. It reaches 7.92 MPa. Flexural strength shows a small drop with increasing LD replacement, with a considerable reduction at the 20% replacement mix and further declines at the 25% and 30% replacement levels. All mixes show a rise in strength over time, despite the initial fall in strength with increasing LD concentration, though none outperforms the control mix.

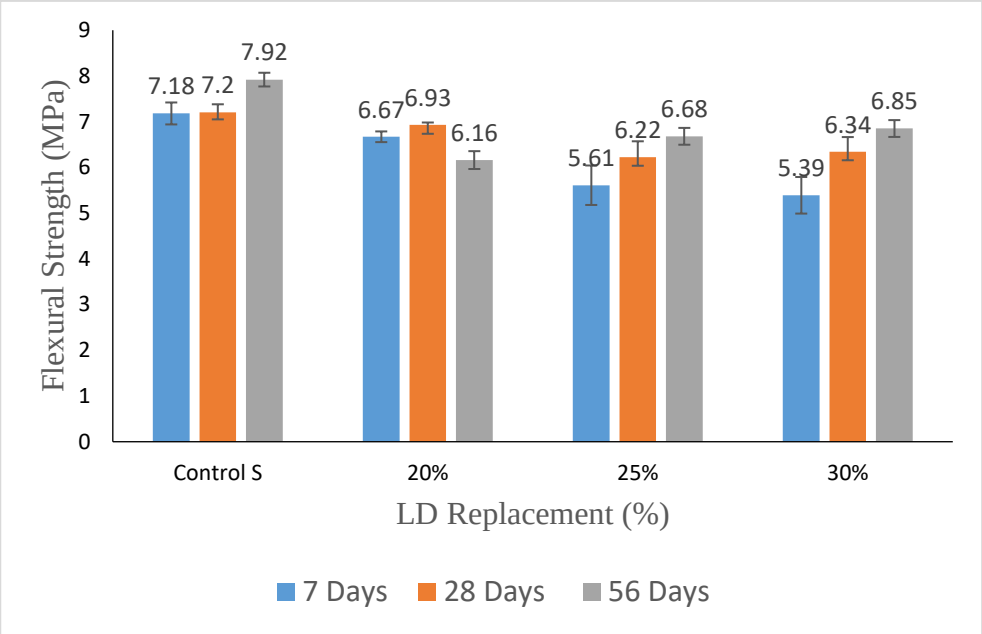

Figure 4.3 (a) Flexural strength of SSC mixes

Flexural strength of concrete specimens incorporating varying percentages of copper slag (CS) (25%, 50%, and 75%). Flexural strength can be seen increasing with higher percentage of copper slag content up to 75%, peaking at 8.45 MPa for 28 days cured specimens. While 25% copper slag also exhibits high strength at 28 days of curing (8.25 MPa), slight decrease is observed compared to 75% replacement of copper slag. Flexural strength gains are more prominent at 28 days than 7 and 56 days.

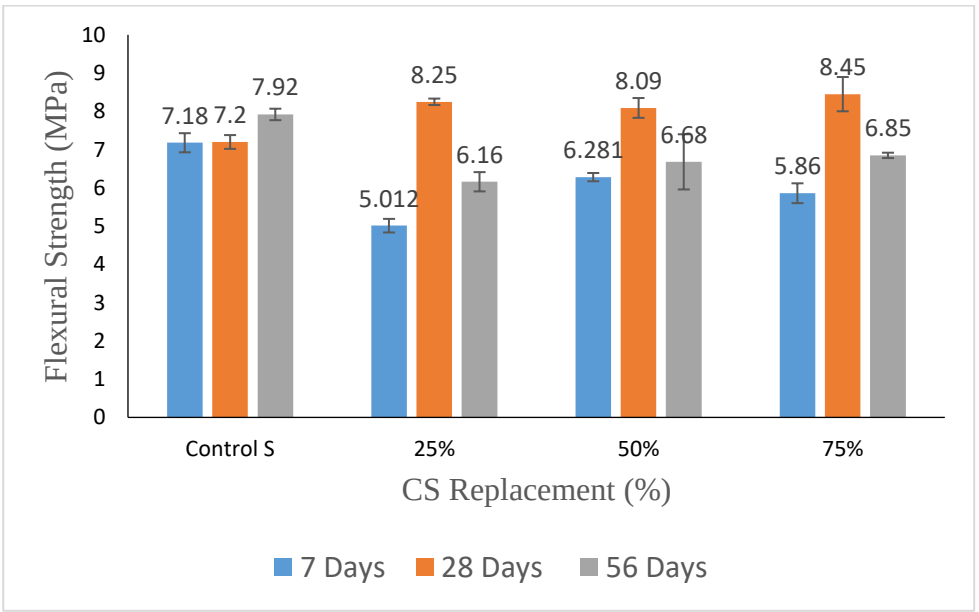

Figure 4.3 (b) Flexural strength of SSC mixes

4.4. Compressive strength

As the content of copper slag increased in self-sensing mixes, the setting time of the concrete was delayed. However, it had no significant impact on the characteristics of concrete, namely the compressive strength of self-sensing concrete mixes containing 25%, 50%, and 75% copper slag throughout the 7, 28, and 56 days of curing. The self-sensing mixes with copper slag demonstrated comparable or greater compressive strength values when compared to concrete mixes consisting just of sand. The compressive strength of the control sample containing 100% sand was found to be 26.52 MPa at 28-day curing period. Maximum enhancement in strength was observed for self-sensing concrete incorporating 50% copper slag showed 44.94 MPa compared to control sample at 28 days curing. Also, 28-day compressive strength improved from 26.52 MPa to 30.14 MPa for mortar mix incorporating 25% copper slag at 28 days of curing. Similarly, 7-day strength increased from 21.92 MPa to 22.22 MPa for 25% of copper slag and 33.23 MPa for 50% of the copper slag replacement as shown in fig 4.4 (a). The increase in strength was mostly related to the physical characteristics of copper slag. The use of copper slag grains effectively raised the stress concentration of the concrete matrix by enhancing the compressibility of the slag particles, as compared to sand. The presence of sharp edges of slag particles enhances the cohesiveness of the concrete matrix (Gupta, et. al 2019). However, insignificant reduction in strength was recorded beyond 50% of copper slag replacement. Although the strength was not less than the SSC mix with 100% sand. Strength was observed that decrease in strength is about 9.01% to 15.27% for SSC mix as 75% of copper slag replacement in comparison to SSC mix with 50% copper slag from 7 to 56 days of curing. The primary cause for the reduction in strength was attributed to the glassy composition of copper slag grains and its low water absorption capacity, resulting in an excessive amount of water.

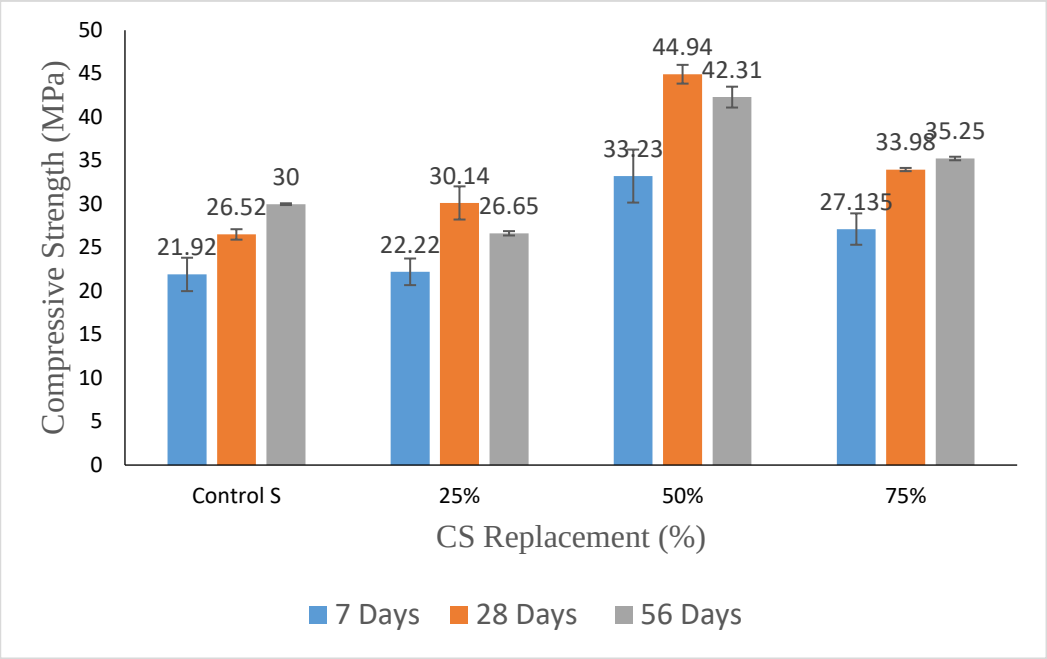

Figure 4.4 (a) Compressive strength of SSC mixes

The compressive strength of self-sensing concrete mixes containing 20%, 25%, and 30% LD slag throughout the 7, 28, and 56 days of curing. Results for compressive strength are shown in Fig 4.4 (b). At 7 days, replacing sand with LD slag results in decrease in strength with an increase in percentage replacement. According to the literature, an increase in slag content initially slows down the internal rate of hydration. This could be because slag's rough surface increases water absorption, which leads to improper cohesion between LD slag and cement paste. Maximum enhancement in strength was observed for incorporating 20% of LD slag was 27.45 MPa compared to control mix at 28 days of curing which was observed 26.52 MPa. Also, 28-day compressive strength improved from 26.52 MPa to 27.22 MPa for mortar mix incorporating 25% LD slag at 28 days of curing. The reason for this could be that the majority of slag particles had rough surfaces and angular shapes, which improved the interfacial transition zone (ITZ) cement and created a strong concrete matrix. Because these LD slag aggregates had a reduced crushing value, their strength values were increased. There has previously been an explanation provided for the increase in compressive strength caused by the superior physico-mechanical characteristics of steel slag aggregates over natural aggregates. Further decrease in strength was observed in incorporating 30% of the LD slag replacement as compared to the control mix. Increasing the amount of LD slag, cement particles might have remained unhydrated due to increase demand of water to

surface properties of slag such as angular, irregular shape, and rough texture. Secondly, the presence of free (unhydrated) lime in slag caused the concrete matrix to expand volumetrically, which decreased strength. (Gupta, et. al, 2019) Although the expansion resulting from free lime is less than 2% for LD slag aggregates, the free lime content increases as the LD slag content increases. However, this becomes a significant factor in compressive strength as we increase the amount of LD slag.

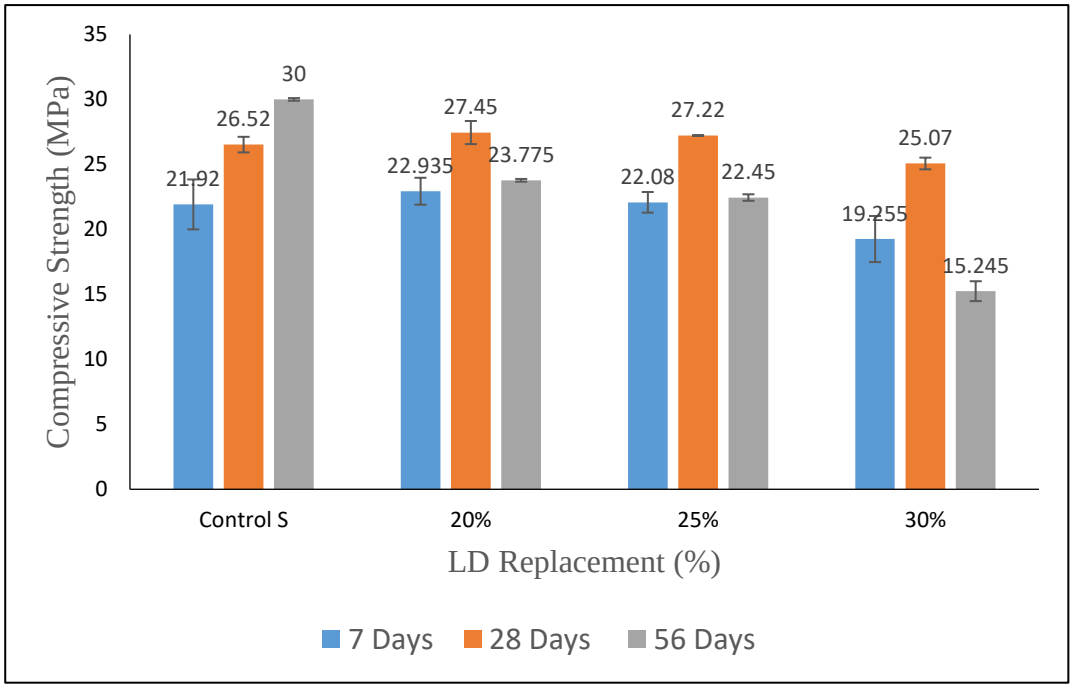

Figure 4.4 (b) Compressive strength of SSC mixes

4.5. Electrical Resistivity

Electrical Resistivity was measured for 7 types of specimens- the control specimen and the specimens that incorporate 20%, 25%, and 30% of LD slag and 25%, 50%, and 75% of copper slag by weight of cement. DC electrical resistivity was measured over time and an increase in resistivity was observed as the days passed. Tests revealed a gradual, insignificant rise in resistivity for various mix proportions as the curing days passed. One of the major reason behind this was the rise in temperature as the result was conducted in the month of May and June so the gradual increase in temperature resulting in affecting the characteristics of the specimens making the specimens surface dry which affect the electrical

characteristics of the different mix proportions. After 7 days, mixes showed gradual decrease in the resistivity making the specimen conductive as compared to the control mix sample that had the value of 156 KΩ-cm after 7 days of curing. On the other hand for copper slag mixes of 25%, 50%, and 75% electrical resistivity comes out to be 17.5 KΩ-cm, 20 KΩ-cm, 19 KΩ-cm respectively. Similarly, for the LD slag incorporating 20%, 25%, and 30% the values observed for electrical resistivity was 8.7 KΩ-cm, 12 KΩ-cm, and 12.6 KΩ-cm respectively. At 28-day testing of copper slag showed slight, decrease in electrical resistivity by 28% approximately as compared to 7-day results, and control mix sample, which showed 409 KΩ-cm making the path conductive of copper slag mix samples due to filling of the unfilled voids of the composition as the copper slag percentage increases. An insignificant increase in electrical resistivity after 56 days because of the gradual increase of temperature and the results, as shown in table 4.1 below.

Table 4.1 (a) Electrical Resistivity at different days for copper slag

No. of samples	7 Days	28 Days	56 Days
Control sample	156 KΩ-cm	709 KΩ-cm	2256 KΩ-cm
CS 25%	17.5 KΩ-cm	12.8 KΩ-cm	1044 KΩ-cm
CS 50%	20 KΩ-cm	16 KΩ-cm	1265 KΩ-cm
CS 75%	19 KΩ-cm	65 KΩ-cm	900 KΩ-cm

Table 4.1 (b) Electrical Resistivity at different days for LD slag

No. of samples	7 Days	28 Days	56 Days
Control sample	156 KΩ-cm	709 KΩ-cm	2256 KΩ-cm
LD 20%	9.5 KΩ-cm	23 KΩ-cm	35 KΩ-cm
LD 25%	9.9 KΩ-cm	38.4 KΩ-cm	69.78 KΩ-cm
LD 30%	7.8 KΩ-cm	25.5 KΩ-cm	62.2 KΩ-cm

Due to significant increase in the electrical resistivity variations due to high temperature, we again cured our casted specimens for the period of 56 days and observed the results in fig 4.5.

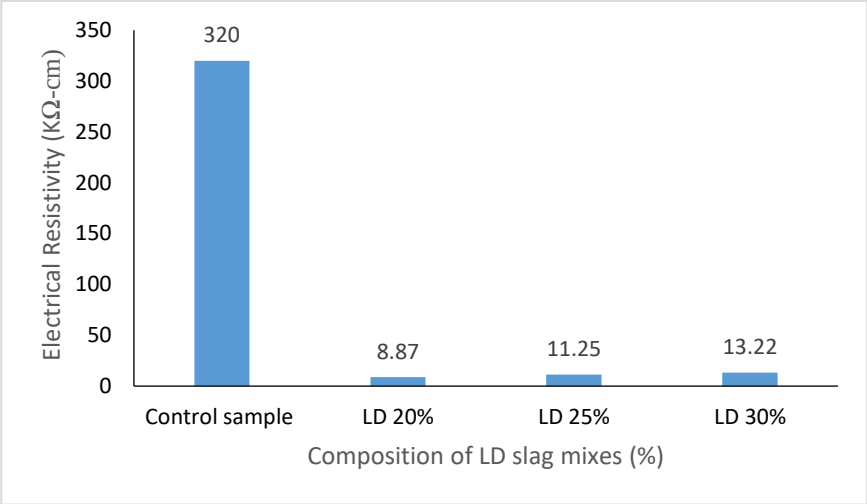

Figure 4.5 (a) Electrical resistivity of SSC mixes for 56 days after wetting

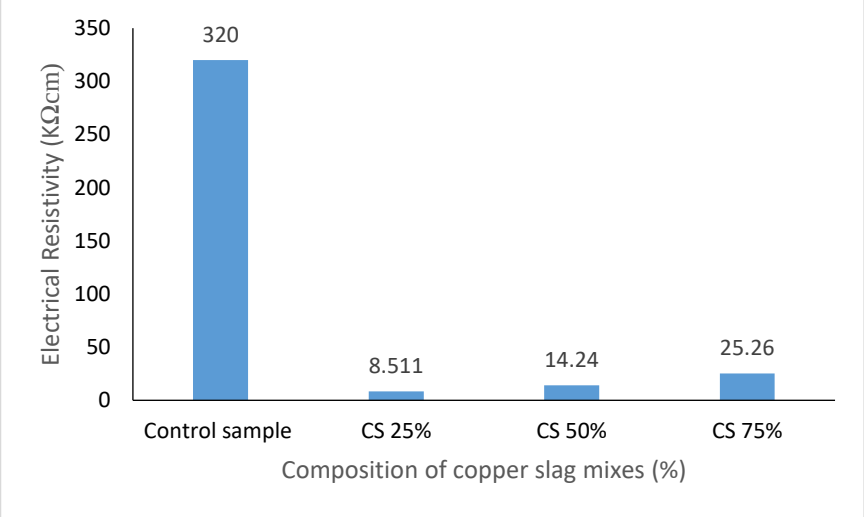

Figure 4.5 (b) Electrical resistivity of SSC mixes for 56 days after wetting

4.6. Piezo-resistivity

The time history correlations between the control mix's FCR and compressive stress for the course of the control mix's 28 days of curing under monotonic compression, beginning with loading and continuing until failure, are shown in Fig 4.6. It demonstrates how the specimen's FCR does not change when the compressive stress does. The maximum FCR for the Control mix is 0%. As seen in Figure 4.7, the control mix showed a maximum stress value of 30.8 MPa at 28 days and 51.5 MPa at 56 days. There was no sign of stress sensitivity in the control specimen.

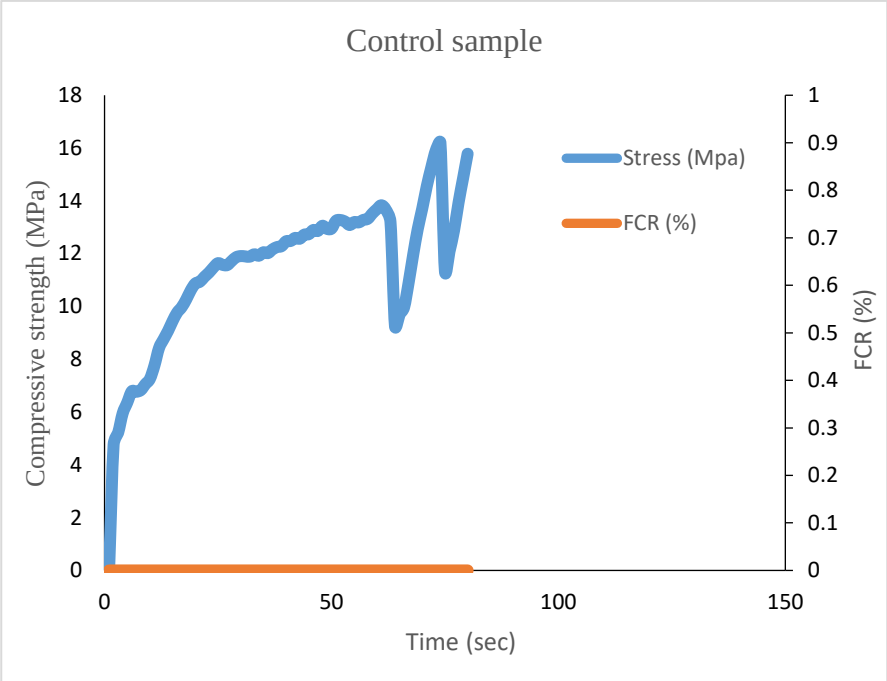

Figure 4.6. Compressive strength vs FCR tested for 28 days

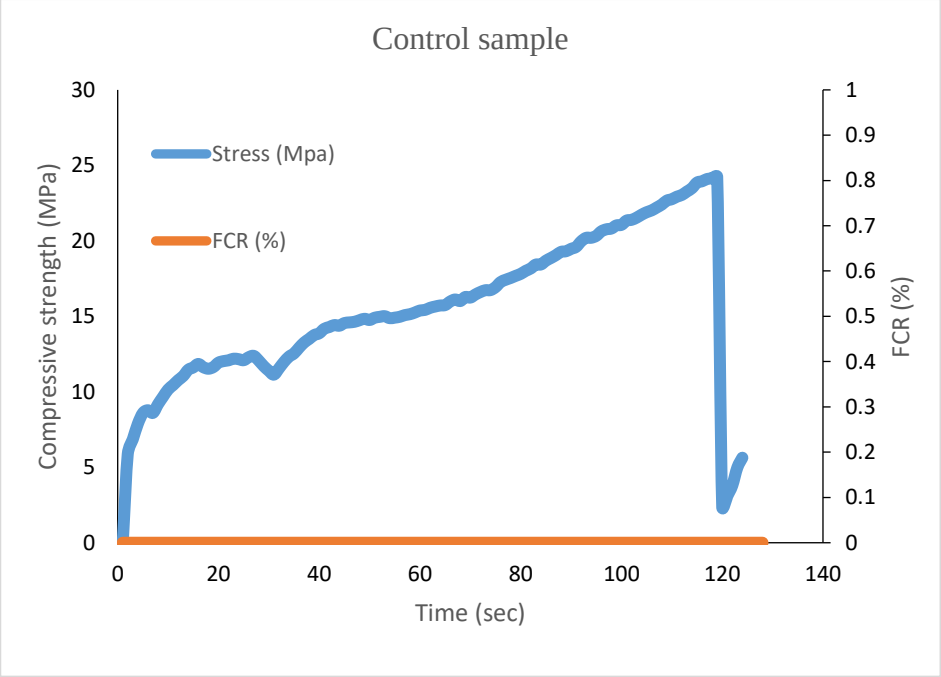

Figure 4.7. Compressive strength vs FCR tested for 56 days

The time history correlations between the copper slag and LD slag of different mixes incorporation i.e. (25%, 50%, and 75%) for copper slag and (20%, 25%, and 30%) for LD slag FCR and compressive stress for the course of the different mixes 28 days and 56 days of curing under monotonic compression. A general trend can be observed between FCR values and the compressive strength of the samples for all copper and LD slag specimens. The FCR values either rise or stay constant as the compressive strength increases, but there is a sharp leap in the FCR values as the sample approaches its yielding point. The sample under compression observes more conductive filler particles coming together as the load increases, which leads to the formation of more conductive networks and explains the fall in the FCR values. This provides an explanation for the leap in the data. However, the graph does not show the very slight decline in the FCR values. These conductive networks, however, are disrupted when the sample yields, which causes an abrupt rise in the resistivity of the sample. This results in the good sensing potential of the specimens and can be used to monitor conductivity changes corresponding to increasing stress.

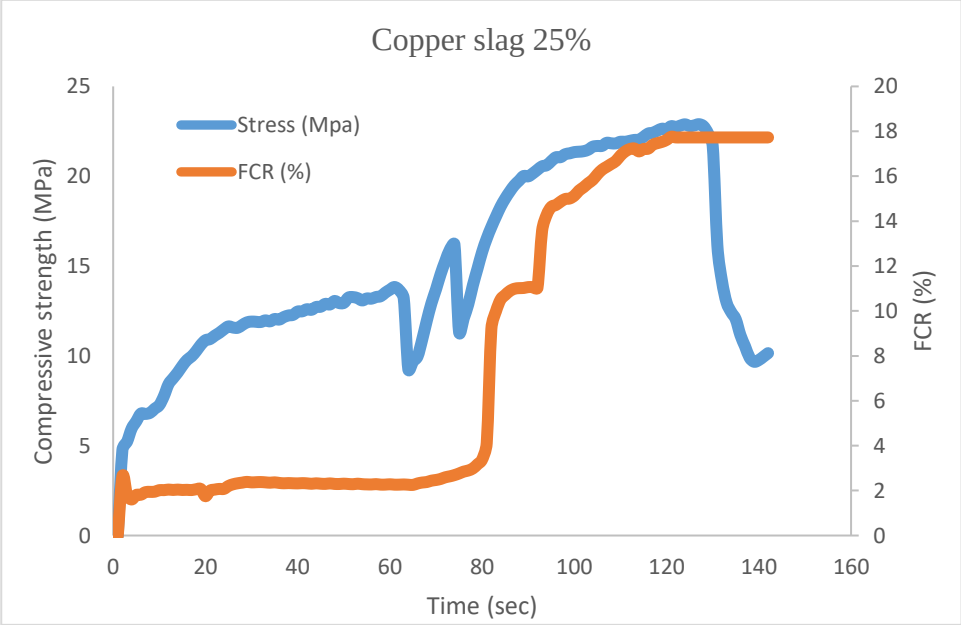

Figure 4.8. Compressive strength vs FCR tested for 28 days

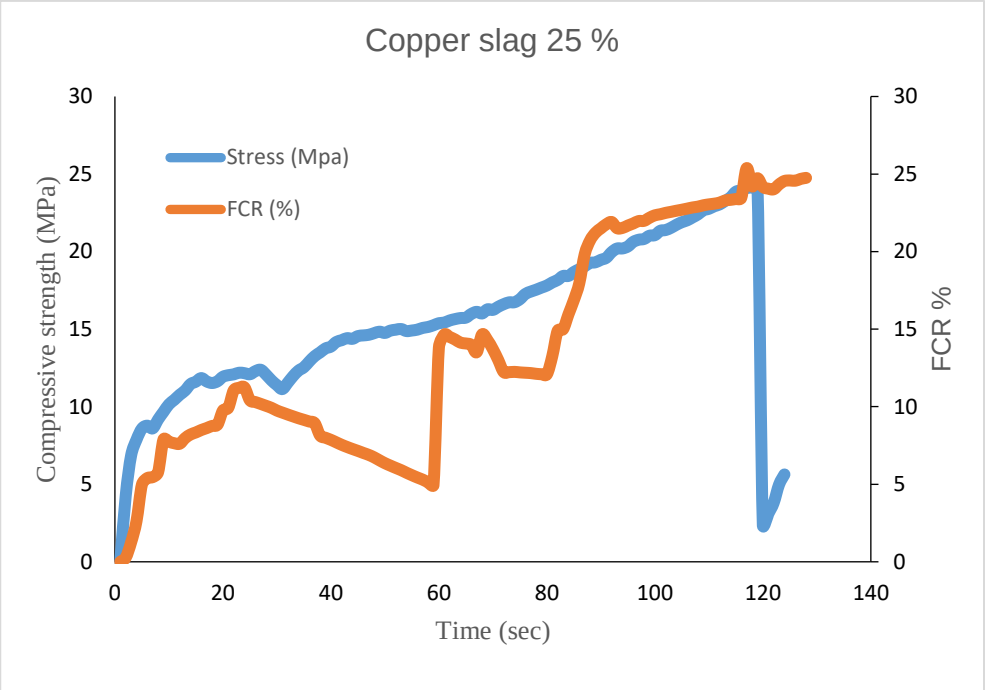

Figure 4.9. Compressive strength vs FCR tested for 56 days

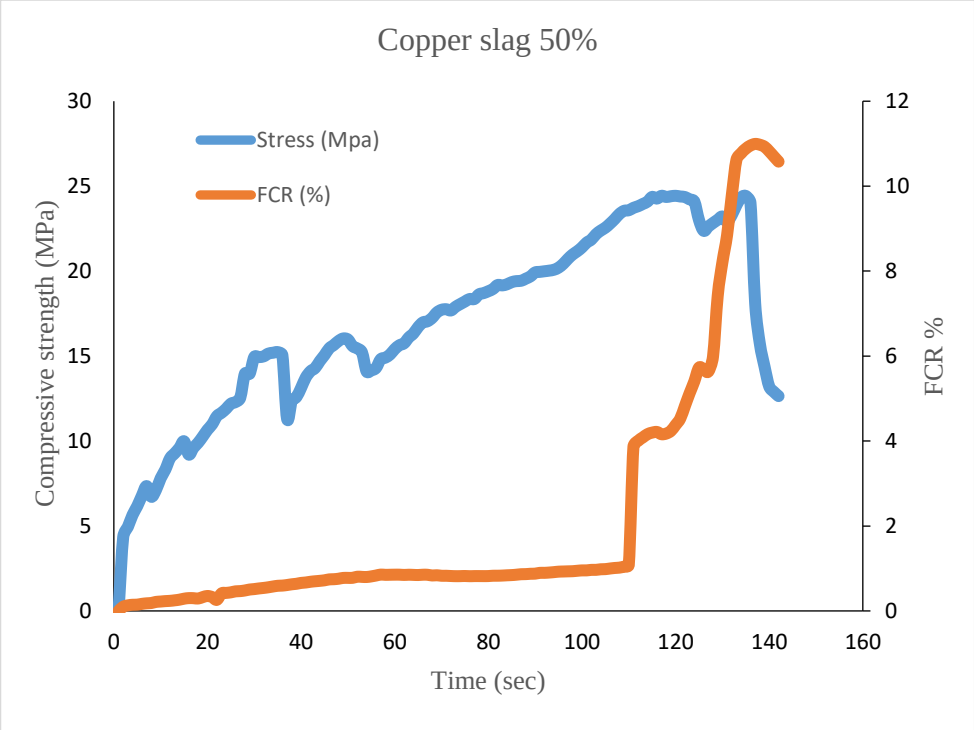

Figure 4.10. Compressive strength vs FCR tested for 28 days

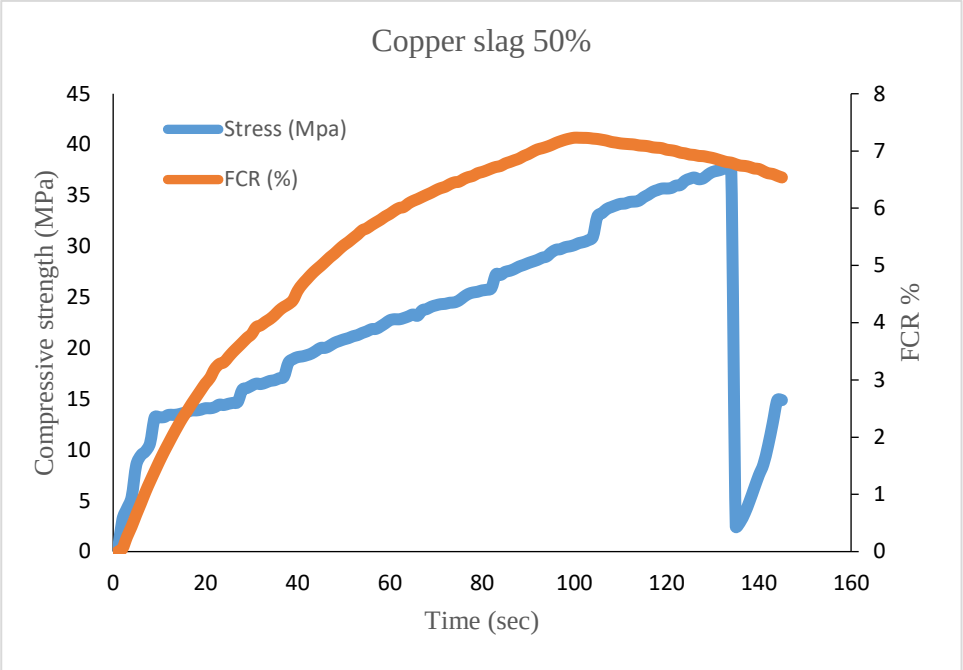

Figure 4.11. Compressive strength vs FCR tested for 56 days

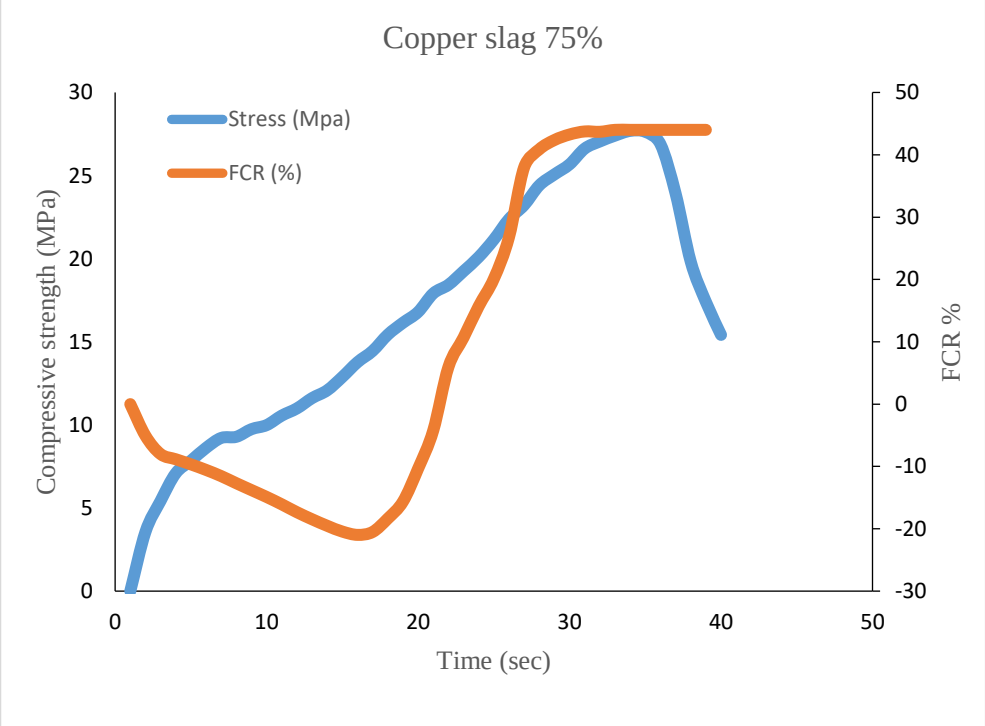

Figure 4.12. Compressive strength vs FCR tested for 28 days

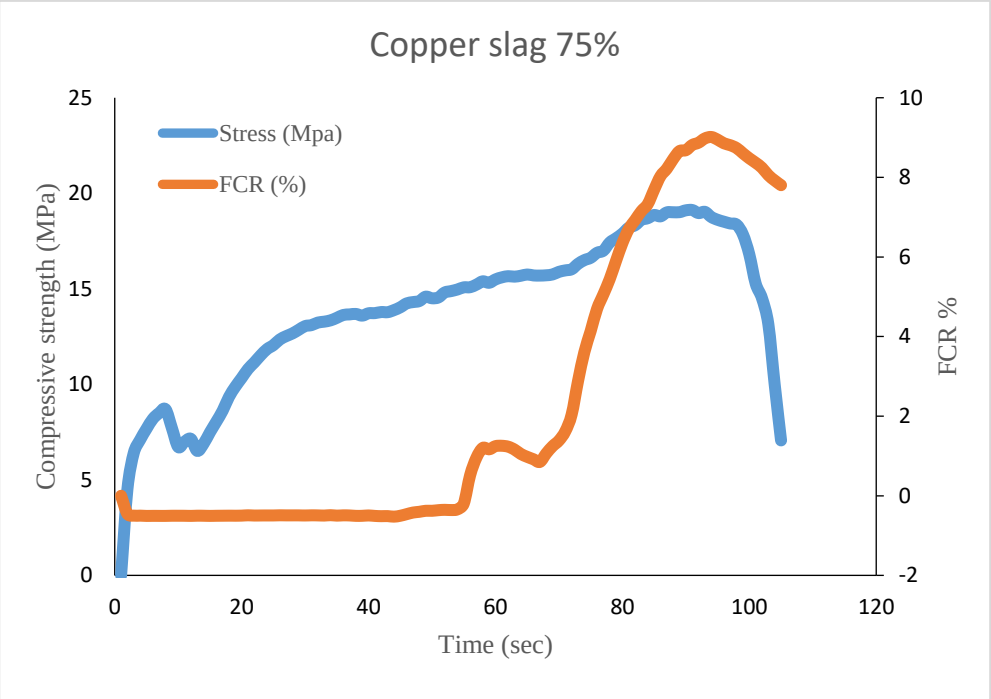

Figure 4.13. Compressive strength vs FCR tested for 56 days

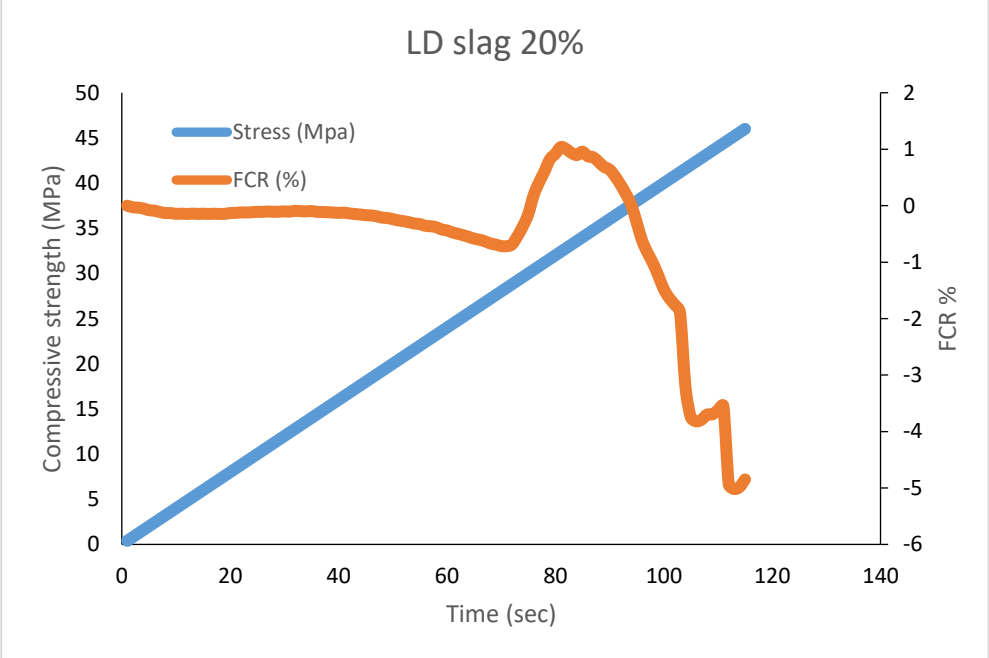

Figure 4.14. Compressive strength vs FCR tested for 28 days

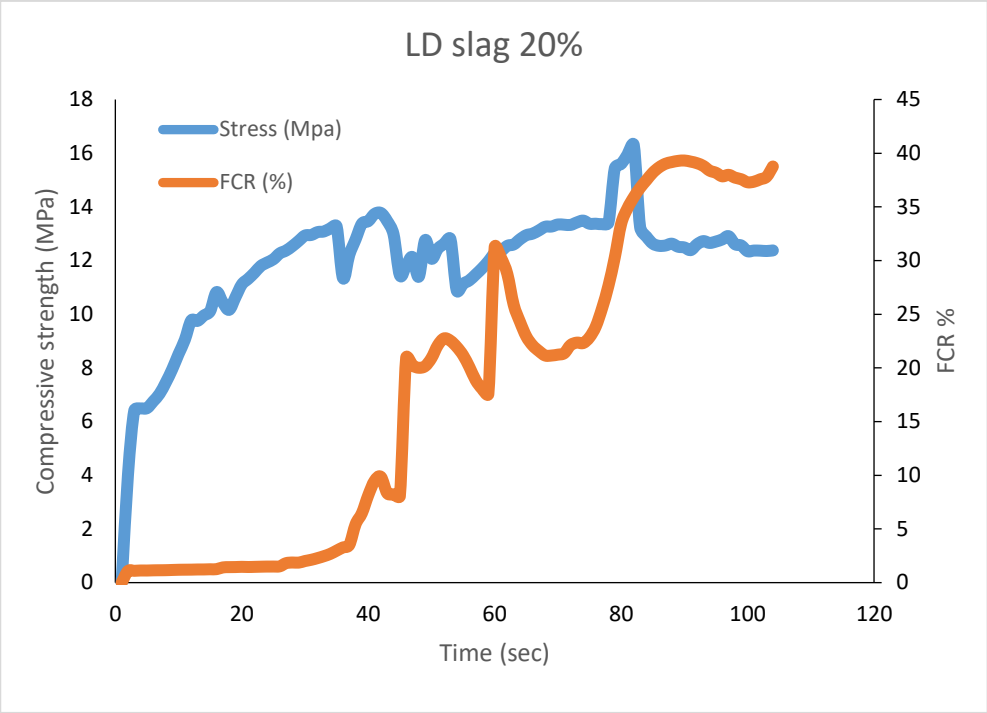

Figure 4.15. Compressive strength vs FCR tested for 56 days

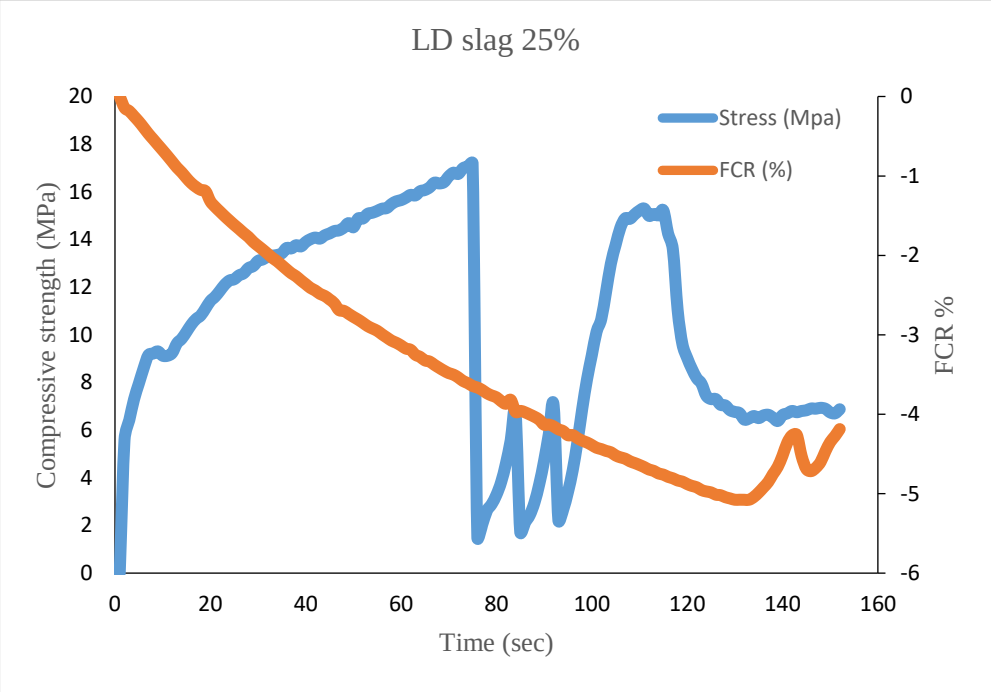

Figure 4.16. Compressive strength vs FCR tested for 28 days

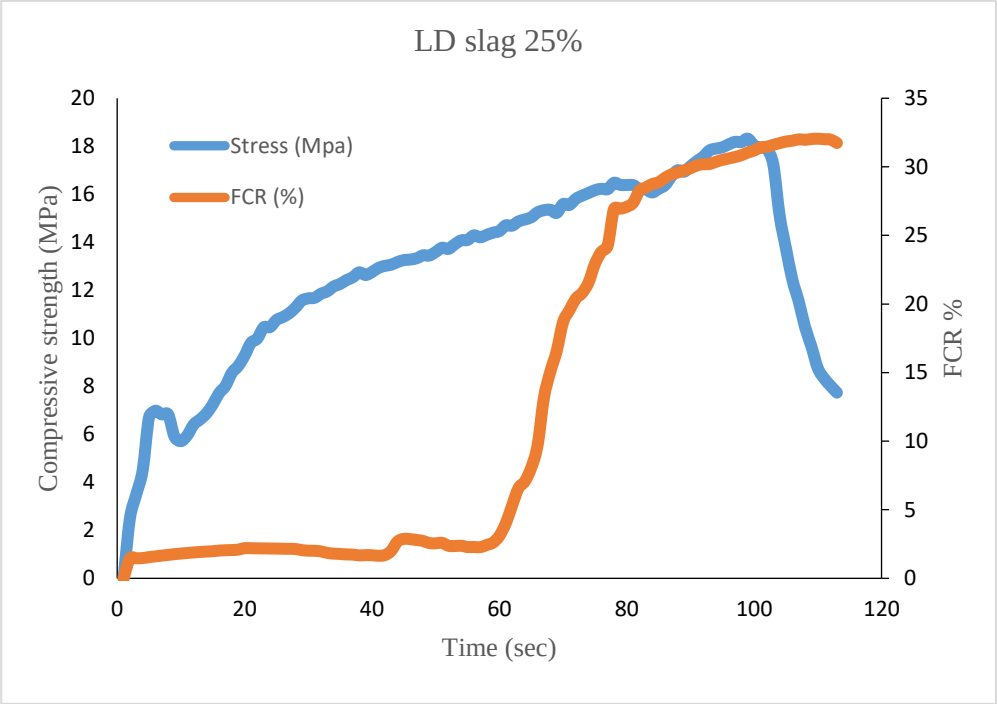

Figure 4.17. Compressive strength vs FCR tested for 56 days

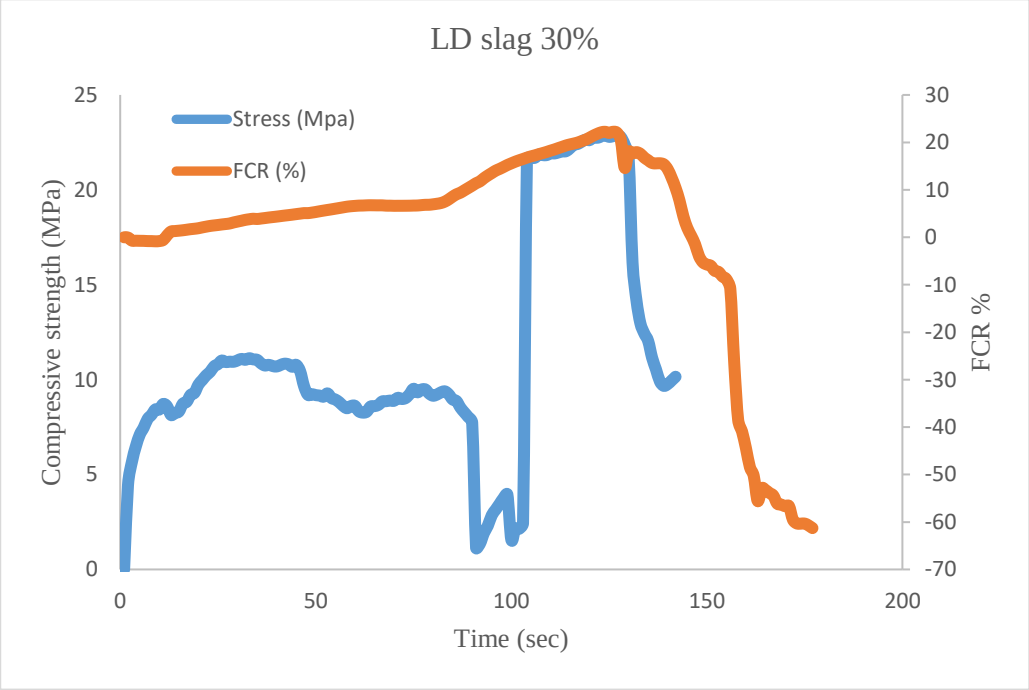

Figure 4.18. Compressive strength vs FCR tested for 28 days

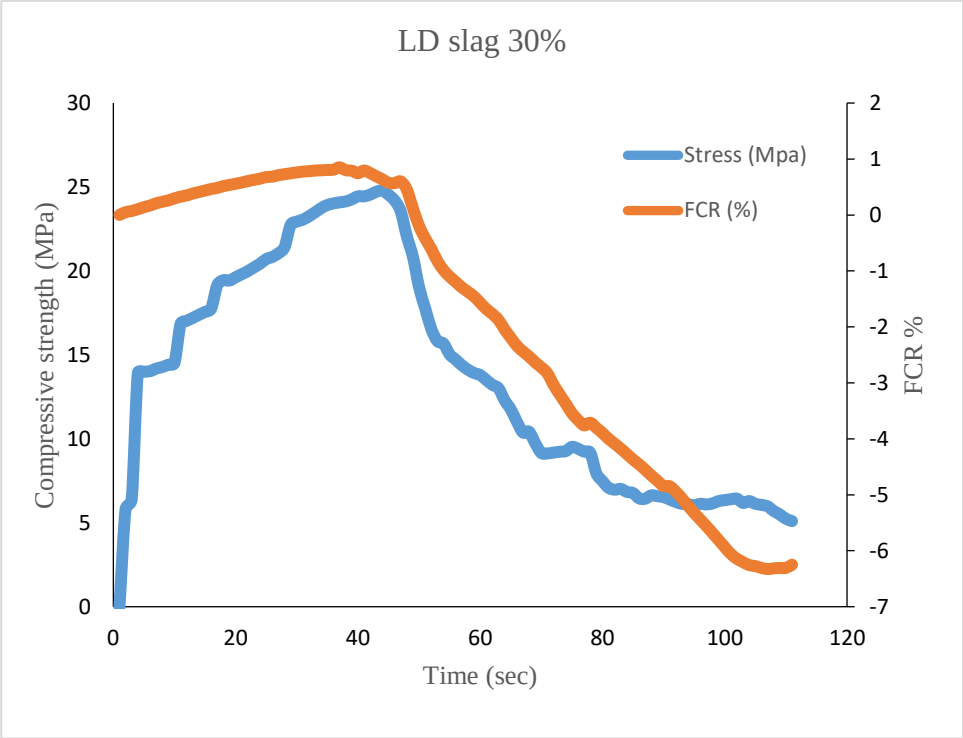

Figure 4.19. Compressive strength vs FCR tested for 56 days

4.7. Fitting curve analysis

Higher R-squared values in samples signify improved composite sensing performance. Figures 4.20 to 4.31, which shows the results for 28 days and 56 days of testing of the specimens, demonstrate high stability and homogeneity, accordingly.

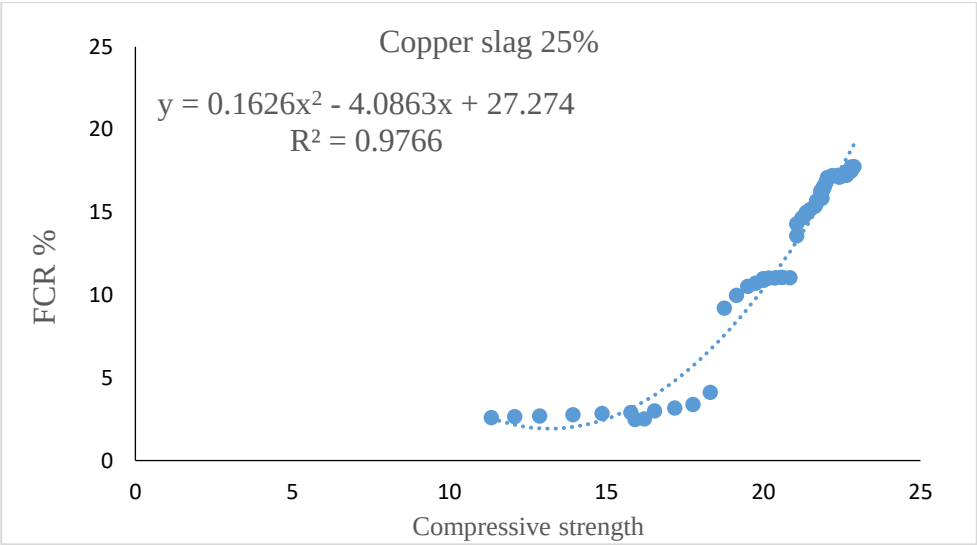

Figure 4.20. Fitting curve between FCR and compressive strength for 28 days

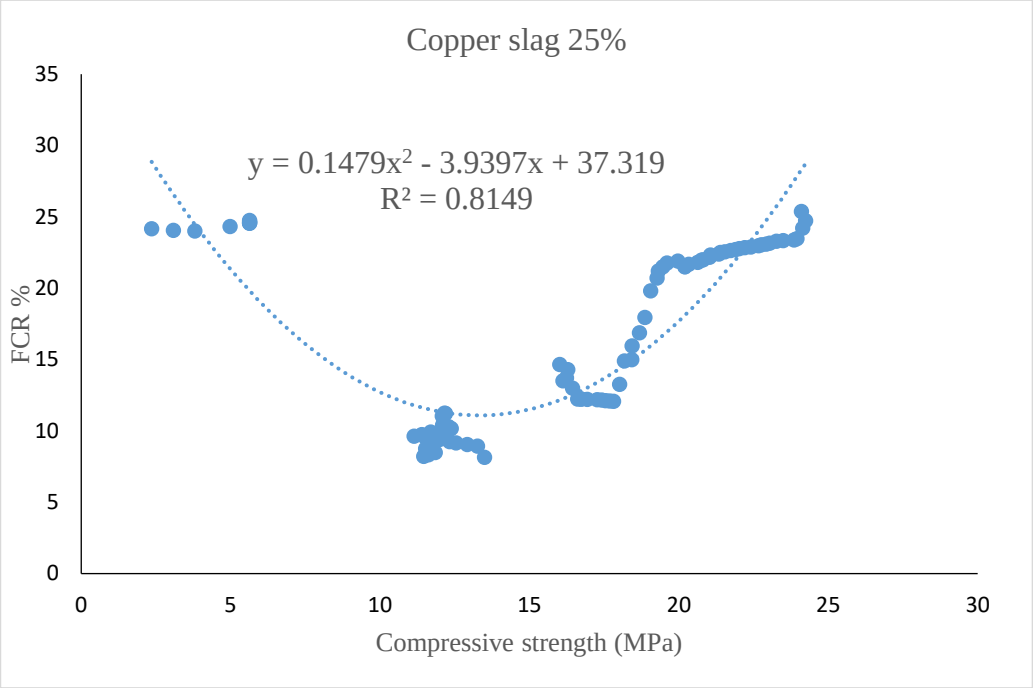

Figure 4.21. Fitting curve between FCR and compressive strength for 56 days

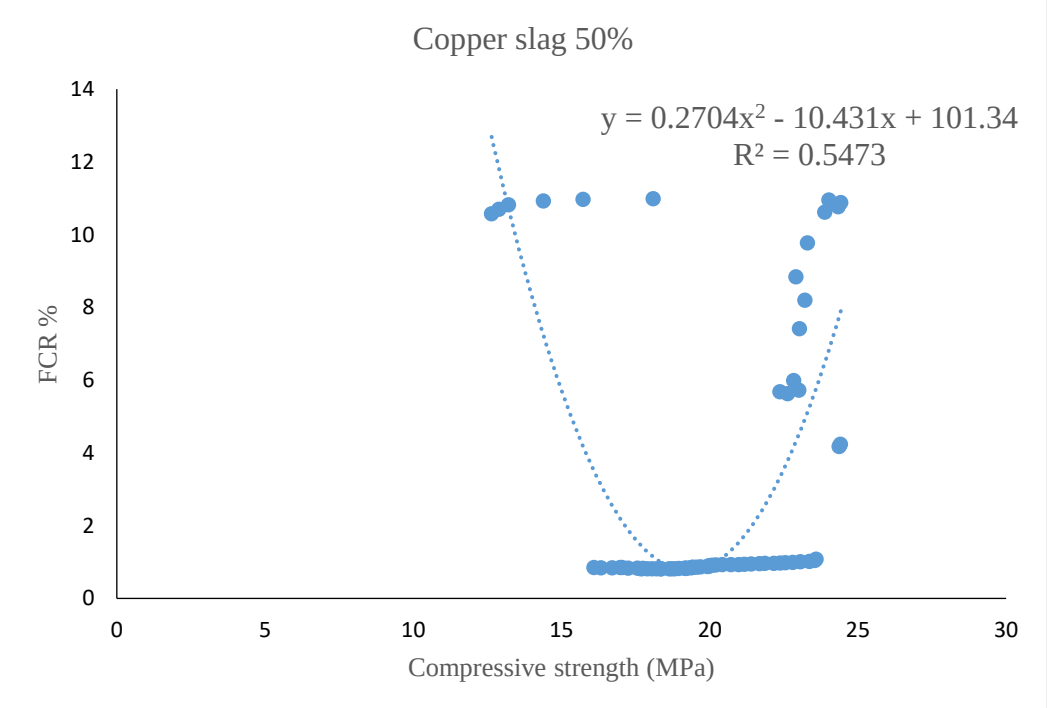

Figure 4.22. Fitting curve between FCR and compressive strength for 28 days

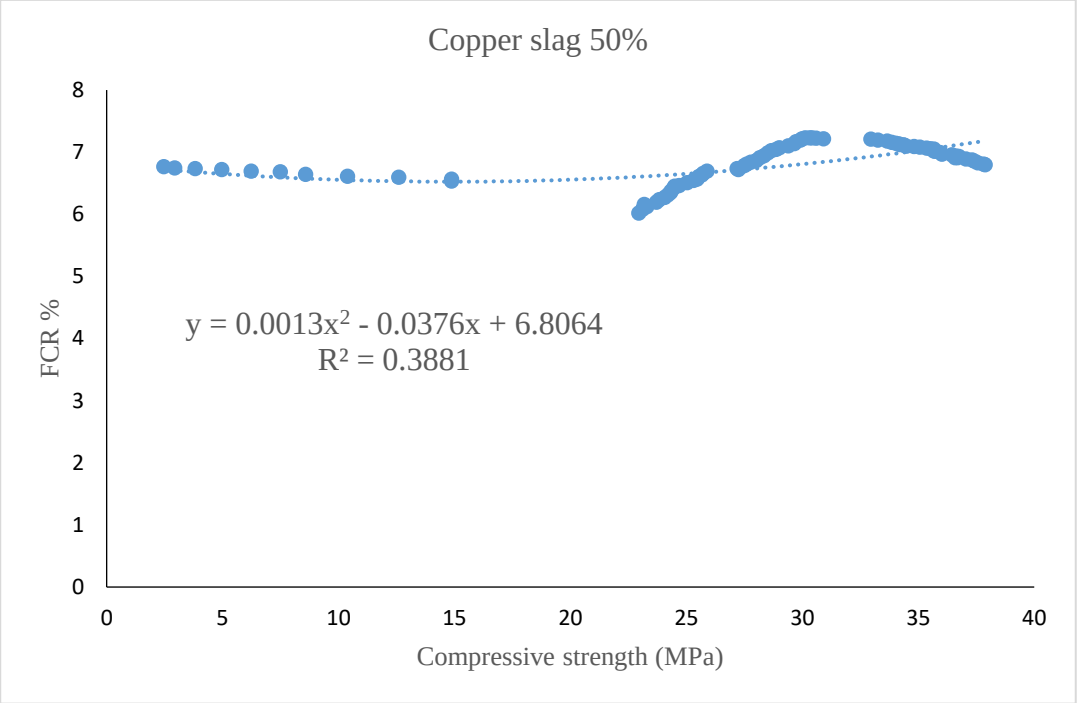

Figure 4.23. Fitting curve between FCR and compressive strength for 56 days

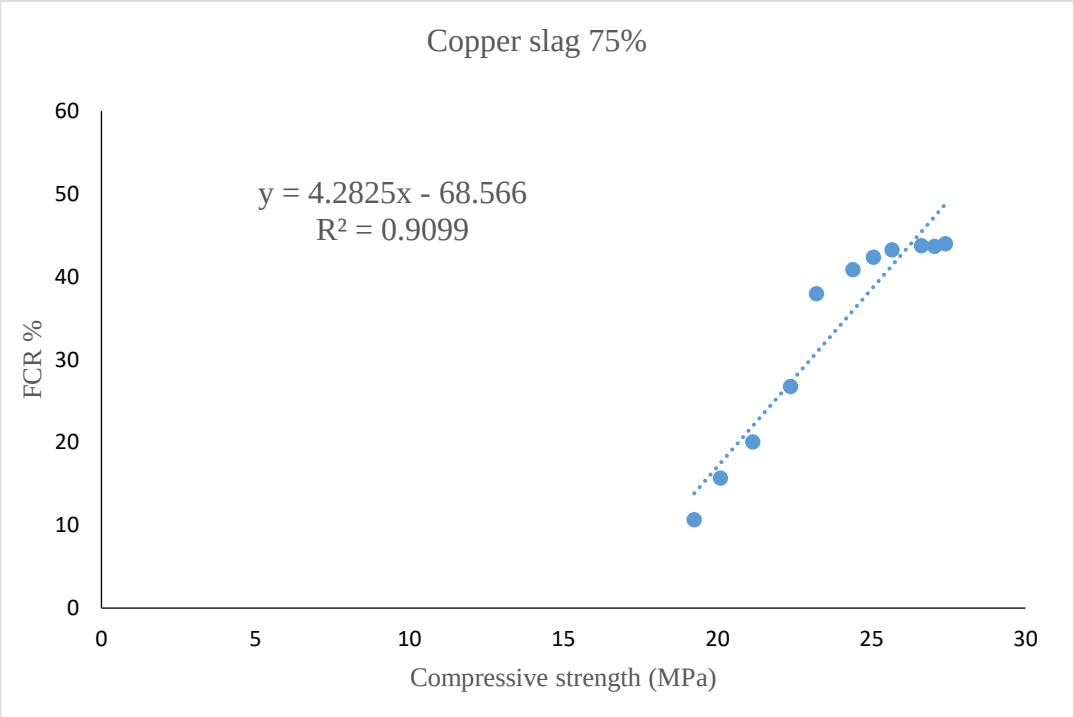

Figure 4.24. Fitting curve between FCR and compressive strength for 28 days

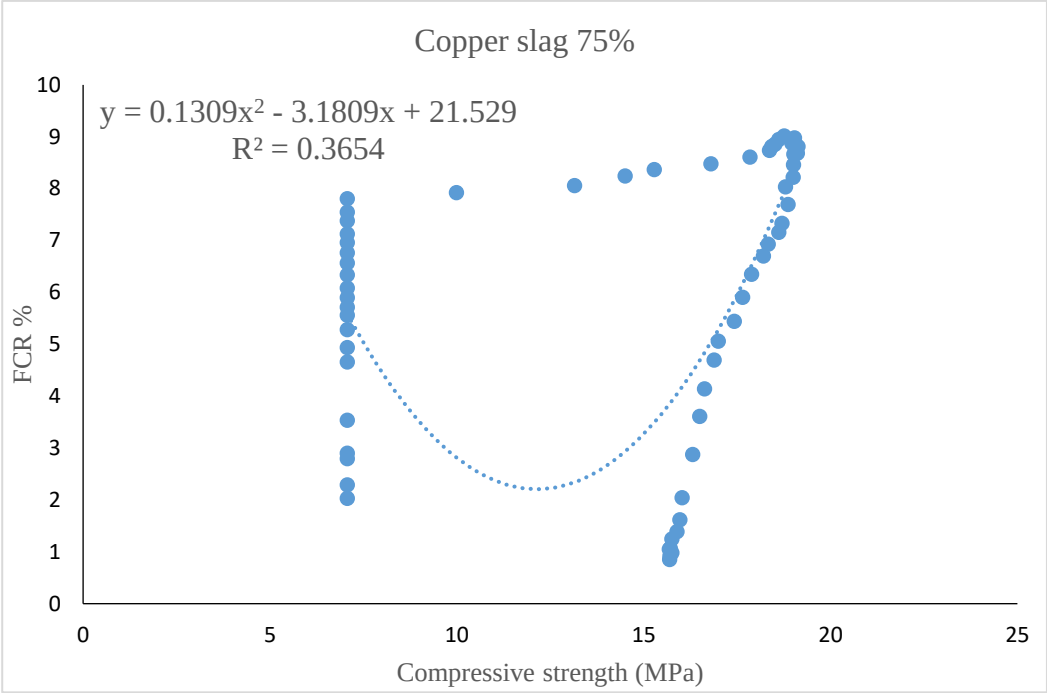

Figure 4.25. Fitting curve between FCR and compressive strength for 56 days

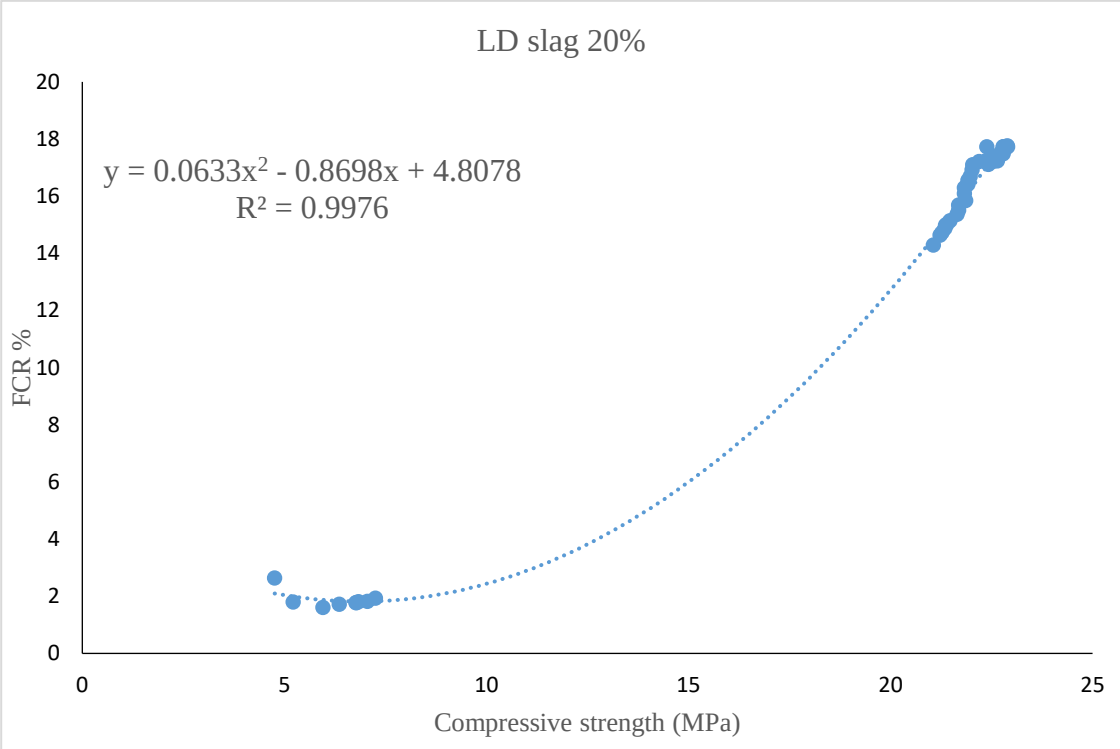

Figure 4.26. Fitting curve between FCR and compressive strength for 28 days

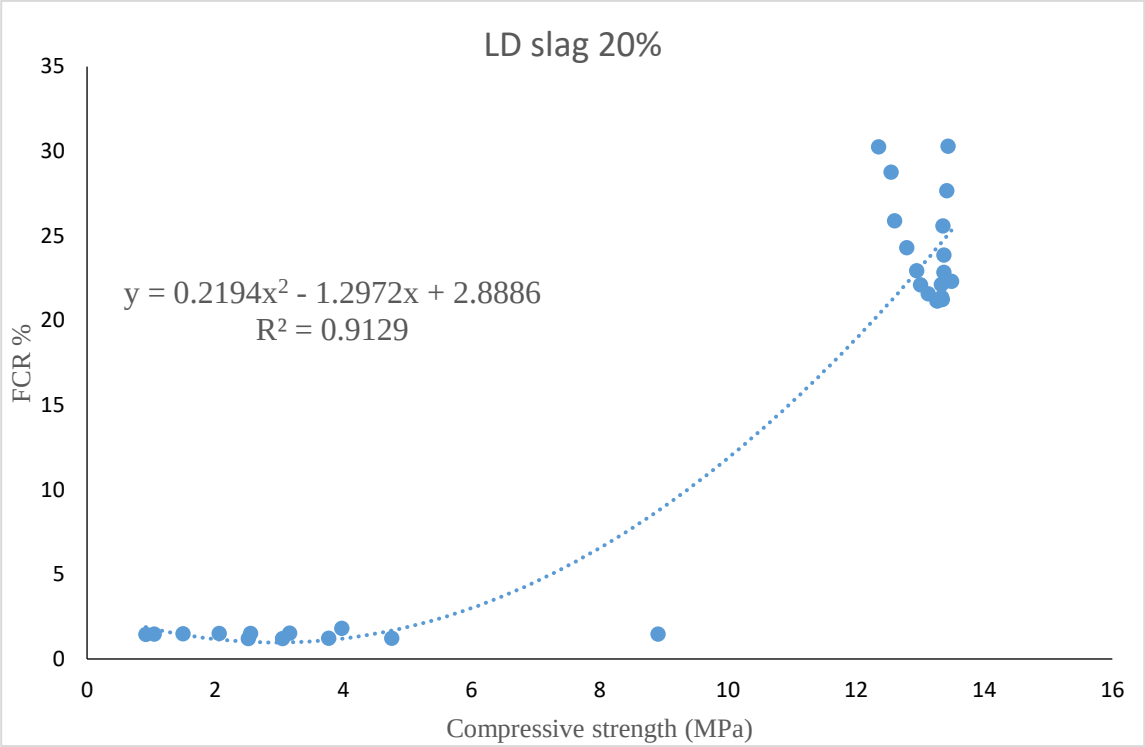

Figure 4.27. Fitting curve between FCR and compressive strength for 56 days

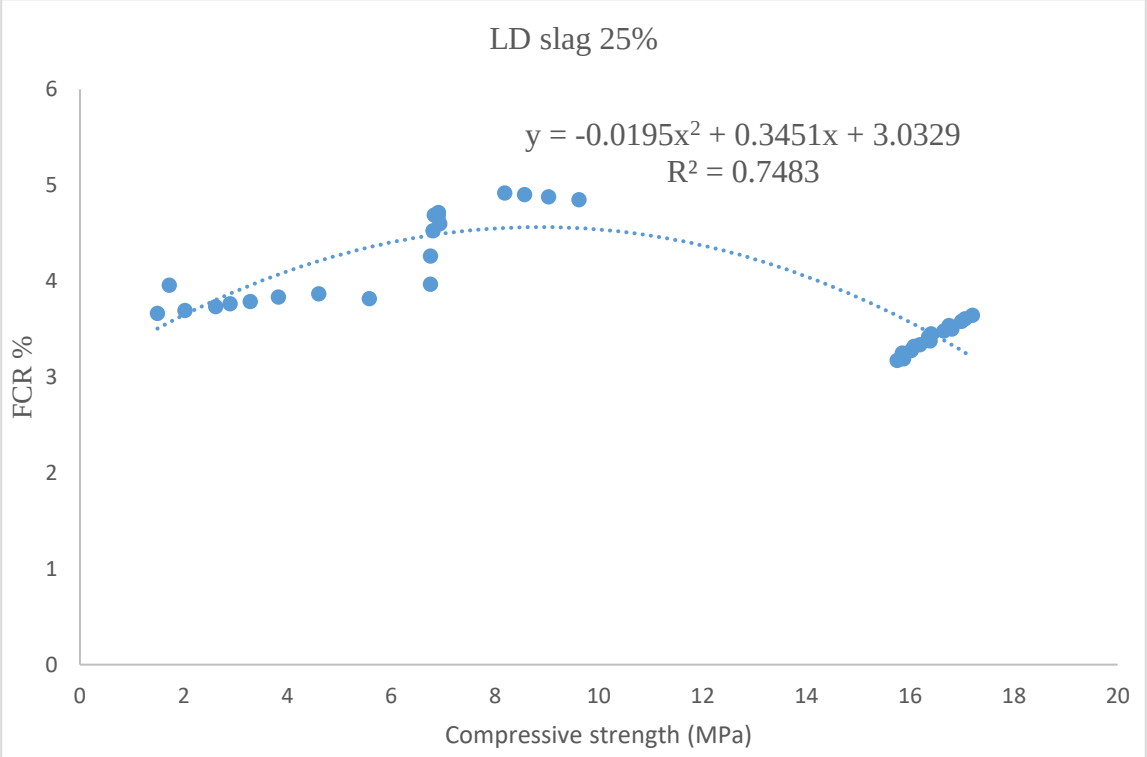

Figure 4.28. Fitting curve between FCR and compressive strength for 28 days

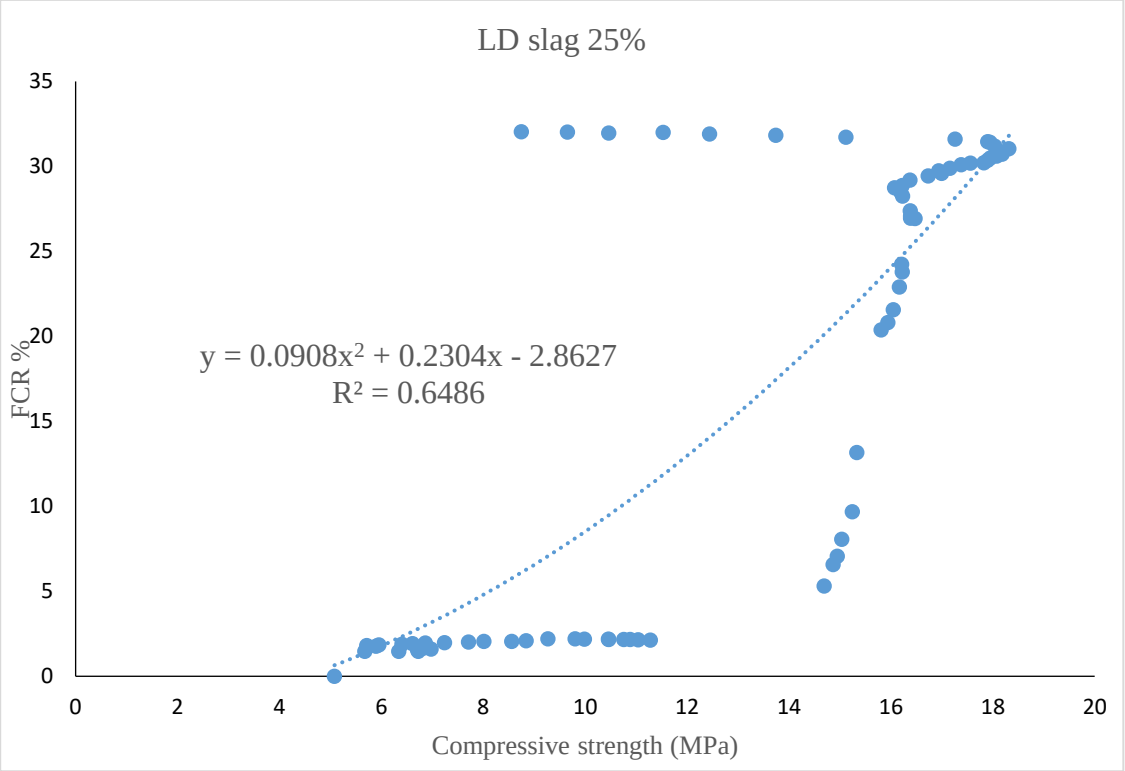

Figure 4.29. Fitting curve between FCR and compressive strength for 56 days

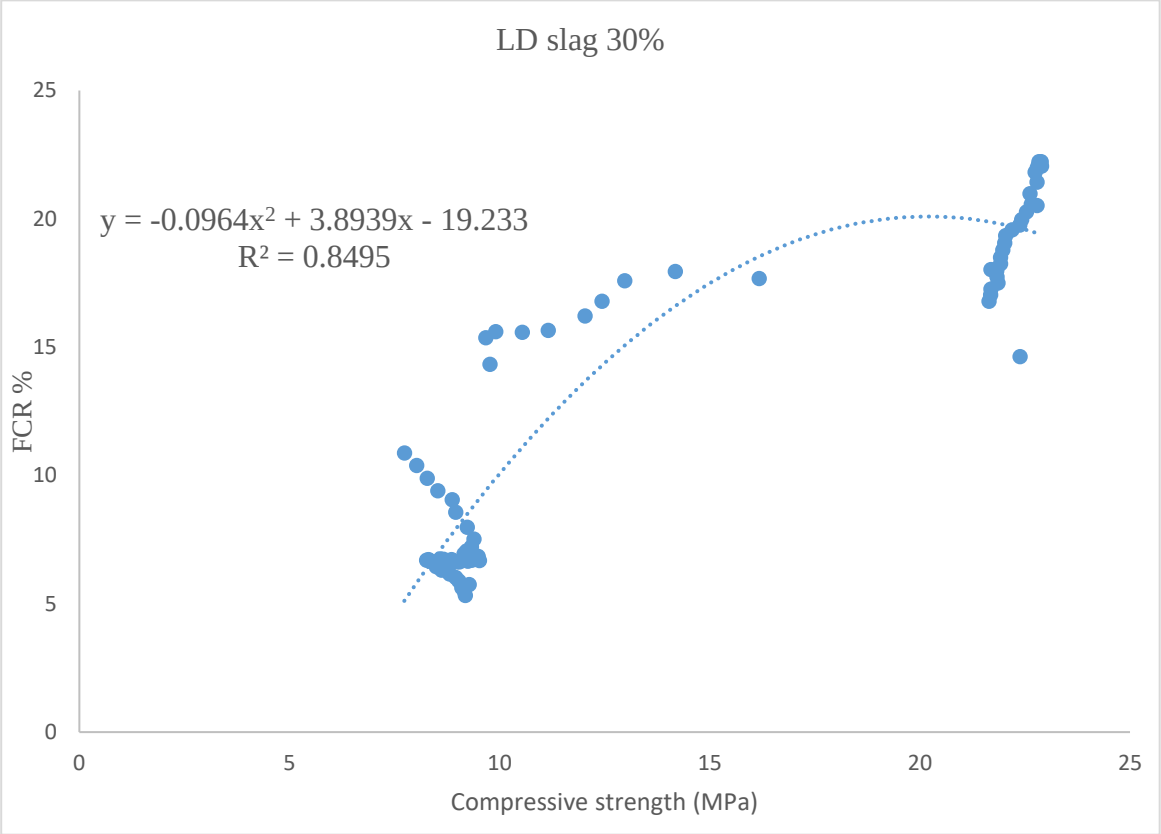

Figure 4.30. Fitting curve between FCR and compressive strength for 28 days

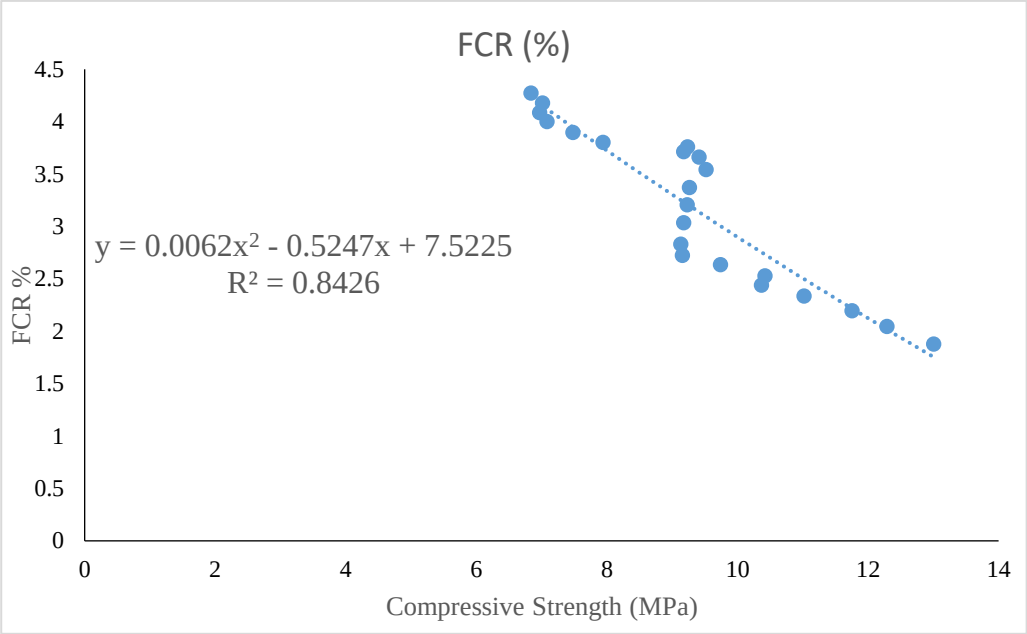

Figure 4.31. Fitting curve between FCR and compressive strength for 56 days

4.8. Analysis of self-sensing reinforced mortar beam incorporating 25% of copper slag

Following flexural stress conditions, the beam's crack growth displayed the following characteristics. The variation in FCR of copper slag mix under the displacement speed of (0.5mm/minute). For mortar beam with electrical characteristics present in it, self-sensing of damage is to be observed from the beginning of load application. Capability of self-sensing reinforced mortar beam was presented and in terms of fractional changes in electrical resistivity was discussed. Therefore, it can be concluded that reinforced mortar beam with greater self-sensing capabilities should yield higher FCR results.

Reinforced mortar after casting is divided into three zones with the set of four copper plates each for three DC power supplies of connection under applied four-point bending loading as shown in fig 4.32. The observed results from figure 4.33 to figure 4.41 shows that the reinforced mortar beam specimen incorporating 25% of the copper slag was successful in registering substantial increments in FCR values. As the unevenly distribution of load in the testing resulted in shear crack formation under the Zone III which insignificantly recorded insignificant drop in the conductivity and therefore resulted in drop of R^2 value by 47.3% approximately. Based on these findings, presence of conductive by-products of industrial waste caused cracks to be detected by the resistivity meter considerably more easily, indicating the significant effects of electrically conductive fillers on the efficiency of self-sensing-sensing capability.

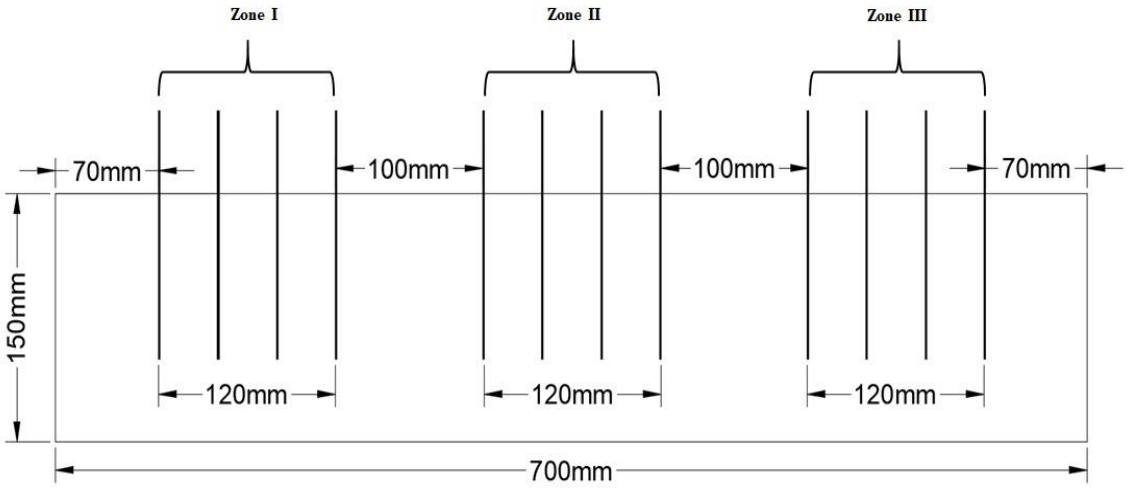

Figure 4.32. Different Zones of beam distributed as per three DC power suppliers

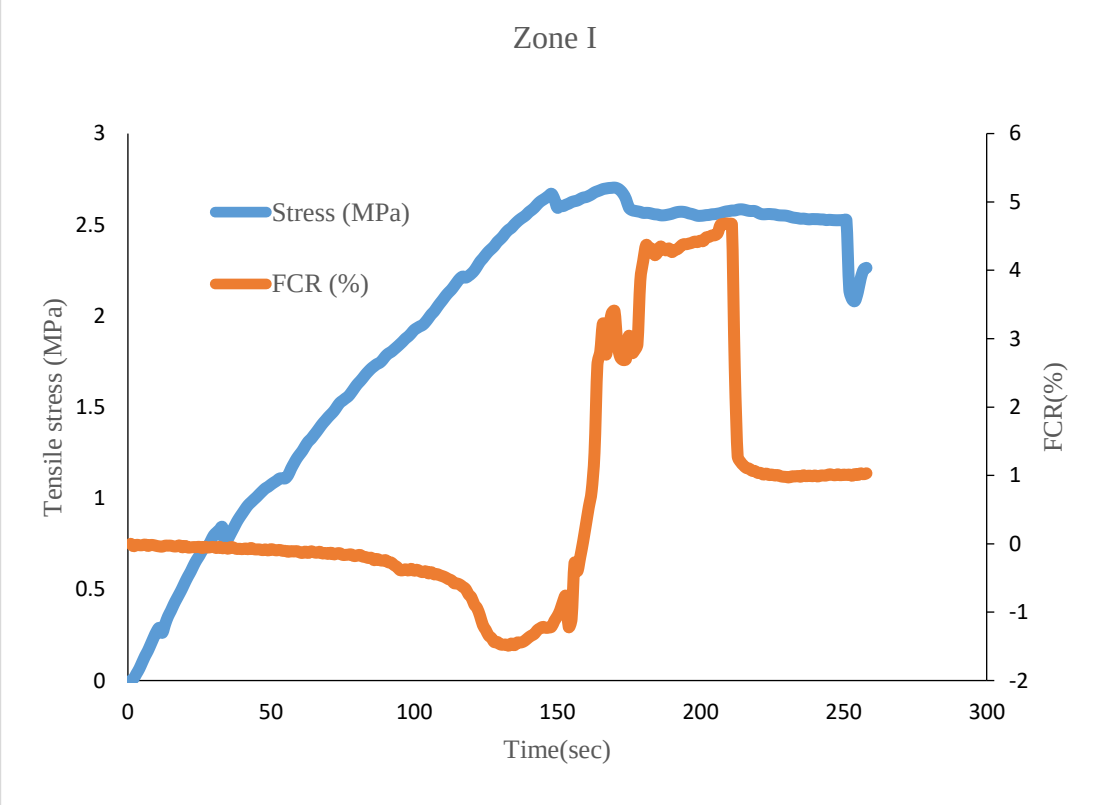

Figure 4.33. Tensile stress vs FCR observed by connection of Zone I

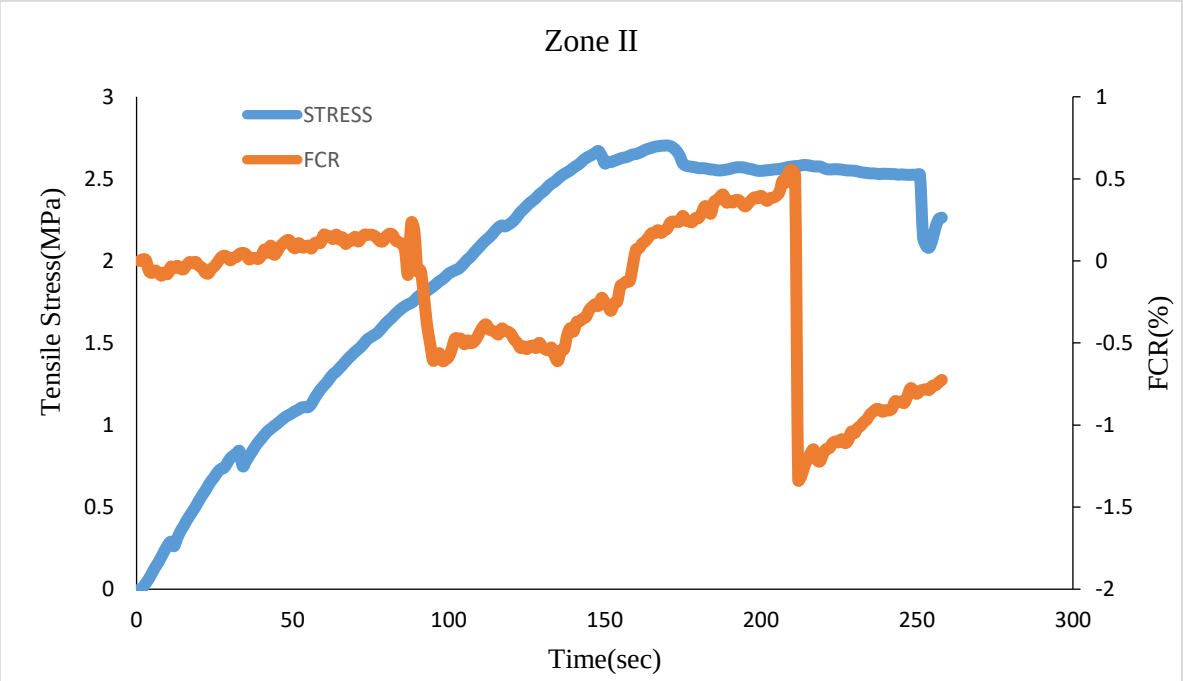

Figure 4.34. Tensile stress vs FCR observed by connection of Zone II

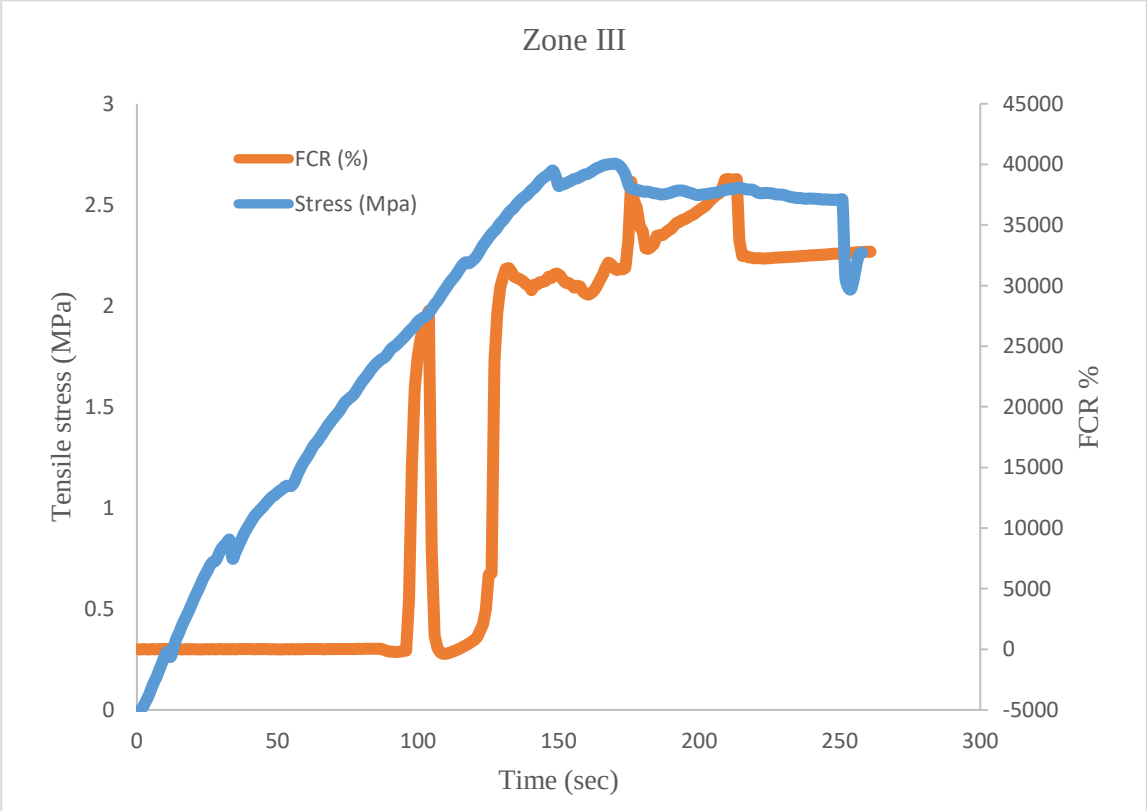

Figure 4.35. Tensile stress vs FCR observed by connection of Zone III

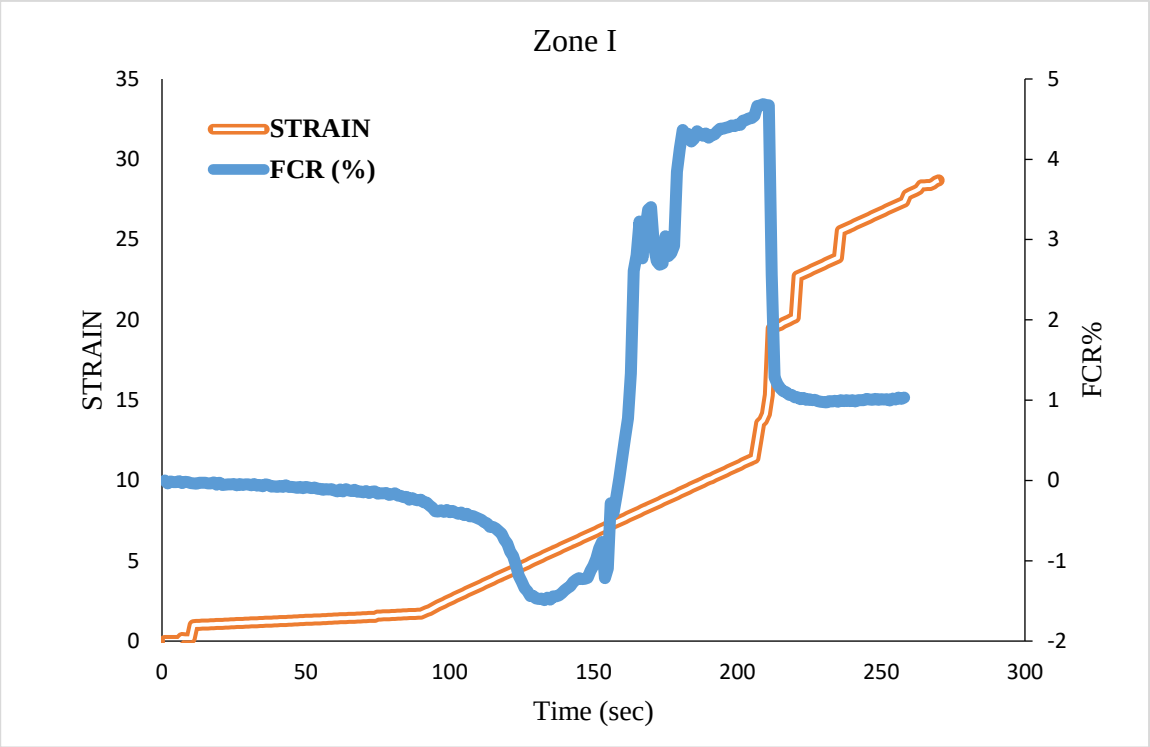

Figure 4.36. FCR vs Strain observed by connection of Zone I

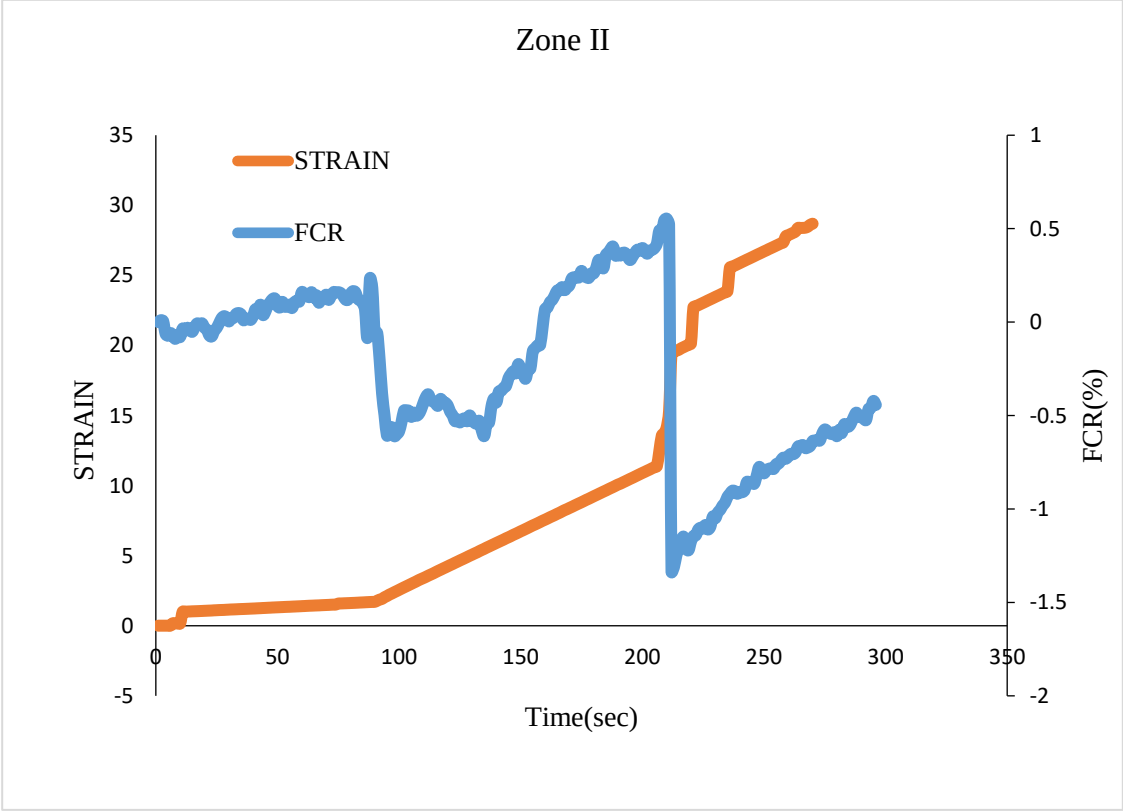

Figure 4.37. FCR vs Strain observed by connection of Zone I

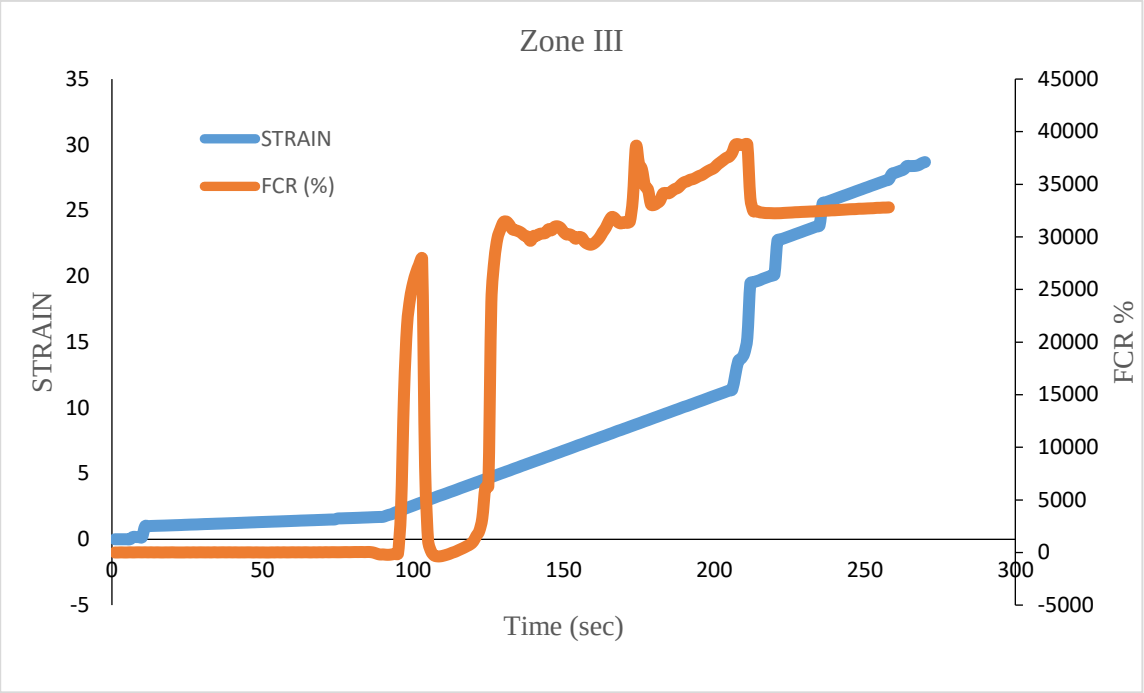

Figure 4.38. FCR vs Strain observed by connection of Zone III

The fitness of FCR and stress for 25% copper slag incorporation in Zone I, Zone II, and Zone III was observed 0.5053, 0.9594, and 0.8018. Greater the value of R^2 greater will be the sensing ability of the beam.

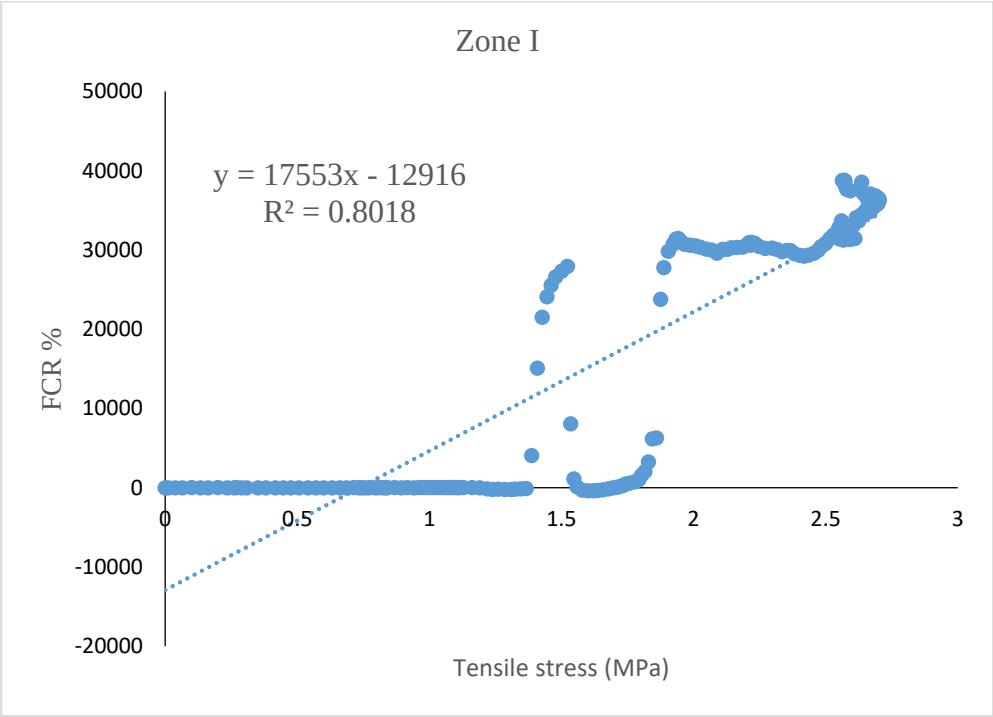

Figure 4.39. Fitting curve between FCR and tensile stress (MPa) of 25% CS in Zone I

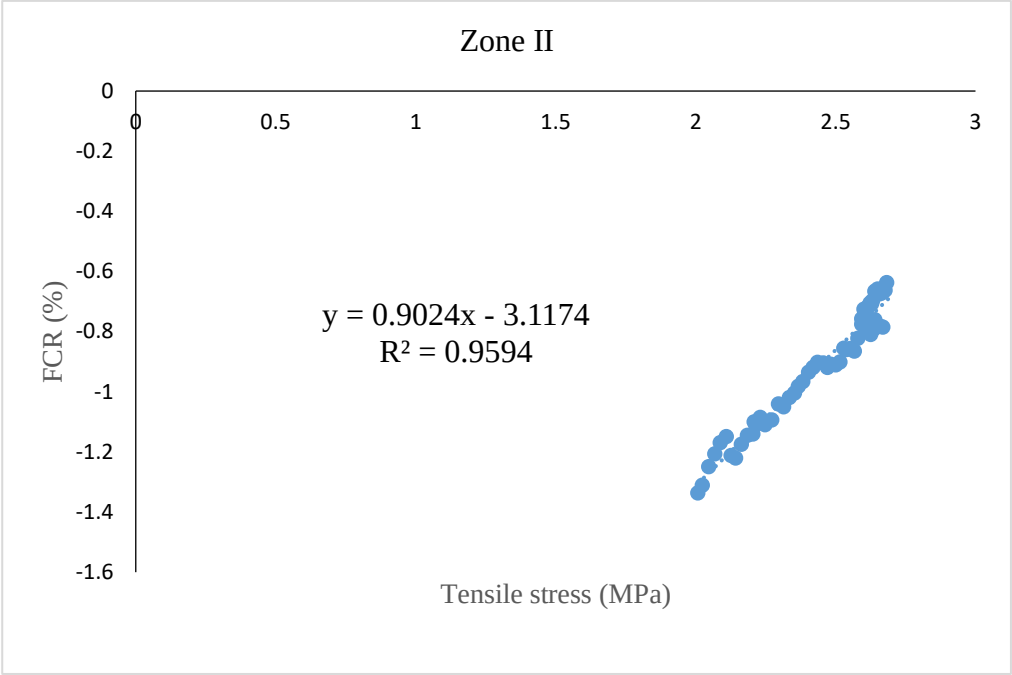

Figure 4.40. Fitting curve between FCR and tensile stress (MPa) of 25% CS in Zone II

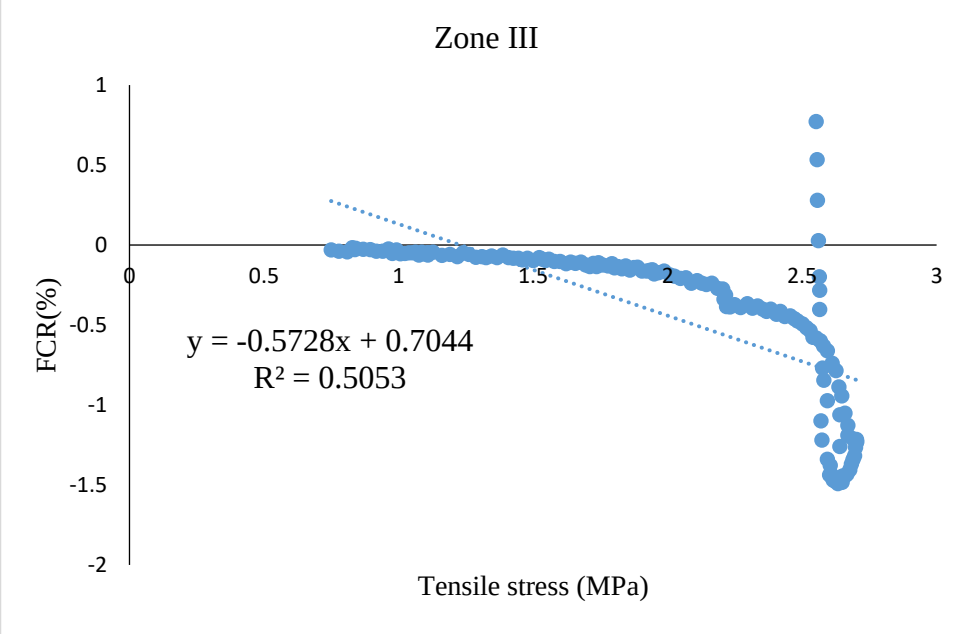

Figure 4.41. Fitting curve between FCR and tensile stress (MPa) of 25% CS in Zone III

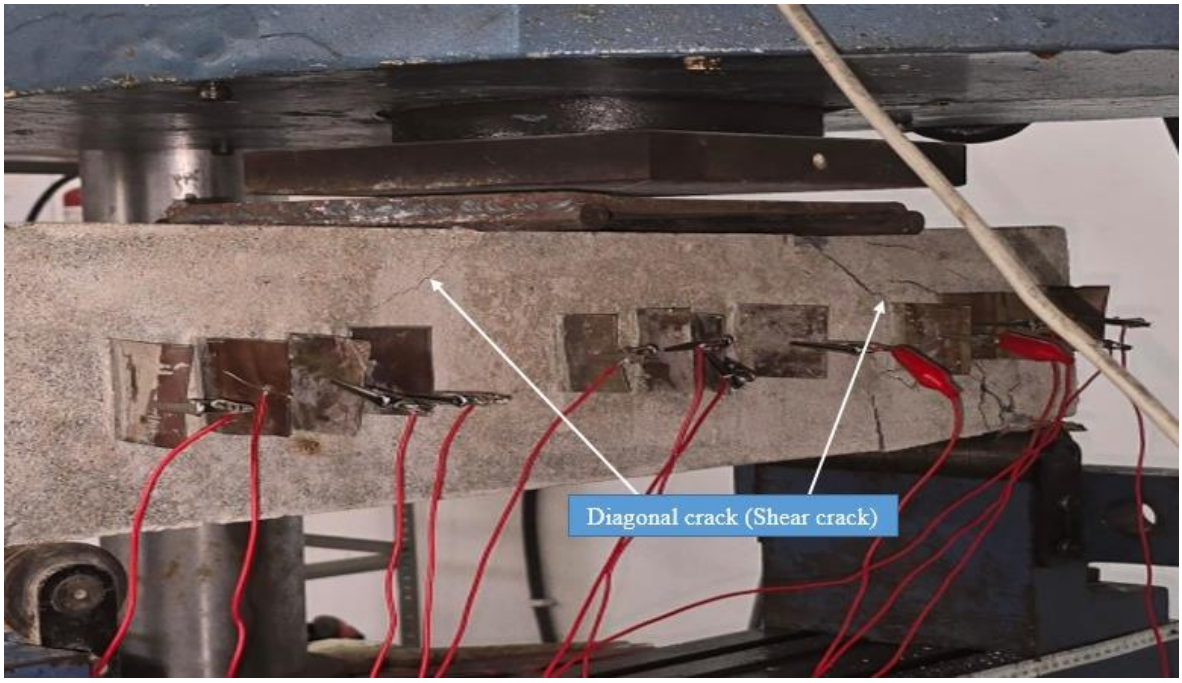

Figure 4.42. Shear failure in Beam incorporating 25% of CS

4.9 Analysis of self-sensing reinforced mortar beam incorporating 20% of LD slag

Similar testing procedure has been done in the case of incorporating 20% of LD slag as a sand replacement as previously done in the case of copper slag reinforced mortar beam. Three zones of beam was divided, (Zone I, Zone II, and Zone III) for the connection of the three DC power suppliers for observing fractional changes in the electrical resistivity. The observed results from figure 4.43 to figure 4.52 shows that the reinforced mortar beam specimen incorporating 20% of the LD slag was successful in registering substantial increments in FCR values. Certain drop in the conductivity was noted in the time of the shear cracks generated at the time of loading but significantly, results observed for LD 20% replacement were much better as compared to only sand samples, which did not show any characteristics of electrical resistivity.

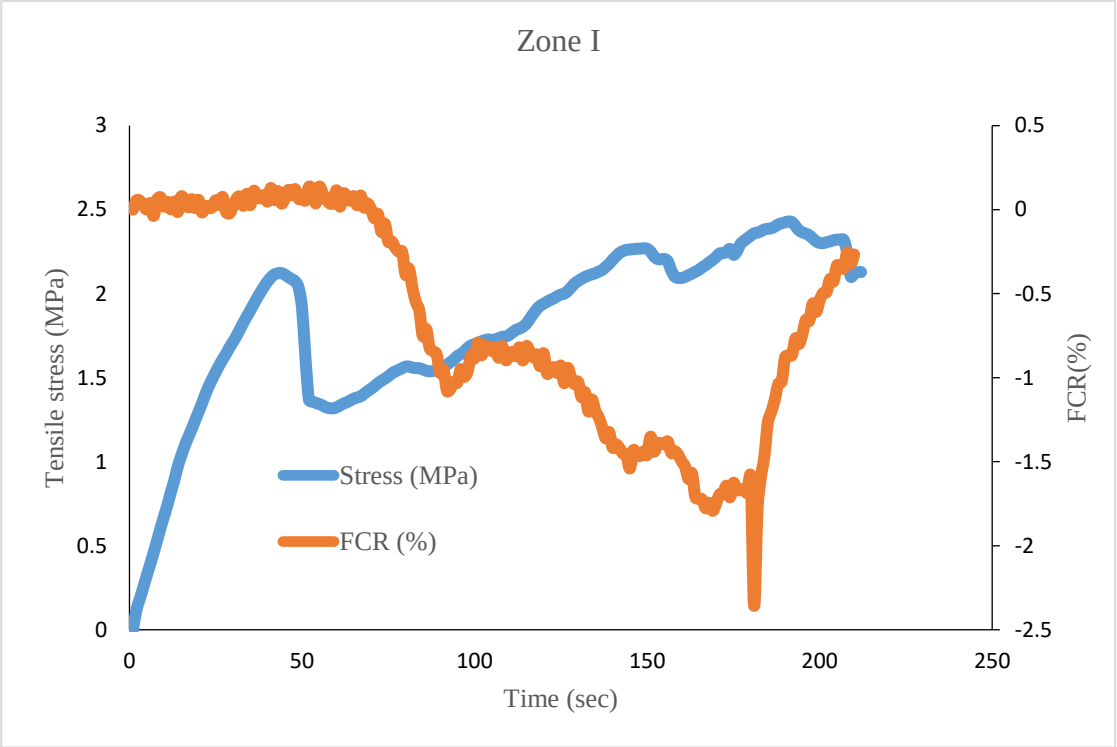

Figure 4.43. Tensile stress vs FCR observed by connection of Zone I

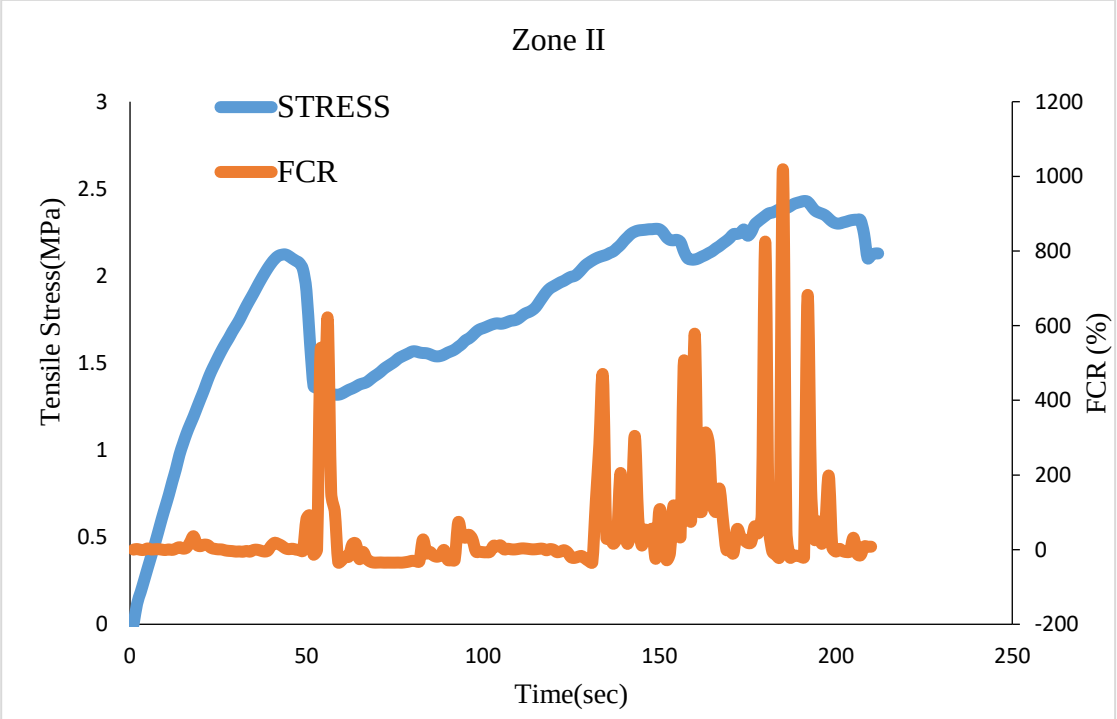

Figure 4.44. Tensile stress vs FCR observed by connection of Zone II

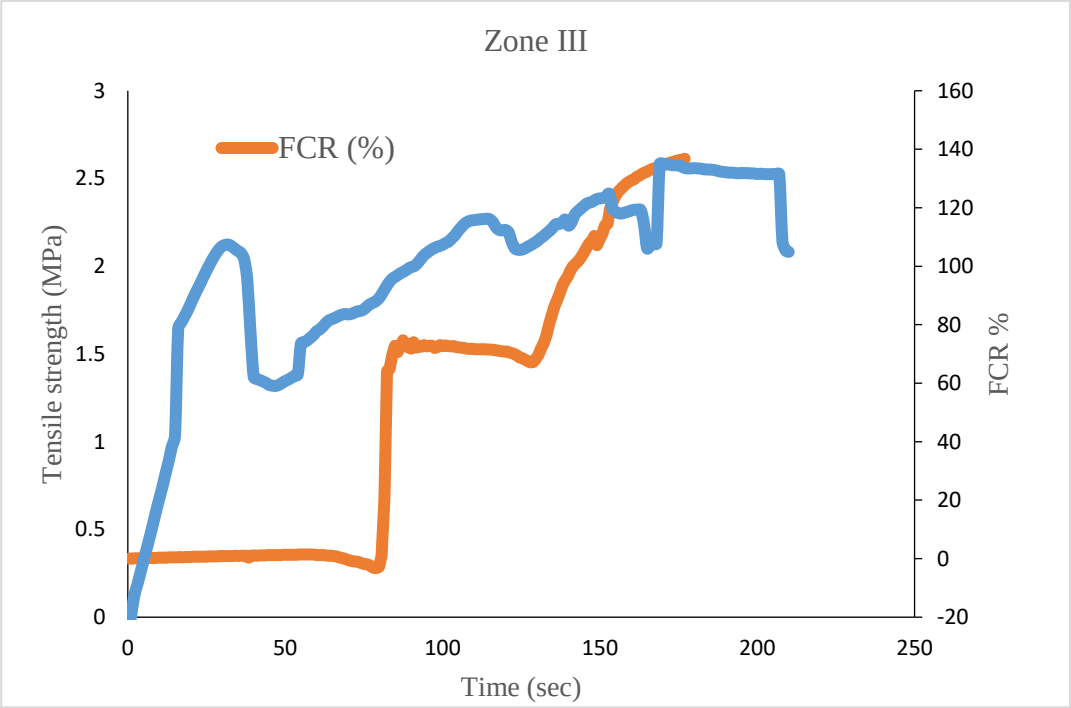

Figure 4.45. Tensile stress vs FCR observed by connection of Zone III

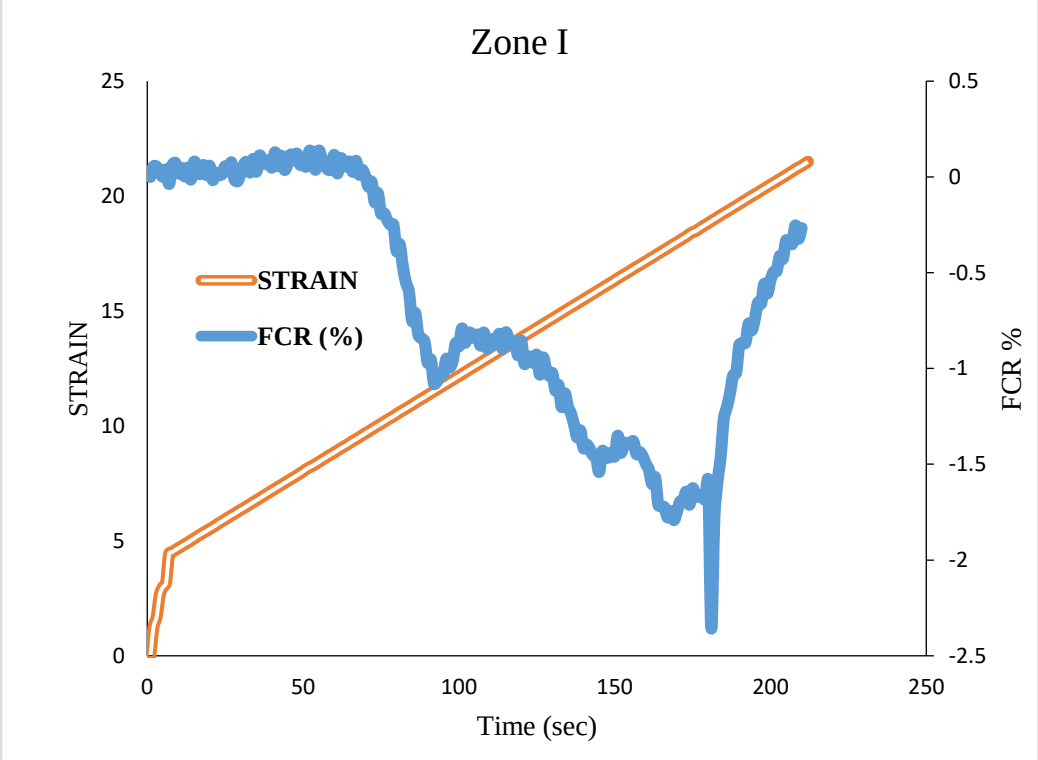

Figure 4.46. FCR vs Strain observed by connection of Zone I

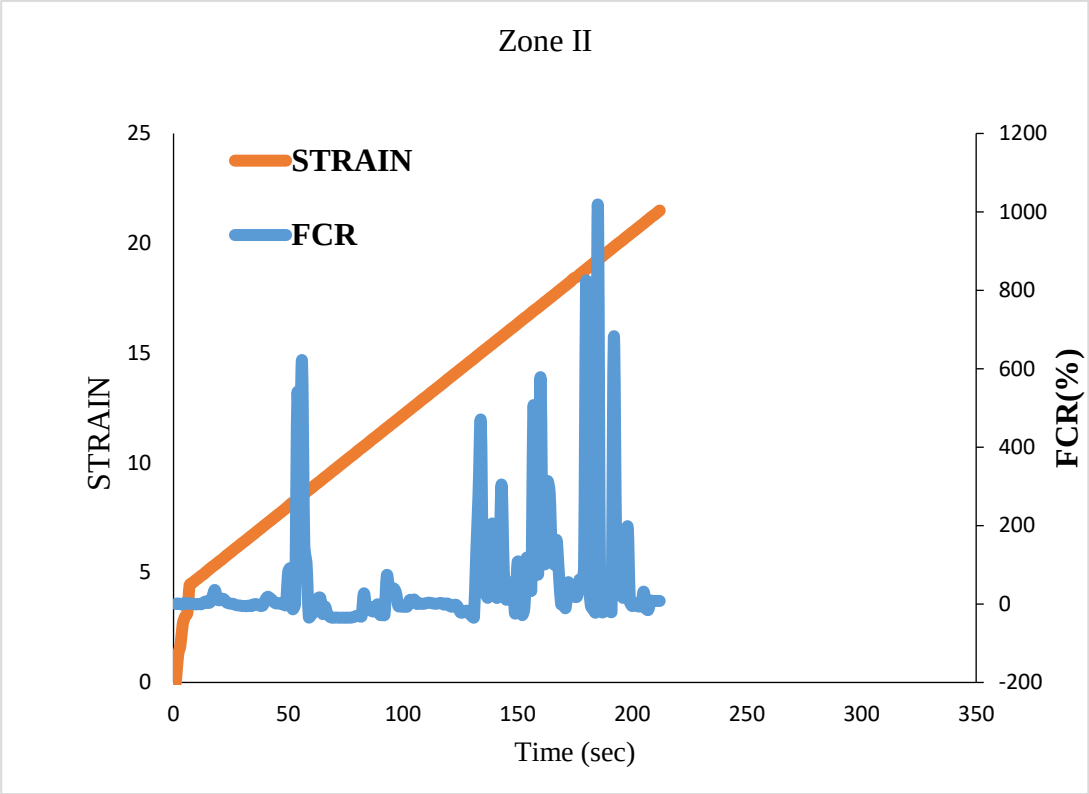

Figure 4.47. FCR vs Strain observed by connection of Zone II

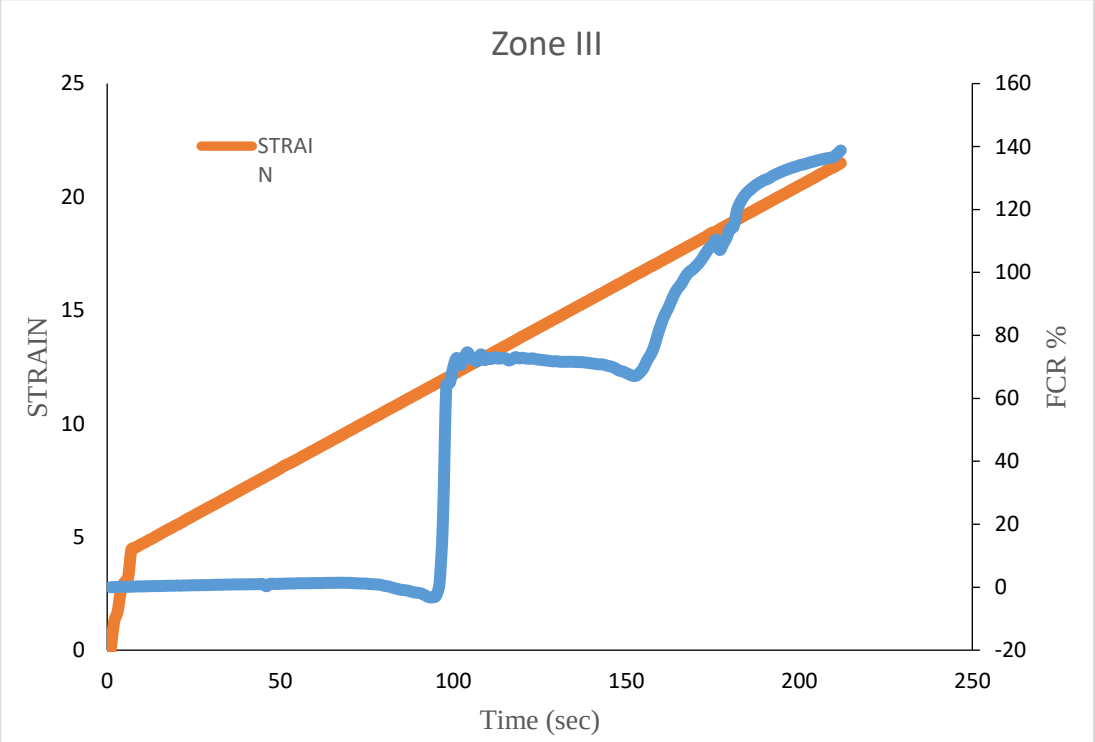

Figure 4.48. FCR vs Strain observed by connection of Zone III

The fitness of FCR and stress for 20% LD slag incorporation in Zone I, Zone II, and Zone III was observed 0.8195, 0.715, and 0.8187. Greater the value of R^2 greater will be the sensing ability of the beam.

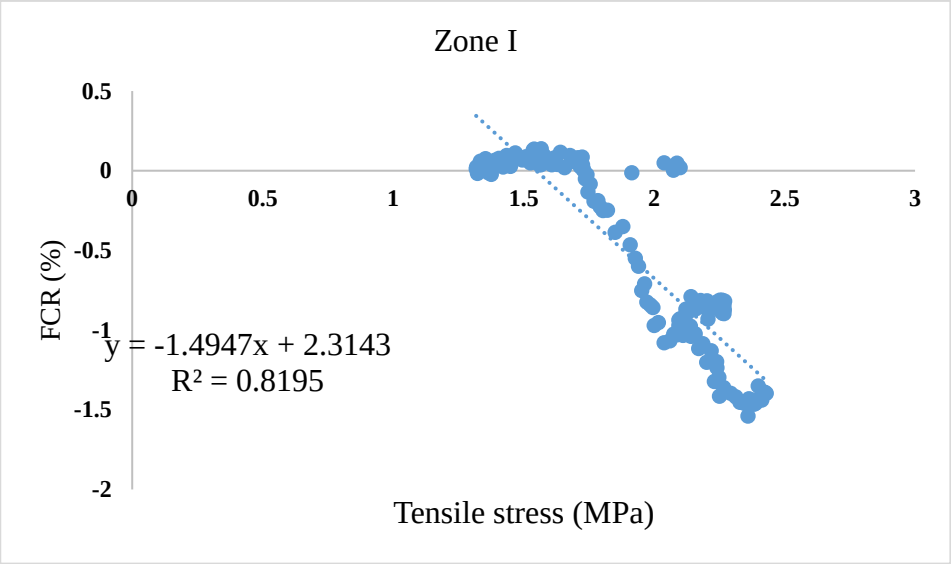

Figure 4.49. Fitting curve between FCR and tensile stress (MPa) of 20% LDslag in Zone I

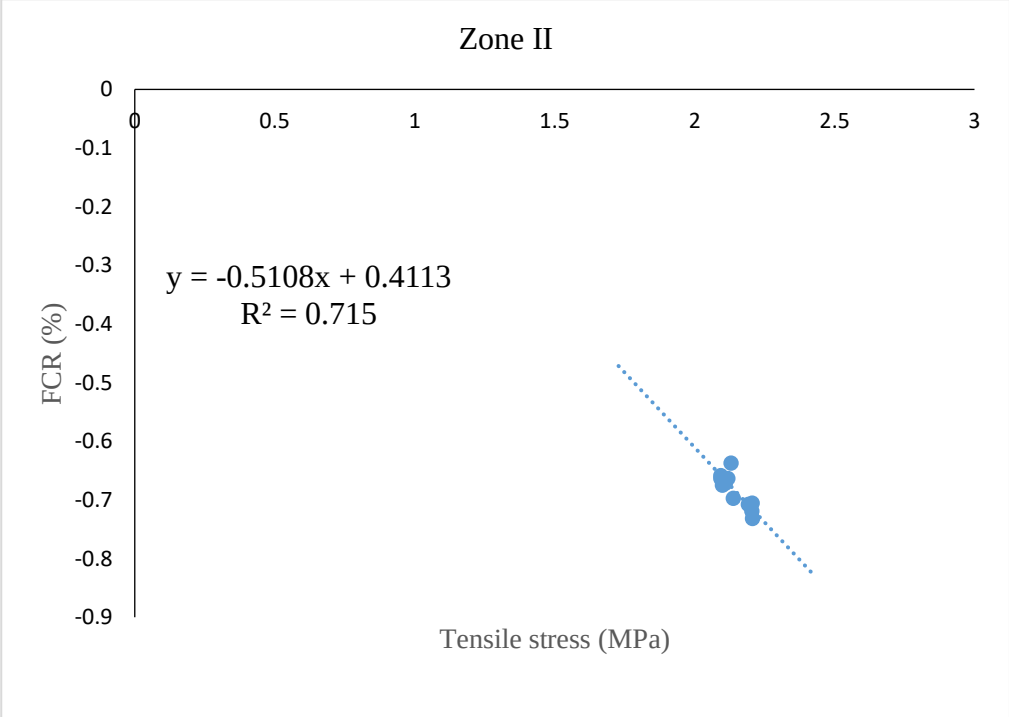

Figure 4.50. Fitting curve between FCR and tensile stress (MPa) of 20% LD slag in Zone II

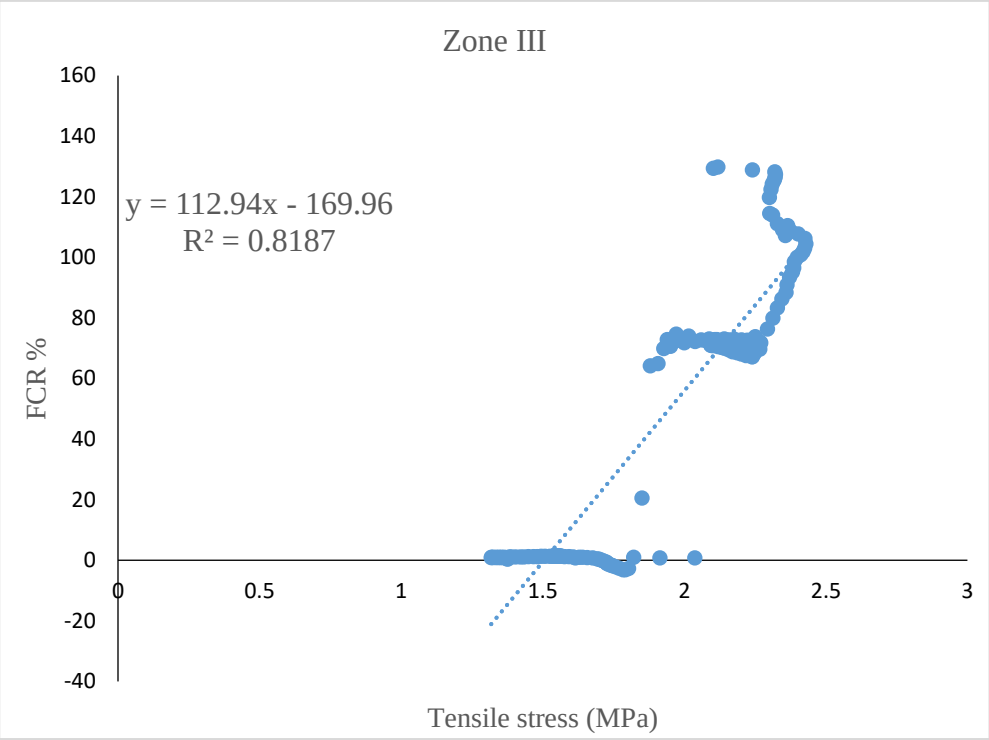

Figure 4.51. Fitting curve between FCR and tensile stress (MPa) of 20% LD slag in Zone III

Figure 4.52. Shear failure in Beam incorporating 20% of LD slag

4.11 Summary

After testing all the casted specimens, the best outcome comes out to be of mortar mix incorporating 25% of the Copper slag as the sand replacement and 20% incorporating of LD slag as a sand replacement. The incorporation of copper slag and LD slag improves the flexural and compressive strengths of the cement mortar. The electrical properties of the mortar are enhanced with addition of conductive industrial by-products, making it suitable for SHM applications. Study finds a significant relationship between strain/stress and changes in electrical resistivity, confirming the self-sensing capability of the composites. Although, in the cases of beam there are some changes in the value of FCR. The value of FCR insignificantly increase due to rise in temperature the specimen becomes dry.

Overall, the results concludes that the use of industrial by-products like copper slag and LD slag can effectively enhance both the mechanical and electrical properties of the cement mortar, making it a better option for self-sensing applications in structural health monitoring.

Chapter 5

CONCLUSIONS

5.1 General

The conclusion of the research in the findings of addition of Copper slag and LD slag replacements for various mechanical and electrical characteristics including electrical resistivity, piezo-resistivity properties allow for the following conclusions to be drawn:

1. By addition of industrial by-products such as Copper slag and LD slag to mortar mix, the material's mechanical properties and electrical characteristics are enhanced. This makes the mortar not only more affordable or durable but also well suited for advanced structural health monitoring (SHM) applications.

2. By turning these by-products into useful building materials, the research tackles important issues facing the construction sector, such as over use of natural resources and disposal of industrial waste.

3. Increasing the percentage of copper slag increases the workability, which can leading to segregation, bleeding thus making the electrical characteristics less. On the other hand, increasing the amount of LD slag as a sand replacement lowers the workability making the specimen dry and decreases the mechanical and electrical characteristics.

4. Addition of copper slag to SSC mixes significantly enhances flexural strength, with a maximum of 8.5 MPa achieved at 28 days with 75% copper slag replacement. While 25% also represents high strength.

5. Copper slag to self-sensing concrete mixes improves compressive strength of the specimens the maximum enhancement in observed for 50% of the sand replacement i.e. 44.94 MPa as compared to control sample at 28-day curing period. Copper slag 25% replacement showed increase in strength at 28-day curing period from 25.52 MPa to 30.14 MPa. Addition of 20% LD slag as a sand replacement generally improves compressive strength, which was observed 27.52 MPa as compared to control mix sample at 28-day of curing period which was 26.52 MPa.

6. When the stress was increased, it was shown that the FCR values for the control specimens did not significantly change at 28 days or 56 days.

7. When a compressive stress is applied, conductive channels are formed and the space between the particles decreases, resulting in the piezoresistive behaviour of the copper slag and LD slag sand replacement. Increased conductivity and a change in FCR follow from this.

8. Certain values of conductivity dropped in the Zone III for copper slag reinforced beam, which insignificantly reached around 30000, 45000% value of FCR breaking the conductive networks between the specimens making it nonconductive at the time of failure.

The research highlights how self-sensing cementitious composites (SSC) can be an innovative and sustainable way to address the needs of the contemporary building sector, encouraging the use of environmentally friendly materials without sacrificing functionality. The results imply that, with additional development and broad implementation, SSC may completely transform the design and upkeep of infrastructure, resulting in longer-lasting, safer, and more environmentally friendly buildings.

References

[1] IS:456-2000, Indian Standard Plain and Reinforced Concrete Code of Practice, Bur. Indian Stand. New Delhi. (2000).

[2] ASTM (2021) 'ASTM C348-21: Standard Test Method for Flexural Strength of Concrete'. American Society for Testing and Materials 1-6

[3] ASTM (1988) 'ASTM C109: Standard Test Method for Compressive Strength of Hydraulic Cement Mortars', American Society for Testing and Materials 4031 (Part 6), 3-7

[4] ASTM C1437 (2007) 'Standard Test Method for Flow of Hydraulic Cement Mortar'. C1437

[5] Bureau of Indian Standard (2013) IS 8112: 2013, Ordinary Portland Cement, 43 Grade Specification. (March)

[6] Gupta, N., & Siddique, R. (2019). Strength and micro-structural properties of self-compacting concrete incorporating copper slag. Construction and Building Materials, 224, 894-908.

[7] Gupta, N., & Siddique, R. (2020). Durability characteristics of self-compacting concrete made with copper slag. Construction and Building Materials, 247, 118580

[8] Ding, Y., Liu, G., Hussain, A., Pacheco-Torgal, F., & Zhang, Y. (2019). Effect of steel fiber and carbon black on the self-sensing ability of concrete cracks under bending.

[9] Dong, W. et al., 2021. Multifunctional cementitious composites with integrated self-sensing and hydrophobic capacities toward smart structural health monitoring.

[10] M.A.G. Dos Anjos, A.T.C. Sales, N. Andrade, Blasted copper slag as fine aggregate in Portland cement concrete, J. Environ. Manage. 196 (2017) 607–613.

[11] Kang, M., Kang, M., Yonis, A., Vashistha, P., & Pyo, S. (2024). Effect of steel slag on the mechanical properties and self-sensing capability of ultra-high performance concrete (UHPC). Development in the Built Environment, 17, 100342.

[12] Han, B., Ding, S., & Yu, X. (2015). Intrinsic self-sensing concrete and structures: A review measurement, 59, 110-128.

[13] Alaneme, K., & Bodunrin, M. (2017). Self-healing using metallic material systems – A review, Applied materials Today, 6, 9-15.

[14] Wang, H., Shi, F., Shen, J., Zhang, A., Zhang, L., Huang, H., Liu, J., Jin, K., Feng, L., & Tang, Z. (2021). Research on the self-sensing and mechanical properties of aligned stainless steel fiber-reinforced reactive powder concrete. Cement and Concrete Composites, 119, 104001.

[15] Singh, P., Roy, A. D., & Singh, H. (2022). Mechanical and durability properties of concrete incorporating weathered coarse Linz-Donawitz (LD) steel slag. Journal of Building Engineering, 61, 105301.

[16] Singh, P., Singh, H., & Roy, A. D. (2023). Sustainably produced concrete using weathered Linz-Donawitz slag as a fine aggregate Substitute: A comprehensive study with Artificial intelligence approach. Structures, 54, 964-908.

[17] Biskri Y, Achoura D, Chelghoum N, Mouret M. Mechanical and durability characteristics of High Performance Concrete containing steel slag and crystalized slag as aggregates. Constr Build Mater 2017;150:167–78.

[18] Venkatesan B, Lijina VJ, Kannan V, Dhevasenaa PR. Partial replacement of fine aggregate by steel slag and coarse aggregate by walnut shell in concrete. Mater Today Proc 2020;37:1761–6.

[19] Gupta T, Sachdeva SN. Laboratory investigation and modeling of concrete pavements containing AOD steel slag. Cem Concr Res 2019;124:105808.

[20] Lam MNT, Le DH, Jaritngam S. Compressive strength and durability properties of roller-compacted concrete pavement containing electric arc furnace slag aggregate and fly ash. Constr Build Mater 2018;191:912–22.

[21] Ali S, Iqbal S, Room S, Ali A, Ur Rahman Z. Value added usage of granular steel slag and milled glass in concrete production. J Eng Res 2021; 9:73–85.

[22] Bharani S, Rameshkumar G, Manikandan J, Balayogi T, Gokul M, Bhuvanesh DC. Experimental investigation on partial replacement of steel slag and E-waste as f ine and coarse aggregate. Mater Today Proc 2020;37:3534–7.

[23] Ren, Z., Sun, J., Zeng, X., Chen, X., Wang, Y., Tang, W., & Wang, X. (2022). Research on the electrical conductivity and mechanical properties of copper slag multiphase nano-modified electrically conductive cementitious composite. Construction and Building Materials, 339, 127650.

[24] W. Meng, K.H. Khayat, Mechanical properties of ultra-high-performance concrete enhanced with graphite nanoplatelets and carbon nanofibers, Compos. B Eng. 107 (2016) 113–122.

[25] R. Zhao, C. Tuan, B. Luo, A. Xu, Radiant heating utilizing conductive concrete tiles, Build. Environ. 148 (2019) 82–95.

[26] Sarwary, M. H., Yıldırım, G., Al-Dahawi, A., Anıl, Ö., Khiavi, K. A., Toklu, K., & Şahmaran, M. (2019). Self-Sensing of flexural damage in Large-Scale Steel-Reinforced mortar beams. ACI Journal, 116(4).

[27] Xu, Z., Zhang, J., Zhang, J., Deng, Q., Xue, Z., Huang, G., & Huang, X. (2024). Influence of steel slag and steel fiber on the mechanical properties, durability, and life cycle assessment of ultra-high performance geopolymer concrete. Construction and Building Materials, 441, 137590.

[28] C.K. Madheswaran, P.S. Ambily, J.K. Dattatreya, N.P. Rajamane, Studies on use of copper slag as replacement material for river sand in building constructions, J. Inst. Eng. (India): Series A 95 (3) (2014) 169–177.

[29] W. Gong, T. Ueda, Properties of self-compacting concrete containing copper slag aggregate after heating up to 400 C, Struct. Concr. 19 (6) (2018) 1873 1880.

[30] Tian, Z., Li, Y., Zheng, J., & Wang, S. (2019). A state-of-the-art on self-sensing concrete: Materials, fabrication and properties. Composites Part B Engineering, 177, 107437.

turnitin

Digital Receipt

This receipt acknowledges that Turnitin received your paper. Below you will find the receipt information regarding your submission.

The first page of your submissions is displayed below.

Submission author:	Arpit GOYAL
Assignment title:	Achleshwar ME Thesis
Submission title:	Thesis ' Achleshwar Singh Raizada' 1 (1).docx
File name:	Thesis_Achleshwar_Singh_Raizada_1_1_.docx
File size:	8.08M
Page count:	108
Word count:	18,324
Character count:	102,549
Submission date:	31-Aug-2024 04:40PM (UTC+0530)
Submission ID:	2441829450

Effect of LD Slag and Copper Slag as Sand Replacement on Self-Sensing Properties of Cementitious Composites

Thesis ' Achleshwar Singh Raizada' 1 (1).docx

ORIGINALITY REPORT

20%	12%	18%	4%
SIMILARITY INDEX	INTERNET SOURCES	PUBLICATIONS	STUDENT PAPERS

PRIMARY SOURCES

1	Zhenhua Ren, Junbo Sun, Xiantao Zeng, Xi Chen, Yufei Wang, Weichen Tang, Xiangyu Wang. "Research on the electrical conductivity and mechanical properties of copper slag multiphase nano-modified electrically conductive cementitious composite", Construction and Building Materials, 2022 Publication	1%
2	Nikita Gupta, Rafat Siddique. "Strength and micro-structural properties of self-compacting concrete incorporating copper slag", Construction and Building Materials, 2019 Publication	1%
3	Pavitar Singh, A.B. Danie Roy, Heaven Singh. "Mechanical and durability properties of concrete incorporating weathered coarse Linz-Donawitz (LD) steel slag", Journal of Building Engineering, 2022 Publication	1%
4	tudr.thapar.edu:8080 Internet Source	1%

5	hdl.handle.net Internet Source	1 %
6	Mohammad H. Sarwary, Gürkan Yıldırım, Ali Al-Dahawi, Özgür Anıl, Kaveh A. Khiavi, Kenan Toklu, Mustafa Şahmaran. "Self-Sensing of Flexural Damage in Large-Scale Steel-Reinforced Mortar Beams", ACI Materials Journal, 2019 Publication	1 %
7	Yunyang Wang, Liqing Zhang. "Development of self-sensing cementitious composite incorporating hybrid graphene nanoplates and carbon nanotubes for structural health monitoring", Sensors and Actuators A: Physical, 2022 Publication	1 %
8	eprints.utar.edu.my Internet Source	1 %
9	www.mdpi.com Internet Source	1 %
10	opus.lib.uts.edu.au Internet Source	1 %
11	Zhuang Tian, Yancheng Li, Jiajia Zheng, Shuguang Wang. "A state-of-the-art on self-sensing concrete: Materials, fabrication and	1 %